

The role of active zone scaffold bassoon in the regulation of presynaptic proteasome

Dissertation

zur Erlangung des akademischen Grades

**doctor rerum naturalium
(Dr. rer.nat)**

genehmigt durch

Fakultät für Naturwissenschaften

der Otto-von-Guericke Universität Magdeburg

von M.Sc. Sandra Fieńko

geb. am. 19. April 1988 in Zielona Góra, Polen

**Gutachter: Prof. Dr. Anna Fejtova
Prof. Dr. Noam Ziv**

eingereicht am 29. August 2017

verteidigt am 26. Februar 2018

Acknowledgments

I would like to express my gratitude to Prof. Dr. Anna Fejtova for the guidance and assistance during the course of my PhD.

I also would like to acknowledge Prof.Dr. Eckart Gundelfinger for enthusiastic discussions during group meetings.

Special thanks to former and present members of the bassoon group Eneko Pina, Anika Dirks, Franzi Altmüller , Carolina Montenegro, Benjamin Berinson, Maru Andre-Alonso, Anil Annamneedi, Santosh Pothula, Daniela Ivanova, Vesna Lazarevic, Yulia Kuleva and Latha Mukunda for all the input, positive energy, encouragement and support!

I also would like to thank Janina Juhle, Isabel Herbert and Jeanette Maiwald for excellent technical assistance.

I would like to thank my friends that I made along the way who simply made this PhD journey unforgettable Maru, Kasia, Marie, Ioana, Marta, Carolina as well as Benjamin and Eneko and all other friends scattered around Europe, especially Asya and Karolina!

Finally, no words can express how grateful I am to my parents and the whole family for their love and support throughout! Thank you!

The work was supported by Deutsche Forschungsgemeinschaft.

Summary

Neuronal proteins are subjected to continued turnover at disparate rates, and this degradative process is of crucial importance for the protein homeostasis. Cellular degradation pathways branch into three constituents: ubiquitin-proteasome system, autophagy and endo-lysosomal pathway. Amongst these, proteasome emerges as the principal machinery in control of protein turnover as well as maintenance of basic neuronal processes that shape and facilitate synaptic plasticity. Proteasome (26S) is a barrel-shaped, multicatalytic complex that consists of 20S and 19S subpopulations. 20S core particle harbors three major proteolytic activities, whereas 19S serves as a regulatory particle that participates in the binding of ubiquitin-tagged substrates, their deubiquitination as well as delivery of client proteins into the proteolytic core. The mere assembly of this intricate machinery is a demanding task, requiring a tightly orchestrated set of steps and several external chaperon cofactors. However, not only auxiliary proteins, but also intrinsic elements of proteasome β subunits play a key role in coordinating 20S assembly process. In this work, we identified a PSMB4 ($\beta 7$) subunit of proteasome as a novel interacting partner of the presynaptic active zone protein (bsn). Studies conducted in the heterologous system of HEK293T cells, cultured cortical neurons as well as cytosolic and synaptic fractions from bsn knock out animals revealed that bsn curbs proteasome activity. Moreover, a series of interaction studies uncovered two independent bsn fragments that bind distinct proteasome subunit segments, which implies a complex role of bsn in the regulation of presynaptic proteasome. As PSMB4 is crucial for the correct proteasome formation, we tested whether bsn by association with this proteasomal subunit, could interfere with 20S assembly. These experiments demonstrated that bsn leads to the accumulation of PAC1, an auxiliary protein, normally degraded following assembly of the functional 20S and thus hampers generation of proteolytically competent proteasomes. These findings are of indisputable relevance as they indicate that bsn acts as a major negative regulator of presynaptic proteasomes. Furthermore, we investigated the impact of proteasome-bsn interaction on the presynaptic vesicles and found that ectopic expression of the short bsn fragments does not affect synaptic vesicle pools. However, optical imaging of synaptic vesicle cycling from bsn deficient neurons showed that inhibition of proteasome activity can still trigger an essential upregulation of, otherwise decreased, recycling pool fraction. These suggest that proteasome and bsn intersect, possibly also with other cellular signaling pathways, to collectively regulate presynaptic phenotype by fine-tuning synaptic vesicular pools.

Zusammenfassung

Neuronale Proteine sind einem ständigen Umsatz unterworfen. Dieser Zerfallsprozess ist wichtig für das Gleichgewicht der Proteinkonzentrationen und findet, proteinspezifisch, zu unterschiedlichen Zeitpunkten statt. Dabei werden beschädigte Proteine entweder in ihre primäre stabile Konformation zurückgefaltet oder durch Proteolyse abgebaut. Die dafür notwendigen strengen Proteinqualitätskontrollmechanismen stellen die Gesundheit der Nervenzellen und die korrekte Hirnfunktion sicher. Zelluläre Abbauwege lassen sich in drei Bestandteile gliedern: Ubiquitin-Proteasom-System, Autophagozytose und Endo-Lysosomaler Weg. Dabei hat sich das Proteasom als der wichtigste Mechanismus zur Kontrolle des Proteinumsatzes und darüber hinaus zum Erhalt basaler neuronaler Prozesse, welche die synaptische Plastizität prägen und fördern, herausgestellt. Das Proteasom (26S) ist ein multikatalytischer Komplex mit einer Faß-ähnlichen Struktur, bestehend aus 20S und 19S Untereinheiten. Die zentrale 20S Untereinheit besitzt die drei wesentlichen proteolytischen aktiven Zentren. Die 19S Untereinheit hingegen hat regulatorische Funktionen, wichtig für die Bindung von mit Ubiquitin markierten Substraten, ihrer Deubiquitinierung und ihres Transportes in die aktiven Zentren. Bereits die korrekte Zusammensetzung dieses komplizierten Komplexes benötigt fein aufeinander abgestimmte Schritte und verschiedene externe Chaperone als Ko-Faktoren. Neben solchen Hilfsproteinen spielen auch intrinsische Elemente, wie der der Proteasom β Untereinheiten, eine wichtige Rolle bei der Koordination des 20S Zusammenbaus.

In dieser Studie identifizierten wir die PSMB4 (β 7) Untereinheit des Proteasoms als neuen Interaktionspartner des an der presynaptischen aktiven Zone lokalisierten Gerüstproteins Bassoon. Wir konnten in heterologen Expressionssystemen mit HEK293T Zellen, in primären kortikalen Kulturen und in zytosolischen und synaptischen Fraktionen von Bassoon Knockout Mäusen zeigen, dass Bassoon die Proteasomaktivität senkt. Darüber hinaus zeigte eine ganze Reihe von Interaktionsstudien, dass zwei unabhängige Fragmente von Bassoon an bestimmte Bereiche des Proteasoms binden können. Diese Komplexität der Interaktion lässt vermuten, dass Bassoon das präsynaptische Proteasom auf zwei verschiedene Wege regulieren könnte. Unsere Experimente zeigten, dass in Gegenwart von Bassoon die Vorläufer der β -Untereinheiten und PAC1, ein Hilfsprotein, welches normalerweise nach dem Zusammenbau der funktionellen 20S Untereinheit abgebaut wird, akkumulieren. Das lässt vermuten, dass Bassoon den Zusammenbau der 20S Untereinheit beeinflusst und somit die Bildung von proteolytisch aktiven Proteasomen hemmt. Diese Ergebnisse demonstrieren erstmalig, dass Bassoon als ein wesentlicher negativer Regulator für presynaptische Proteasomen fungiert.

Darüber hinaus wurde in dieser Arbeit der Einfluss der Proteasom-Bassoon Interaktion auf presynaptische Vesikel studiert. Es konnte gezeigt werden, dass die ektopische Expression der kurzen Bassoon Fragmente die verschiedenen Pools der synaptischen Vesikel nicht beeinflusst. Dennoch zeigten Experimente in Bassoon Knockout Kulturen, die eine Aussage über Endo- und Exozytose von

synaptischen Vesikels zulassen, dass eine Unterbindung der Proteasomaktivität zu einem vergrößerten Recycling Pool der synaptischen Vesikel führt. Diese Unterschiede in der Größe des Recycling Pools waren auch im Vergleich zu Wildtyp Neuronen signifikant. Das lässt auf ein Zusammenspiel zwischen Proteasom und Bassoon - und womöglich auch zwischen diesen und anderen Signalwegen - schließen, um so gemeinsam den präsynaptischen Phänotyp durch Anpassung der synaptischen Vesikel Pools zu regulieren.

Table of Contents

1. Introduction	1
1.1 Ubiquitin conjugating apparatus	1
1.2 The proteasome	3
1.2.1 Anatomy of the 20S proteasome	4
1.2.1.1 β-ring	4
1.2.1.2 α-ring	5
1.2.2 Anatomy of the 19S regulatory particle	5
1.3 Tissue specific forms of the proteasome	7
1.4 Molecular mechanisms controlling proteasome assembly	8
1.4.1 α-ring formation	9
1.4.2 β-ring assembly	11
1.4.3 Dimerization of the half-proteasomes	12
1.5 The role of the ubiquitin-proteasome system in the brain	13
1.6 The architecture of the chemical synapses	13
1.6.1 Bassoon as an example of the prominent active zone protein	14
1.7 The Synaptic vesicle cycle	15
1.7.1 Synaptic vesicle pools	15
1.8 Hebbain and Homeostatic plasticity	17
1.9 Role of the UPS in the synaptic plasticity: the case of Aplysia	17
1.10 Influence of the UPS on the mammalian synaptic plasticity	18
1.11 Proteasome at the post synapse	18
1.12 UPS at the presynapse	20
1.13 Aim of the study	23
2. Materials and Methods	24
2.1. Materials	24
2.1.1 Antibodies	24
2.1.2 Animals	24
2.1.3 Molecular biology reagents	24

2.1.4 Cell culture media and reagents for mammalian cells	25
2.1.5 Culture media for bacterial cells and yeast.....	25
2.1.6 Pharmacological reagents.....	26
2.1.7 Commonly used buffers and reagents for biochemical /imaging experiments	26
2.1. Methods	27
2.2.1 Genotyping of mutant mice.....	27
2.2.2. Cloning of DNA constructs	28
2.2.3. Mapping of interaction domain by yeast two hybrid screening (Y2H)	30
2.2.4. Lentiviral particles production	30
2.2.5. Primary neuronal cultures and viral infections	31
2.2.6. Co-recruitment assays in COS7 cells	32
2.2.7. Immunoprecipitation from HEK293T cells and Western blotting.....	32
2.2.8. Mouse brain subfractionation	33
2.2.9. Native gel electrophoresis and Zymography	34
2.2.10. Proteasome activity assay from HEK293T cells, cortical cultures and brain fractions.....	34
2.2.11. Measurement of the UPS activity in HEK 293T cells with the fluorescent proteasome reporter	35
2.2.12. Glycerol density gradient ultracentrifugation.....	35
2.2.13. CypHer5E and synapto-pHluorin imaging.....	36
2.2.14. Statistical analysis	37
3. Results	39
3.1 Bsn interacts with the proteasomal subunit β 7 (aka PSMB4)	39
3.2 Bsn recruits endogenous UPS	45
3.3 Bsn is ubiquitinated but not constitutively degraded	48
3.4 Bsn overexpression impairs proteasome activity	49
3.5 Bsn deficiency modulates proteasome activity	55
3.6 Bsn interferes with proteasome assembly.....	59

3.7 Bsn overexpression does not induce changes in the SV pool sizes	62
3.8 Bsn and proteasome intersect to trigger alternations in the SV pool sizes	65
4. Discussion	69
4.1 Functional interaction of the active zone protein bsn with a crucial subunit of the 20S proteasome	69
4.1.1 Multiple binding interfaces in Bsn2 are involved in the interaction with PSMB4	70
4.1.2 Bsn4 associates specifically with C-terminus of PSMB4 and acts as a hub for many protein interactions	71
4.2 Bsn acts as a major regulator of the presynaptic proteasome activity	73
4.3 Potential role of bsn in the assembly of 20S proteasomes	77
4.4 Increased proteasome activity contributes to the deregulation of synaptic vesicle pool sizes observed in bassoon knockout animals	79
5. Bibliography	83
6. Abbreviations	90
7. Scientific publications	95

1. Introduction

Proteostasis constitutes groundwork for the development and maintenance of a healthy organism. In order to ensure proper cellular functions and to prevent any disease from occurring protein balance has to be strictly guarded but at the same time highly dynamic to allow for the adaptation to ever-changing environment. Whereas protein biogenesis has been extensively studied, the concept of protein degradation has not been widely acknowledged and has long received only scarce attention. It has been rather believed that proteins function as stable entities. However, this view was challenged by Rudolf Scheonheimer who, by using radiolabeling experiments, showed that proteins are in a state of flux, constantly undergoing multiple rounds of synthesis and degradation (Ciechanover, 2005).

The first one to shed light on proteolysis was a Belgian scientist Christian de Duve who discovered a lysosome (De Duve et al., 1955). The lysosome is a membrane-bound organelle containing hydrolytic enzymes responsible for a breakdown of various biomolecules, including proteins. The discovery of the lysosome soundly implied that all proteins are subjected to degradation within this organelle. Nevertheless, it was hard to conceive how omnivorous lysosomal system can precisely regulate the fate of different proteins that are characterized by different lifespan and should undergo degradation at different time points and under changing pathophysiological conditions. This question was resolved with a finding of ubiquitin-proteasome system (UPS) by Avram Hershko, Aaron Ciechanover and Irwin Rose, who received a Nobel Prize for their discovery in 2004 (Ciechanover et al., 1980; Ciechanover, 2005).

1.1 Ubiquitin conjugating apparatus

UPS composes one of the biggest and most refined protein complexes in the cell. It is engaged in the regulation of a myriad of homeostatic functions, including transcription, cell cycle and differentiation, antigen presentation, apoptosis, signal transduction, receptor-mediated endocytosis, protein quality control and metabolism. The UPS is tailored to purge cells of misfolded, aggregated or no longer necessary proteins with a high temporal and spatial resolution. The system is energy dependent and uses ATP hydrolysis to fuel highly specific elimination of its substrates. In the center of the pathway stays a small, (76 amino acids) highly conserved protein called ubiquitin (Ub). Conjugation of ubiquitin molecules to the target protein is called ubiquitination and constitutes a commonly encountered

posttranslational modification that essentially acts as a death tag for the protein which is subsequently degraded. Recent evidence, however, indicates that ubiquitination is not only involved in protein degradation, but also plays a pivotal role in cellular signaling and communication, participating in kinase activation, receptor endocytosis, lysosomal degradation or vesicle trafficking (Herrmann et al., 2007; Chen and Sun, 2009).

Moreover, ubiquitination is a dynamic modification, that is reversed by the action of deubiquitinating enzymes (DUBs) (Glickman and Ciechanover, 2002; Shabek and Ciechanover, 2010).

Degradation of client proteins proceeds in two phases: 1) the substrate is tagged with the regulatory protein-ubiquitin and 2) the tagged protein is broken down by a large protease-26S proteasome. The specificity of the process is conferred by the members of the ubiquitination cascade which includes a cooperative action of three enzymes, namely Ub-activating enzyme (E1), Ub-conjugating enzyme (E2) and an Ub-protein ligase (E3). The cascade is typically initiated by E1 enzyme that activates ubiquitin moiety in an energy dependent manner to produce high-energy thiolester bond between catalytic cysteine of E1 and terminal glycine (G76) of ubiquitin. The activated ubiquitin moiety is next transferred to E2 which generates another thiolester lineage with G76 of ubiquitin. In the last step, ubiquitin is accepted by the E3 ligase, the enzyme that catalyzes a covalent attachment of ubiquitin moieties to lysines within the substrate (Figure 1). More specifically, Ub molecule is added via its C-terminal glycine to an ϵ -amine group of a lysine residue of a client protein to produce an isopeptide bond. Interestingly, it has been recently discovered that Ub might also be conjugated to the N-terminal residue of the protein to create a linear linkage or to threonine, serine or cysteine to create an ester or thiolester bond. In the course of the successive reactions, multiple Ub molecules become conjugated to the internal lysine 48 of the previously added Ub; however any of the 7 lysine residues present in ubiquitin can be used for the creation of the isopeptide bond. This process termed polyubiquitination generates polymerized ubiquitin chain (polyUb) that forms the basis for the recognition and degradation by the proteasome (Glickman and Ciechanover, 2002; Shabek and Ciechanover, 2010).

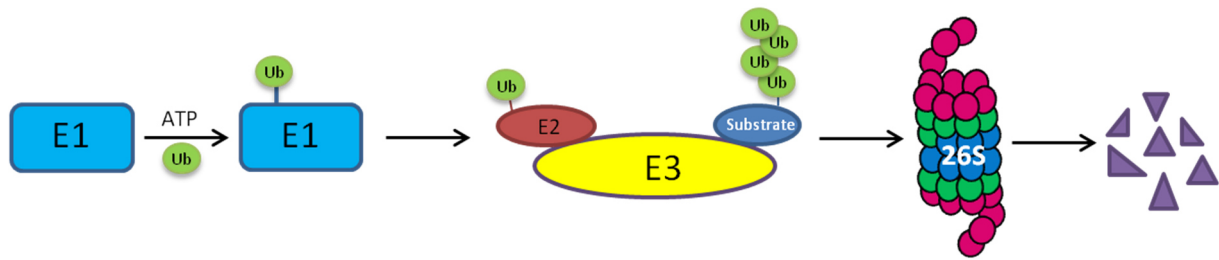


Figure 1. Schematic representation of the ubiquitin-proteasome system. Through a concerted action of three enzymes: E1, E2 and E3 the substrate to be disposed is tagged with ubiquitin moieties. This polyubiquitin chain serves as a signal for the proteasome and in the following step protein is degraded.

1.2 The proteasome

Proteasome is a large, multisubunit, catalytically active complex, present throughout all three domains of life: archaea, bacteria and eukarya. Evolutionary conservation of the proteasome highlights its major role in the cells. In bacteria two types of proteasomes have been identified: the first one- HsIV and its homologues, are related to proteasomal subunits and assemble into a simpler form consisting of two hexameric rings harbouring proteolytic activity, flanked by an ATP-ase of the Clp family. This complex is detected, for example, in *Escherichia coli*. Second type of proteasome-like complex is found in Actinomycetales including *Mycobacterium* and *Rhodococcus* and is a four ring structure capped by regulatory particle and practically identical to eukaryotic and archaeal proteasomes in the overall architecture (Murata et al., 2009).

Proteasomes are involved in the degradation of numerous proteins inhabiting different cellular compartments; therefore they are defined as molecular devices capable of a spatio-temporally controlled substrate catabolism. They can be found in both nucleus and cytoplasm (Wojcik et al., 2000b, a) in addition, proteasomes can also associate with endoplasmatic reticulum (ER) membranes and cytoskeletal elements (Klare et al., 2007).

1.2.1 Anatomy of the 20S proteasome

26S proteasome is comprised of two subcomplexes: the catalytic core particle (CP, also called 20S proteasome) of roughly 700kDa, capped at one or both sides by a regulatory particle (RP, 19S proteasome) of approximately 700kDa. 20S proteasome, whose name derives from the sedimentation constant, constitutes catalytical part of the 26S complex which is responsible for ATP-dependent, non-lysosomal breakdown of polyubiquitinated proteins. 20S proteasome resembles a hollow barrel-like structure and is comprised of four axially stacked heteroheptameric rings (Tomko and Hochstrasser, 2013). In eukaryotes the outer rings are built of seven distinct α subunits, whereas the inner rings are composed of seven distinct β subunits arranged in $\alpha_{1-7}\beta_{1-7}\alpha_{1-7}\beta_{1-7}$ complex (Murata et al., 2009; Jung and Grune, 2012).

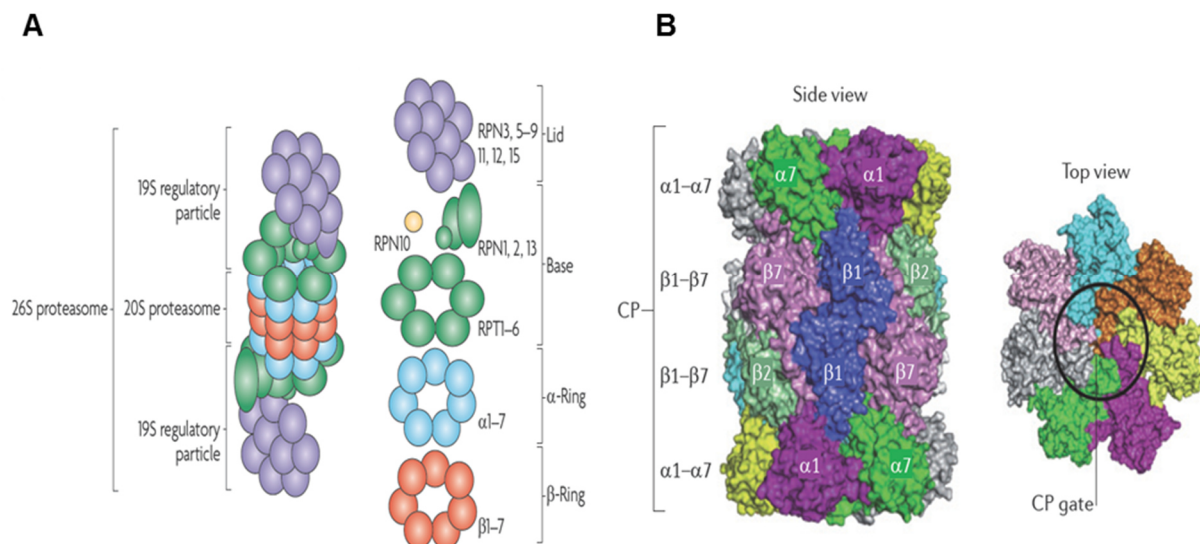


Figure 2. Basic structure of the proteasome. a) 26S proteasome is composed of two outer α -rings and two inner β -rings capped by 19S regulatory particle which can be further subdivided into the base and the lid. b) side and top view of the yeast 20S from the X-ray structure analysis. Modified from: (Murata et al., 2009; Maupin-Furlow, 2011) .

1.2.1.1 β -ring

Two adjacent β rings form a catalytic cavity, which harbours six proteolytic sites- three per each β ring. These proteolytic sites are buried within the inner chamber of the proteasome in order to prevent reckless degradation of the folded proteins. Proteasomes belong to the family of N-terminal nucleophilic hydrolases (NTN hydrolases) and their catalytic activity is formed by N-terminus of β 1, β 2 and β 5 subunits, which are associated with caspase-like, trypsin-like

and chymotrypsin-like activities, respectively. Crystal-structure analysis revealed that N-terminal threonine (Thr1) residue plays a crucial role in the catalysis and its substitution to serine results in a lower effectiveness of hydrolysis (Sorokin et al., 2009).

Further to the three principal proteolytic centers, two additional proteolytic activities have been proposed: 1) cleaving the peptide bonds after branched chain amino acid residues (BrAAP; branched chain amino acid peptidase) and 2) cleaving the peptide bonds after small neutral amino acid residues (SNAPP; small neutral amino acid peptidase). The latter activity is supposedly located on $\beta 7$ subunit as inferred on the basis of mutagenesis analysis as well as inspection of the X-ray crystal structure of the bovine proteasomes (Unno et al., 2002; Jung and Grune, 2012).

1.2.1.2 α -ring

The entry to the catalytic chamber of the proteasome is preceded by two antechambers made collectively by one α and one β ring on either side. Essentially, α subunits are responsible for a formation of a gated channel that supervises the transfer of the substrate proteins into the proteolytic cavity. In order for the client protein to access this cavity and subsequently undergo degradation, N-terminal regions of α subunits must be subjected to conformational changes (Jung and Grune, 2012). The most prominent role in the channel formation is ascribed to $\alpha 2$, $\alpha 3$ and $\alpha 4$ subunit, which mechanistically occlude the entrance to the catalytic center (Sorokin et al., 2009; Jung and Grune, 2012).

The opening of the gate can be also aided by docking of the regulatory particle onto 20S proteasome. These regulatory particles contain HbYX (hydrophobic-tyrosine-X) motives at their C-terminus that insert in the pockets created by α rings. The insertion displaces the α -ring N-terminal chains from the CP and unplugs the substrate entry pore (Jung and Grune, 2012; Wani et al., 2015).

1.2.2 Anatomy of the 19S regulatory particle

Enzymatically active proteasome is flanked on one or both sides by 19S regulatory particle. This complex has multitude functions: it binds polyubiquitinated proteins, performs deubiquitination as well as substrate unfolding, it also helps to thread client protein into the hydrolytic chamber and last but not least it participates in the gate opening and thus activation of the latent 20S proteasome. 19S consists of approximately 19 subunits, divided into two

classes: regulatory particle of triple ATPase (Rpt) subunits and regulatory particle of non-ATPase (Rpn) subunits. RP is made up of two subcomplexes: the lid and the base (Sorokin et al., 2009).

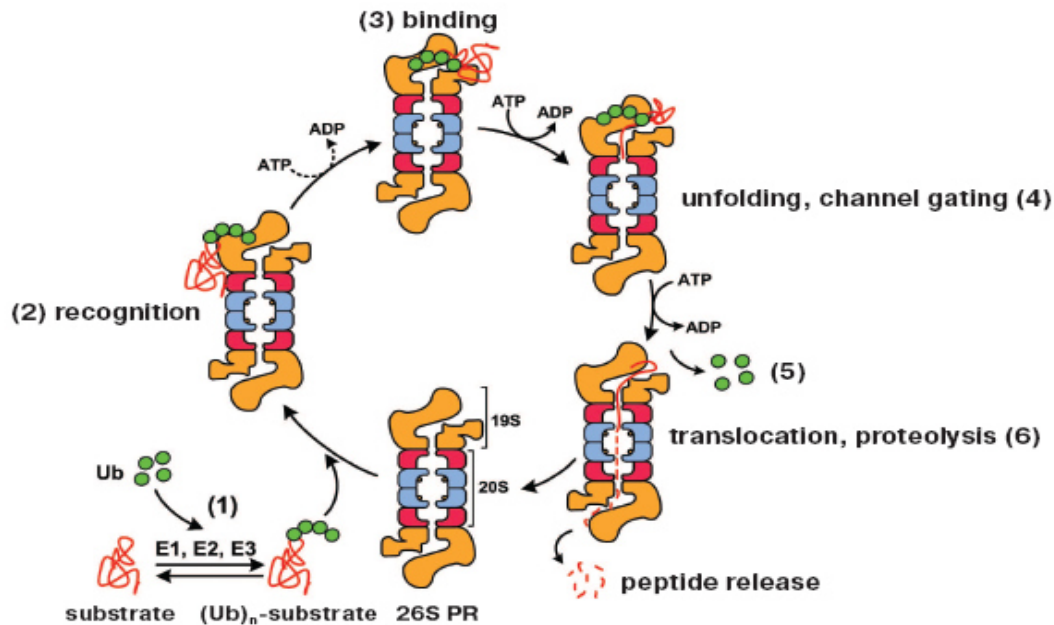


Figure 3. Simplified scheme of the ubiquitin-proteasome pathway. 1) Ubiquitination of the target protein is a stepwise process and requires consecutive action of three enzymes: E1, E2 and E3. 2) Polyubiquitin chain is recognized by the Ub receptors in the lid complex. 3) The substrate is bound atop regulatory particle. 4) Protein is unfolded. 5) The substrate is deubiquitinated. 6) and translocated into the proteolytic chamber of the 20S proteasome (Adapted from: (Sorokin et al., 2009).

The base is formed by six ATPases of the AAA+ superfamily Rpt (Rpt1-6) and four Rpn subunits (Rpn1, Rpn2, Rpn10, Rpn13). Rpt subunits form a hexameric ring that sits directly atop 20S proteasome. This ATPase ring catalyzes energy-dependent unfolding of proteins, a process indispensable for their translocation into the 20S CP. This step is of critical importance as the catalytic core of the proteasome is too narrow to fit proteins with a developed tertiary conformation. Rpn10 and Rpn13 function as intrinsic ubiquitin receptors—they are equipped with the sequences that recognize and bind polyubiquitinated proteins. Furthermore, there are other external UBL-UBA (ubiquitin-like-ubiquitin-associated) ubiquitin receptors that bind polyubiquitinated molecules via their UBA domain and shuttle proteins for degradation via interaction through UBL domain with proteasomal Rpn1 subunit. Rpn1 and Rpn2 are believed to have a role in non-specific binding of the substrate, thereby retaining it on the proteasome (Tanaka, 2009; Tomko and Hochstrasser, 2013).

The lid subcomplex associates laterally with the base-CP structure. It consists of nine Rpn subunits: Rpn3, 5-9, 11, 12 and 15. Up till now the most significant role is ascribed to Rpn11, which is involved in release of Ub conjugated to the substrate. Rpn11 is *de facto* a deubiquitinating enzyme hydrolyzing the polyubiquitin chain at a proximal site. There are also other DUBs, like Usp14 and Uch37, loosely associated with the proteasome that process ubiquitin molecules at a distal site.

A biogenesis of 19S is an extremely complicated process assisted by many auxiliary proteins, which only recently began to be deeply investigated (Tanaka, 2009; Jung and Grune, 2012; Tomko and Hochstrasser, 2013).

1.3 Tissue specific forms of the proteasome

In mammals, proteasome system has developed substantial variety among the catalytic subunits-four additional catalytic β subunits have been found. $\beta 1$, $\beta 2$ and $\beta 5$ in the constitutive proteasome are replaced by $\beta 1i$, $\beta 2i$ and $\beta 5i$ with the formation of so called immunoproteasome. The generation of this type of proteasome is aided by IFN- γ stimulation and requires de novo proteasome biogenesis (Jung and Grune, 2012). Immunoproteasome has higher trypsin-like and chymotrypsin-like activities in comparison to the constitutive one and plays a pivotal role in immune response. Exchange of the subunits also renders it more eligible for processing of antigenic peptides that will be later displayed in the context of major histocompatibility complex (MHC) class I molecules. Underscoring importance of immunoproteasomes, investigation of the mouse strain deficient for $\beta 1i$, $\beta 2i$ and $\beta 5i$ revealed that these animals exhibit abnormal antigen processing followed by compromised immunological response (Tanaka, 2009).

Thymoproteasome represents yet another subtype of the proteasome, which can be found in cortical thalamic epithelial cells (cTEC) in the thymus. Thymoproteasomes participate in the positive selection of developing thymocytes, hence they are involved in maturation process as well as acquirement of the immunocompetence by T-cells. In contrast to immunoproteasomes, where chymotrypsin-like activity is boosted, thymoproteasomes are characterized by a substantial drop in this activity without changes in trypsin-like and caspase-like activities. This activity alternation is conceivable as thymoproteasomes incorporate another type of $\beta 5$ subunit, namely $\beta 5t$ subunit, specific exclusively for the proteasomes residing in the thymus, along with $\beta 1i$, $\beta 2i$. Emergence of alternative subunits is said to arise as a result of tandem duplication of the genes encoding constitutive subunits (Tanaka, 2009). Intermediate

proteasomes containing, for instance, two types of immune subunit and one type of constitutive subunit have also been discovered, however their role requires further elucidation. Moreover, *Tanaka et al.* reported existence of a mammalian testis-specific proteasome that incorporates $\alpha 8$ subunit instead of $\alpha 4$ (Tanaka, 2009).

In addition to the diversity of the catalytic subunits in the 20S CP, other types of regulatory particles that cap 20S proteasome exists that confer different properties upon the proteolytic machinery. They include PA28 also called 11S regulator (REG), which can be further subdivided into two forms: PA28 $\alpha\beta$ and PA28 γ , as well as PA200.

PA28 $\alpha\beta$ is built up of seven α and seven β subunits and forms ring shaped complex. It is mainly found in the cytoplasm. Cellular abundance of PA28 is upregulated in response to IFN- γ , thereby this structure can play essential role in the adaptive immunity, abutting immunoproteasomes. PA28 γ is largely detected in the nucleus, where it performs various functions, including modulation of cell proliferation and body growth in mice, as well as guidance over centrosomes and chromosomal stability (Tanaka, 2009).

20S proteasomes can be capped by more than one type of regulatory particle, which leads formation of so called hybrid proteasomes. This structure is a result of a simultaneous binding of two different activators, creating, for example, 19S-20S-PA28 variant. Expression and incorporation of PA28 into 19S-20S is markedly enhanced by IFN- γ , which again suggest a prominent role in the generation of MHC class I related antigens. Furthermore, hybrid proteasomes increase processing of small peptides and create distinct pattern of peptides then 26S proteasome (Tanaka, 2009).

1.4 Molecular mechanisms controlling proteasome assembly

Assembly of 20S proteasome requires an orchestrated set of steps in order to ensure correct positioning of α and β subunits within the complex. As proteasome biogenesis is a fairly elaborate process, consisting of many stages and producing different intermediate species, it comes as no surprise that the assembly is supported by an array of dedicated chaperon proteins. First, an α -ring is generated which will then serve as a platform for subsequent incorporation of β subunits, prompting precursor complex formation. Dimerization of these precursors is triggered by $\beta 7$ subunit integration.

1.4.1 α -ring formation

The assembly of the proteasome starts with formation of α rings. This assumption was inferred on the basis of experiments carried out in *E. coli*, where expression of α subunits from archaeobacteria *Thermoplasma acidophilum* was enough in order to produce double homoheptameric ring structures without apparent participation of any auxiliary proteins. β subunits alone, however, were unable to self-assemble into ring structures, which indicates that α -ring forms a scaffold to which β subunits are recruited. The assembly of eukaryotic α rings is far more complex, mainly because each of seven distinct α subunits occupies strictly defined position in the α -ring (Ramos and Dohmen, 2008; Murata et al., 2009; Matias et al., 2010). Consistently, auxiliary proteins have been discovered that help to correctly orientate α subunits into the ring structures. PAC1 and PAC2 (proteasome assembly chaperones) are two accessory proteins that interact with α subunits and thereby stimulate production of α -ring structures. Deletion of PAC1 or PAC2 in human cells results in the accumulation of α -ring dimers and off- pathway intermediate species. This reveals that PAC1- PAC2, in addition to the initiating role in α -ring assembly, also act to prevent dimerization of the α rings and thus creation of any aberrant products that could hamper the biogenesis of the functional 20S proteasomes (Hirano et al., 2005; Tanaka, 2009; Matias et al., 2010). Treatment with a proteasome inhibitor-MG132 stabilizes PAC1-PAC2 dimer that concentrates in the fractions with fully assembled 20S, unveiling that these proteins remain bound to the proteasome intermediates until the end of the assembly process and are degraded by the newly formed mature proteasome (Hirano et al., 2005; Ramos and Dohmen, 2008). Furthermore, structural analysis indicates that PAC1-2 possess HbYX motif at their C-terminus which binds α rings and impedes premature association of RP with CP (Sasaki et al., 2010; Stadtmueller et al., 2012; Kock et al., 2015; Wani et al., 2015)

Studies carried out in a mammalian line of HEK293T cells reveal existence of another chaperone pair, namely PAC3-PAC4. PAC3-PAC4 bind to $\alpha 5$ and interact with its neighboring $\alpha 4$ and $\alpha 6$ subunits. This complex might play essential role in the initiation of the α -ring formation and allegedly partake in the correct positioning of the last α subunits- $\alpha 3$ and $\alpha 4$ (Rosenzweig and Glickman, 2008). The dimer is found on the inner surface of the emerging α -ring. This position would be conflicting with binding of one of the β subunits- namely $\beta 4$ on the top of $\alpha 3$ and $\alpha 4$, therefore PAC3-PAC4 dissociates from the precursor complexes upon $\beta 4$ incorporation, which is in agreement with the finding that these chaperon proteins are not present in the later proteasome assembly species (Ramos and Dohmen, 2008).

Interaction of PAC3-PAC4 with the two first added β subunits- $\beta 2$ and $\beta 3$ raises the possibility that this dimer could participate in the initiation of the incorporation of β subunits onto α rings (Hirano et al., 2006). Noteworthy, PAC3-PAC4 bears structural similarity to β subunits, what might clarify their common anchoring site on the α rings (Tanaka, 2009). Knockdown of PAC3 in human cells mitigates α -ring production, moreover these cells show decreased proteasome activity as well as increased accumulation of polyubiquitinated species. In the triple knockdown of PAC1/2/3 even more significant downregulation of the proteasomal activity is observed in comparison to PAC3 or PAC1/2 depleted cells, and the same phenomenon is noticed for the upregulation of polyubiquitinated proteins (Hirano et al., 2006). Furthermore, PAC3 knockdown does not cause accumulation of α dimers as in the case of PAC1/2 deficient cells, and the ectopic expression of PAC3 in the PAC1/2 knockdown background does not rescue this phenotype, speaking for a distinct role of this chaperons in α -ring formation and implying an additive effect of the knockdowns (Hirano et al., 2006; Ramos and Dohmen, 2008). Kusmierczyk *et al.* showed that yeast strains deficient in Pba3-Pba4 (yeast ortholog of human PAC3-PAC4) forge alternative proteasomes that contain two copies of $\alpha 4$ in one α -ring (Kusmierczyk et al., 2008). These proteasomes are deprived of $\alpha 3$, the crucial gating subunit, and therefore they are constitutively open. Cells harboring this alternative proteasomes show increased resistance to stress conditions, including tolerance to heavy metal and oxidative stress (Velichutina et al., 2004; Kusmierczyk et al., 2008; Rosenzweig and Glickman, 2008).

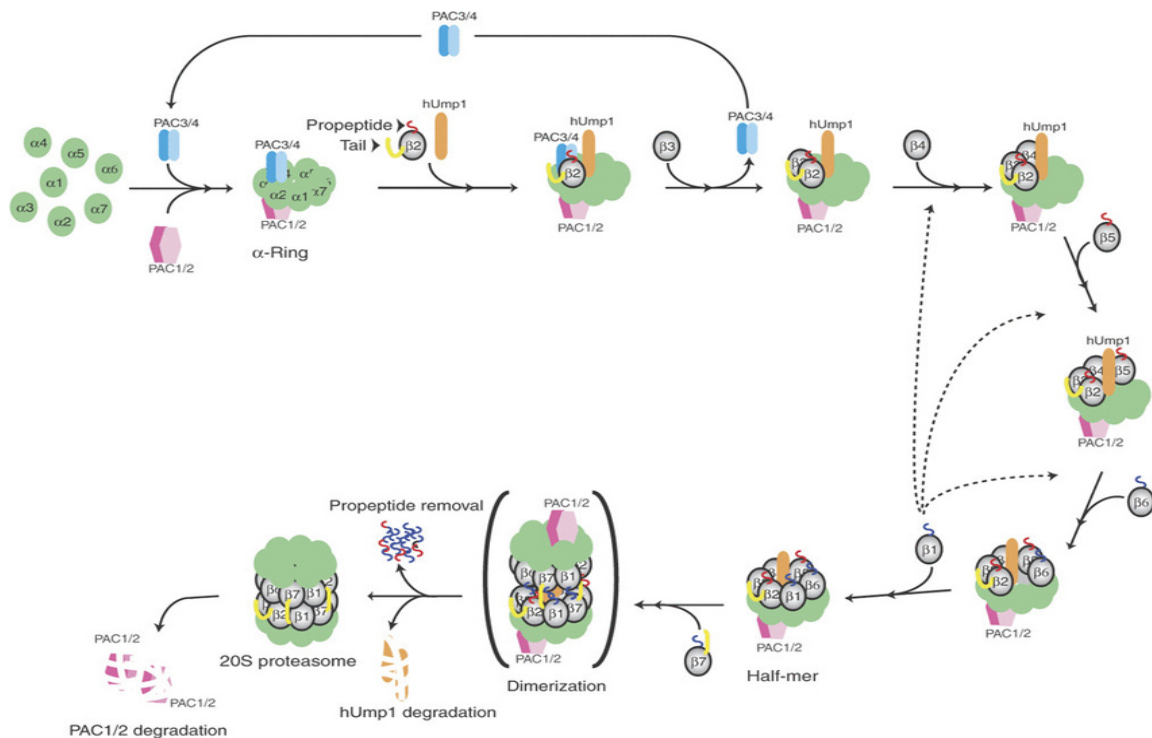


Figure 4. A model of 20S proteasome assembly. α -ring assembly is assisted by two pairs of the heterodimeric proteins: PAC1-PAC2 and PAC3-PAC4. After completion of α -ring formation, β subunits are added in a defined order, starting with $\beta 2$. Incorporation of this subunit is coupled with hUmp1 recruitment which initiates the assembly of β -ring. This is followed by the sequential association of $\beta 3$, $\beta 4$, $\beta 5$, $\beta 6$ and $\beta 1$ (which supposedly can be incorporated at any other step marked by the dotted line). In the final stage the C-terminus of $\beta 7$ subunit brings two half-proteasomes together, chaperons hUmp1 and PAC1-PAC2 are degraded, while propeptides of $\beta 2$, $\beta 5$, $\beta 6$, $\beta 7$ subunits are cleaved- the biogenesis of 20S proteasome is completed. Adopted from: (Hirano et al., 2008).

1.4.2 β -ring assembly

Once α -ring is completed, it will serve as a platform for β subunits incorporation, which proceeds in a strictly controlled and guided fashion. Five out of seven β subunits, including catalytic subunits $\beta 1$, $\beta 2$ and $\beta 5$ as well as non-catalytic $\beta 6$ and $\beta 7$ are synthesized with N-terminal propeptide sequences that either protect catalytic centres of β subunits from acetylation, and thus inactivation, or aid in the productive incorporation of other β subunits. At the end of the assembly process the N-terminal propeptides are cleaved to produce mature and proteolytically competent 20S proteasomes. The cleavage is an autocatalytic process that reveals catalytic Thr1 residue of the active subunits, a residue critical for functionality of proteolytic centers (Chen and Hochstrasser, 1996; Murata et al., 2009; Gallastegui and Groll, 2010).

Progressive addition of β subunits to α rings results in the production of proteasome precursors, first of them- an intermediate complex of 13S, comprised of one α -ring as well as

unprocessed $\beta 2$, $\beta 3$ and $\beta 4$ subunits has been described in both yeast and mammal. Additionally, half-mers ($-\beta 7$) consisting of α -ring and all β subunits with an exception of $\beta 7$ has been identified (Murata et al., 2009). β -ring formation and half-proteasome biogenesis progress stepwise and are accompanied by extrinsic as well as intrinsic chaperon proteins.

Ump (ubiquitin mediated proteolysis) has been characterized in yeast strains faulty for ubiquitin mediated proteolysis. It is also the first discovered extrinsic accessory protein of 20S proteasome assembly pathway (Ramos and Dohmen, 2008; Tanaka, 2009; Sa-Moura et al., 2013). Its human ortholog, hUMP1 (also termed proteasemblin or POMP) is present in the precursor species comprising α rings and unprocessed β subunits and is degraded upon termination of the proteasome biogenesis, similarly to PAC1-PAC2 (Burri et al., 2000; Ramos and Dohmen, 2008). siRNA mediated knockdown analysis in HEK293T cells, unveiled an essential role of hUMP1 in promoting β -ring formation, namely that hUMP1 is able to attach to α -ring devoid of any β subunit, and its incorporation is coupled with $\beta 2$ recruitment (Hirano et al., 2008). Besides external auxiliary factors, N-terminal propeptides and C-terminal extensions of some of the β subunits function as intramolecular chaperons facilitating 20S proteasome assembly. In human cells, the leader sequence of $\beta 5$ is required for $\beta 6$ integration. Also, propeptide sequence as well as C-terminal tail of $\beta 2$ subunit that winds around $\beta 3$ subunit are of particular significance as their deletion causes failure of $\beta 3$ incorporation and is thus fatal (Hirano et al., 2008; Ramos and Dohmen, 2008; Murata et al., 2009).

1.4.3 Dimerization of the half-proteasomes

The last and simultaneously rate limiting step in the proteasome assembly is the incorporation of $\beta 7$ subunit. This subunit has a unique C-terminal extension, localized on the outer surface of β -rings that is engaged in the interactions not only within but also across β rings. The C-terminal tail of $\beta 7$ intercalates into a groove between $\beta 1$ and $\beta 2$ on the opposite ring, thereby bringing two half-proteasomes together and stabilizing newly formed 20S. It also contributes to the maturation of $\beta 1$ active site. Dimerization of two half-mers is followed by the cleavage of N-terminal propeptide sequences of β subunits, accompanied by hUMP1 and PAC1-PAC2 degradation (Murata et al., 2009). The assembly process of 20S proteasome is completed and in the next stage 20S proteasome will be flanked by regulatory particle creating fully competent 26S machine ready to destroy incoming proteins.

1.5 The role of the ubiquitin-proteasome system in the brain

Primary, the interest in the UPS function in the brain started with a discovery of its notorious role in the neurodegenerative diseases. Myriad publications implied a massive accumulation of polyubiquitinated proteinaceous inclusions as well as modulation of the proteasomal activity. This encompasses, but is not restricted to neurofibrillary tangles in Alzheimer's disease, Pick bodies in Pick's disease, intracellular deposits of huntingtin in Huntington's disorder and Lewy bodies in Parkinson's disease (Yi and Ehlers, 2007). On the other hand, more recent reports have divulged a paramount task of UPS in the neuronal development and survival, synaptic function and plasticity as well as memory formation.

Neurons are intricate and highly specialized brain cells and their unique morphology, with an axon reaching up to few meters in length and extremely elaborate dendritic arborizations, imposes certain challenges and restrictions upon cellular degradation machinery. First and foremost, neuronal proteolysis should be locally confined in order to achieve high specificity and avoid any collateral damage. This is accomplished by restricting UPS components to defined compartments, like pre- and postsynaptic zones. Additionally, posttranslational modifications including phosphorylation render protein substrates as well as ubiquitin ligases more vulnerable to subsequent ubiquitination. The activity of the proteasome has also been showed to be differentially regulated depending on the neuronal compartment (Tai and Schuman, 2008). However, before we delve into neuronal protein degradation, it will be helpful to provide a brief description of the general architecture and plasticity of a neuronal synapse.

1.6 The architecture of the chemical synapses

A synapse is defined as a connection between two neurons, where communication process and information processing takes place. The typical chemical synapse consists of a presynaptic releasing part precisely aligned with a postsynaptic receiving compartment, separated by a narrow gap of around 20 nm called synaptic cleft. At these specialized chemical synapses efficient transmission is achieved by quantal release of neurotransmitter, stored in the synaptic vesicles (SV), in response to the action potential-driven increase of intracellular calcium (Sudhof, 2004). Subsequently, this neurotransmitter binds to the receptors present on the membrane of the postsynaptic neuron.

Exocytosis of SV, a process where synaptic vesicles fuse with the presynaptic membrane, occurs at the specialized domains of the presynaptic compartment, an active zone (AZ). The active zone is formed by the presynaptic membrane and a proteinaceous electron-dense lattice, the cytomatrix at the AZ (CAZ). Molecular constituents of the CAZ include two large homologous proteins piccolo (pclo) and bassoon (bsn), Rab3-interacting molecules (RIMs), RIM-binding protein (RBP), ELKS, cytomatrix at the active zone associated structural protein (CAST), α -liprins and Munch-13 (Gundelfinger and Fejtova, 2012). All these proteins participate in a functional as well as spatiotemporal orchestration of the neurotransmitter release.

1.6.1 Bassoon as an example of the prominent active zone protein

Bsn is a large, scaffolding protein and as a multidomain molecule it is involved in many interactions, which contribute to the numerous functions of the presynaptic compartment (Gundelfinger and Fejtova, 2012; Gundelfinger et al., 2015). Bsn participates in the assembly process of the AZs and together with pclo is the first protein to arrive at the sites of synapse establishment. Bsn, pclo and CAST form vesicle transport (PTV) structures that are delivered to nascent synapses, where their deposition together with other vesicles containing presynaptic material initiates AZ formation in response to transsynaptic signals (Fejtova and Gundelfinger, 2006; Gundelfinger et al., 2015). Latest reports also assert the role of bsn in the clustering of the presynaptic voltage gated calcium channels, specifically P/Q calcium channels. Here, via interaction with RBP, bsn positions P/Q-type channels in the vicinity of SV release sites at the hippocampal synapses, thus enabling rapid response to incoming action potential (Davydova et al., 2014). What is interesting, upon partial knockout of bsn (Bsn Δ Ex4/5), conventional central synapses show only mild disturbances in neurotransmitter release. However, in retina the same mutation revealed the importance of bsn in the anchoring of synaptic ribbons to the presynaptic zone, as in bsn deficient synapses, ribbons are floating freely in the cytoplasm, which leads to the impairment of synaptic transmission (Altrock et al., 2003; Dick et al., 2003). Severe morphological and functional alternations are also detected at another sensory synapse, namely cochlear inner hair cell synapse, where partial knockout of bsn prompts decrease in the number of readily releasable vesicles as well as impairment in the rate of their replenishment together with disassociation of synaptic ribbons from release sites (Khimich et al., 2005). Moreover, complete bassoon deficiency (Bsn^{-/-} knockout of the whole gene) results in the augmentation of short-term synaptic depression at

cerebellar mossy fiber to granule cell synapses as well as faulty vesicle reloading (Hallermann et al., 2010). Compellingly, bsn is also involved in the maintenance of the synaptic integrity (Waites et al., 2013), what is described in the great detail in the section 1.12.

1.7 The Synaptic vesicle cycle

As mentioned above neurotransmitter in the presynapse is kept in the synaptic vesicles. SVs are virtually implicated in the entire array of presynaptic functions. In order to maintain continuous rounds of neurotransmitter release, synaptic vesicles are subjected to the trafficking cycle, which can be grouped into several successive stages. It starts with the loading of the SVs with the neurotransmitter through an electrochemical gradient-mediated active transport of the neurotransmitter into the SVs. In the next step, SVs are clustered at the AZ, which is followed by association of SVs with the plasma membrane termed docking and acquisition of the fusion competence in a priming process. Docked and primed vesicles are prepared for fusion with presynaptic membrane upon increase in the intracellular calcium levels triggered by the incoming action potential. Subsequently, SVs undergo endocytosis, where they are retrieved and recycled back in the presynaptic terminal (Sudhof, 2004).

1.7.1 Synaptic vesicle pools

Synaptic vesicles in the presynaptic terminal are divided into three functionally distinctive pools: readily releasable pool (RRP), recycling pool (RP) and resting pool (RtP). RRP consists of the vesicles that are docked at the AZ and primed for release upon incoming action potential (Rizzoli and Betz, 2005). This group of vesicles is characterized by the highest release probability. The size of the RRP at the typical hippocampal synapse was evaluated to amount to 5-10 vesicles; however this might greatly differ between individual synapses and has been found to be dependent upon bouton volume and AZ area (Welzel et al., 2011). Repetitive frequency stimulation rapidly depletes RRP, which is subsequently refilled by vesicles from RP. It has been shown that depletion of readily recycling pool underscores short term depression (STD) of synaptic transmission. The rate of RRP exhaustion and its consequent replenishment regulate the rate and the time span of STD and thereby the synaptic strength and neuronal network function (Blitz et al., 2004; Rizzoli and Betz, 2005; Guo et al., 2015). Prolonged and physiological stimulation mobilizes vesicles from RP, which do not

reside in the close proximity of the active zone and therefore do not partake in the fast synaptic transmission. This pool is believed to contain about 5-20% of all vesicles.

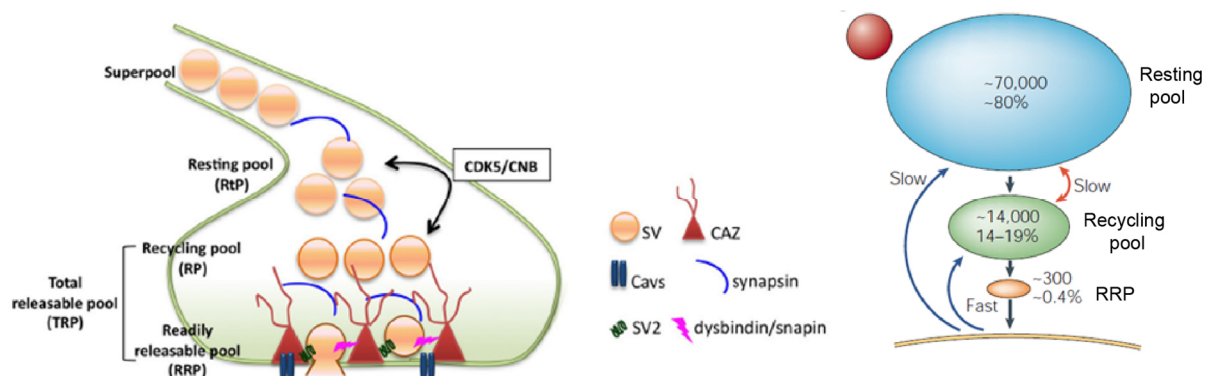


Figure 5. Scheme of the presynaptic bouton comprising distinct synaptic vesicles pools. Presynaptic vesicles that can be ascribed to three major pools: readily releasable pool, recycling pool that together make total recycling pool, resting pool and a rapidly transiting superpool. The figure on the right depicts the pool sizes at a rough estimate of rat cultured hippocampal neurons (Modified from: (Rizzoli and Betz, 2005; Lazarevic et al., 2013)).

Mixing between RRP and RP is fairly quick and vesicles from both pools seem to be rapidly recovered by endocytosis. The resting pool comprises vesicles that are reluctant to undergo exocytosis and their release occurs only in response to intense stimulation. These vesicles represent the majority of the vesicles present at the presynaptic terminal (~80%) and they are typically localized away from the AZ and allegedly clustered together with the help of synapsin I and actin (Rizzoli and Betz, 2005). It has also been proposed that this pool might contribute to the “super pool”-an array of vesicles dynamically exchanged between neighbouring synapses (Fernandez-Alfonso and Ryan, 2008).

1.8 Hebbain and Homeostatic plasticity

Chemical synapses are not static units. They constatly tune efficacy of information processing, that is, they go through the process of synaptic plasticity, which is defined as the capability of synapses to undergo strengthening or weakening, gradually with time following changes (reinforcement or drop) in their activity. Synaptic plasticity can be subdivided into short-term plasticity, that lasts from seconds to minutes and relies on the alternations in the neurotransmitter release as well as modulation of the postsynaptic receptors and preexisting proteins and long term synaptic plasticity (Kandel and Schwartz, 1982; Blitz et al., 2004). Long term synaptic plasticity, on the other hand, produces long-lasting effects that can persist

from several hours up to the lifetime and is believed to underscore learning and memory formation. This Hebbian form of durable synaptic plasticity can be broken down into two components: long term potentiation (LTP) and long term depression (LTD). However, unrestrained and uncontrolled synaptic strengthening or weakening can lead to hyperexcitability or synaptic elimination, respectively. In order to prevent this pathological processes a counteracting force, termed homeostatic plasticity must enter. Homeostatic plasticity works as a negative feedback mechanism to “stabilise” neuronal circuits and maintain adequate levels of synaptic transmission (Vitureira and Goda, 2013).

1.9 Role of the UPS in the synaptic plasticity: the case of Aplysia

One of the first experiments highlighting the role of proteolysis in the synaptic plasticity was carried out in *Aplysia*, a sea slug, and investigated biochemical basis of long-term facilitation (LTF), a simpler form of long term potentiation (LTP) in higher animals (Greenberg et al., 1987; Hegde et al., 1993). LTF is initiated by release of neurotransmitter serotonin which triggers activation of cAMP signaling pathways. Upregulation of cAMP induces a downstream kinase PKA (protein kinase A), persistent activation of which is indispensable for LTF expression. PKA is comprised of the regulatory and the catalytic subunits and the enzyme is inactive when both subunits are associated. cAMP binding to the regulatory subunit liberates the catalytic subunit of the enzyme, which translocates to the nucleus. Once in the nucleus, it phosphorylates and thus activates a transcription factor CREB (cAMP-response-element-binding protein) inducing immediate-early genes expression (Hegde et al., 1993; Tai and Schuman, 2008) that will eventually result in synaptic strengthening. One of the immediate-early genes includes Ap-Uch (*Aplysia* ubiquitin C-terminal hydrolase) a deubiquitinating enzyme that interacts with the proteasome and boosts proteolysis by recycling monomeric ubiquitin. This enzyme contributes to the proteasomal degradation of PKA regulatory subunit and therefore allows for persistent activation of the catalytic subunit and synaptic remodeling (Hegde et al., 1997; Chain et al., 1999).

1.10 Influence of the UPS on the mammalian synaptic plasticity

Ample evidence has also been amassed for a prominent role of the proteasome in the regulation of synaptic plasticity in mammals. Studies conducted by Dong *et al.* suggest that proteasome inhibitors distinctly influence induction and maintenance phases of the late long

term potentiation (L-LTP) (Dong et al., 2008). Inhibition of proteasomal activity has a potentiating effect on the early stages of L-LTP, due to the build-up of translational activators, like eIF4E and eEF1A (Dong et al., 2014). Conversely to the effect on early L-LTP, proteasome blockers, impede maintenance phase of L-LTP by promoting stabilization of transcriptional repressors, including CREB repressor ATF4 (Dong et al., 2008), as well as translational repressors, like polyadenylate-binding protein interacting protein 2 (Paip2) and 4E-BP2 (Dong et al., 2008; Dong et al., 2014). Moreover, recent studies suggest that manipulation of the proteasome activity considerably influences LTD. Application of DHPG (dihydroxyphenylglycine) triggers activation of group I metabotropic glutamate receptors (mGluR) and thus induction of mGluR-mediated LTD, which is significantly enhanced in the presence of proteasome inhibitors, whereas another type of chemical LTD, induced by NMDA treatment is insensitive to blockers of proteasomal degradation (Citri et al., 2009). Interestingly, another study reported that NMDA-dependent LTD robustly affects proteasome as it reduces its proteolytic capacity and promotes its disassembly (Tai et al., 2010).

In vivo studies also provide considerable evidence for the role of the proteasome in the regulation of long-term memory formation and retrieval. Specifically, fear conditioning leads to CAMKII-mediated increase in the phosphorylation of the proteasomal subunit Rpt6 what results in a substantial upregulation of the proteasome activity in the amygdala and local inhibition of the proteasome severely interferes with fear memory formation and stability (Jarome et al., 2011; Jarome et al., 2013). These findings highlight the importance of the proteasome in the synaptic plasticity and establish it as an essential regulator of long-term memory formation.

1.11 Proteasome at the post synapse

Long term synaptic plasticity engages both AMPA (AMPA) and NMDA (NMDAR) receptors. For the expression of LTP and strengthening of the synapse however, readily recycled AMPARs have to be efficiently inserted and stabilized at the synapse, what is ensured by a scaffolding protein PSD-95 (postsynaptic density protein) and its regulatory partner stargazin (Colledge et al., 2003; Vandenberghe et al., 2005). In this line, substantial number of studies reveal that postsynaptic receptors as well as structural and regulatory proteins are subjected to the control by the UPS. PSD-95 together with stargazin creates docking sites for AMPA receptors. Therefore, degradation of PSD-95 indirectly affects AMPARs, reducing their availability on the surface of the plasma membrane and weakening

synaptic strength (Colledge et al., 2003). Additionally, Lussier *et al.* demonstrated that AMPARs are prone to activity-dependent ubiquitination. They identified E3 ligase termed RNF167 that is responsible for the ubiquitination of AMPARs, which greatly decreases the amount of AMPARs on the synaptic surface (Lussier et al., 2012) and therefore contributes to the downregulation of synaptic transmission. RNF167 is not the only E3 ligase targeting AMPARs. Another protein, namely Nedd4-1 (Neural precursor cell expressed developmentally down-regulated protein 4) has been described to preferentially ubiquitinate AMPARs. Nedd4-1 catalyses polyubiquitination of AMPA receptors that are subsequently internalized and sent for degradation, this lowers the overall AMPAR cell surface location and induces suppression of synaptic transmission (Lin et al., 2011). Recent reports indicate that Nedd4-1 redistributes to dendritic spines upon AMPAR, but not NMDAR, stimulation. Interestingly, NMDAR activation antagonizes Nedd4-1-mediated polyubiquitination of AMPARs, promoting their deubiquitination by a DUB termed USP8. These two enzymes, thus, have an opposing effect on synaptic strength where decrease in USP8 favours Nedd4-1 recruitment and weakens synaptic strength, while activation of USP8 counteracts Nedd4-1 actions and contributes to upscaling of synaptic strength (Scudder et al., 2014).

Furthermore, several reports have shown that the levels of NMDARs are also tightly controlled by the UPS. Mind Bomb-2 (Mib2) E3 ligase associates and ubiquitinates GluN2B subunit of NMDARs in Fyn kinase-dependent fashion (Jurd et al., 2008), whereas ubiquitination of GluN1 subunit is mediated by Fbx2 E3 ligase in response to neuronal activity (Kato et al., 2005). More recent evidence demonstrates that NMDARs, notably GluN2B-containing receptors, regulate AMPAR trafficking by partaking in the docking of the synaptic proteasome. In the light of this, it has been shown that Glu2B deficient neurons substantially decrease both Glu2A as well as GluN1 clustering and are subsequently unable of homeostatic upregulation of NMDARs in response to chronic activity deprivation (Ferreira et al., 2015). Furthermore, AMPARs are also dramatically affected, specifically their surface and synaptic levels are markedly increased in GluN2B^{-/-} neurons together with the impairment of their endocytosis. Curiously enough, proteomic analysis of GluN2B^{-/-} neurons revealed a significant downregulation of some of the proteasomal subunits as well as upregulation of deubiquitinating enzymes, implying that UPS is changed in GluN2B^{-/-} neurons. The control of surface AMPAR levels seems to involve binding of CaMKII to GluN2B, since upregulation of AMPAR in GluN2B^{-/-} neurons was rescued by wild type GluN2B but not by GluN2B mutant unable to associate with CaMKII (Ferreira et al., 2015). The interplay between

CaMKII, synaptic plasticity and proteasome is further emphasized by Bingol *et al* who discovered that CaMKII is essential for the activity-mediated recruitment of proteasome to dendritic spines (Bingol and Schuman, 2006). Upon neuronal depolarization (induced by 1.5 min 60 mM KCl application) as well as NMDAR activation, proteasome redistributes from dendritic shafts to dendritic spines within minutes and this accumulation last for at least one hour. In this scenario, neuronal activation leads to the sequestration of the proteasome in spines mostly through a reduction of the spine exit rate. Interestingly, biochemical studies revealed that NMDA stimulation strengthened the association of the proteasome with actin cytoskeleton revealing mechanism for its dendritic spine confinement (Bingol and Schuman, 2006; Bingol *et al.*, 2010). Moreover, CaMKII can also stimulate proteasome activity by the phosphorylation of Ser120 on Rpt6 subunit of 19Sregulatory complex. This phosphorylation is crucial for modulating synaptic strength and further influences homeostatic scaling (Djakovic *et al.*, 2012).

1.12 UPS at the presynapse

Although much less investigated, the significance of UPS in the fine-tuning of presynaptic function becomes progressively appreciated. Any modifications of the presynaptic proteome by the UPS would affect the size of synaptic vesicle pools as well as vesicle release and therefore profoundly impinge upon short and/or long term synaptic plasticity. One of the key constituents of the AZ- RIM1 was found to be selectively polyubiquitinated and degraded by the proteasome. RIM1 has a prominent role in the neurotransmitter release by confining calcium channels to the active zone and participating in the priming of synaptic vesicles for exocytosis (Kaeser *et al.*, 2011). At the synaptic sites RIM1 binds E3 ligase SCRAPPER, which controls its levels by sending it for the proteasomal degradation, thereby collaterally contributing to the regulation of neurotransmitter release. It has been shown that in the SCRAPPER knockout (SCR-KO) hippocampal neurons the frequency of miniature excitatory post synaptic currents (mEPSC) is markedly increased, what can be rescued by RIM1 knockdown. Furthermore, SCR-KO mice also display apparent changes in the short term plasticity (Dobie and Craig, 2007; Yao *et al.*, 2007). Interestingly enough, UPS is engaged in the regulation of another paramount AZ molecule, namely Munc-13. This protein interacts with RIM and participates in the priming step by reading synaptic vesicles for release. Tada *et al.* describe a novel E3 ligase: Fbxo45 that targets Munc-13 for degradation thereby keeping neurotransmission in check (Tada *et al.*, 2010). These reports demonstrate that UPS functions

to shape synaptic transmission. Nonetheless, UPS itself can be subjected to the regulation by presynaptic proteins. Essentially, bsn and pclo limit presynaptic protein turnover by repressing the activity of the E3 ligase Siah1 (seven in absentia homolog) and therefore preventing synaptic loss. It has been found that in the neurons where bsn and pclo expression was knocked down there is a significant loss of the synaptic material, including SV proteins, SNAP-25 and synapsin. Elimination of these proteins leads to pronounced changes in the synaptic morphology with aberrantly elongated/enlarged SVs, upregulation of pleomorphic vesicles and disintegration of the postsynaptic density that develop over time (Waites et al., 2013). The loss of synaptic material is precluded when the double knock down (DKD) cultures are treated with proteasomal and ubiquitination inhibitors. Furthermore, bsn and pclo interact directly with a RING domain of Siah1, which is normally engaged in the interaction with E2 conjugation enzymes. Therefore, bsn and pclo seem to compete with E2 enzymes for binding to Siah1, acting as negative regulators of Siah1 action and consequently promoting synapse maintenance and integrity (Kononenko et al., 2013; Waites et al., 2013). Interestingly, recent report describes the role of bsn in the modulation of yet another surveillance system, namely autophagy (Okerlund et al., 2017). This indicates that not only UPS, but also other proteolytic pathways are controlled by bsn and that in the absence of this protein SVs catabolism is upregulated, which has serious repercussions for synaptic stability. UPS also regulates recycling of synaptic vesicles in hippocampal cultures. Experiments using FM styryl dyes (dye molecules penetrate synaptic vesicles, enable their visualization and study of synaptic vesicle recycling) reveal proteasome inhibitor-mediated increase of about 70% in the size of the total recycling vesicle pool. This increase is activity dependent as 15 min of heightened neuronal activity in the presence of the proteasome blocker is enough to trigger the same increase in the size of the total recycling pool as that seen by the application of the proteasome inhibitor alone. No changes in the kinetics of dye uptake or release were observed, suggesting that inhibition of the proteasome probably modulates synaptic vesicle pools and promotes recruitment of SVs from the resting pool into the total recycling pool. Thereby, proteasome can be defined as a presynaptic homeostatic regulator that keeps tight reins on neurotransmitter release during times of boosted activity (Willeumier et al., 2006). This goes in line with the finding that the block of the proteasome occludes induction of activity-dependent presynaptic silencing. Persistent presynaptic silencing, produced by 4 h elevation of extracellular K^+ , resulted in decreased EPSC amplitude as well as smaller size of RRP of SVs in hippocampal neurons. In addition, synaptic levels of Munc-13 and RIM1

proteins were substantially reduced (Jiang et al., 2010). Inhibition of the proteasome introduced together with the depolarizing challenge was able to prevent all these alternations and thus abolish induction of persistent presynaptic silencing. Compellingly, overexpression of RIM1 had similar effect, implying that UPS-mediated RIM1 degradation is of crucial importance for the induction of presynaptic muting (Jiang et al., 2010). Another study, conducted by Lazarevic *et al.*, indicated that global network activity silencing, induced by 48 h treatment with AMPAR and NMDARs antagonists, prompts molecular reshaping of the release machinery i.e. synaptic levels of bsn, pclo, Munc13-1, RIM1 and ELKS/CAST were considerably decreased in the silenced hippocampal cultures. Moreover, two of the vital CAZ proteins bsn and α -liprin were selectively targeted by UPS upon activity silencing, establishing the involvement of the proteasome in the modulation of the levels of the presynaptic scaffolds during activity depletion (Lazarevic et al., 2012). In contrast to the aforementioned long-term effects of proteasome blockage, short-term effects have also been described. Application of the proteasome inhibitor to the hippocampal cultures leads to the increase in the frequency of spontaneous and miniature EPSCs as well as mIPSCs (miniature inhibitory postsynaptic currents) within minutes. Interestingly, the same effect is triggered by the treatment with E1 inhibitor ziram, illustrating that not only proteasomal degradation but also dynamic ubiquitination of the substrate proteins can rapidly modulate neurotransmitter release (Rinetti and Schweizer, 2010).

1.13 Aim of the study

Initial work carried out by Prof. Dr. Anna Fejtova and Dr. Wilko Altmann identified one of the core proteasome subunit-PSMB4 as an interaction partner of a large, multidomain CAZ protein bsn. As recent studies highlight the importance of the proteasome in the regulation of neurotransmitter release and synaptic vesicle cycling, we were encouraged to further scrutinize its role at the presynaptic terminals. Additionally, because bsn has emerged as a major negative regulator of presynaptic protein polyubiquitination, endo-lysosomal system and autophagy, we were motivated to investigate potential impact of bsn on many facets of proteasome function. Moreover, since bsn is largely engaged in the determination of presynaptic efficacy and proteasome appears to act as a homeostatic modulator of vesicular release, we decided to explore the involvement of bsn-proteasome interaction in the synaptic vesicle cycling.

The goal of our study was to address the following questions:

1. What interaction interfaces on bsn and PSMB4 mediate the binding between these two proteins?
2. What is the physiological outcome of this interaction?
 - 2.1 Is bsn ubiquitinated and degraded by the proteasome?
 - 2.2 Does bsn interfere with the activity of the ubiquitin-proteasome system?
 - 2.3 Is bsn implicated in the assembly of the proteasome?
3. What is the role of bsn-PSMB4 interaction in the regulation of presynaptic function?
 - 3.1 Does bsn-proteasome interaction bear any consequences for presynaptic vesicle cycling?

2. Materials and Methods

2.1. Materials

2.1.1 Antibodies

The following antibodies were used in the study: mouse antibodies against; anti-flag (immunocytochemistry (ICC) 1:1000, Western blotting (WB) 1:1000, Sigma-Aldrich, F1804), anti-synaptotagmin1 luminal domain CypHer5E-labeled (ICC 1:200, Synaptic Systems, 105311CpH), anti-SNAP25 (WB 1:1000, Synaptic Systems, 111 011), anti- β -actin (WB 1:1000, Sigma), anti- α 4 (ICC and WB 1:1000, MCP34; PW8120), anti- α 5 (WB 1:1000, MCP196), anti- α 6 (WB 1:1000, MCP20; PW8100), anti- α 7 (WB 1:1000, MCP72; PW8110), anti- β 2 (WB 1:1000, MCP168; PW8145), anti- β 3 (WB 1:1000, MCP102), anti- β 7 (WB 1:1000, MCP205; PW8135), anti-Rpt6 (WB 1:1000, p45-110) and anti-FK2 (ICC and WB 1:1000; PW8810). All antibodies against proteasome were purchased from Enzo Life Sciences; rabbit antibodies: anti- β -Tubulin III (WB 1:1000, Sigma-Aldrich), anti-PSMG1/PAC1 (WB 1:1000, Cell Signaling, #13378), anti-PSMC4 (WB 1:1000, Bethyl Laboratories Inc), anti-GFP (WB 1:1000, Abcam, ab 6556), anti-RFP (ICC and WB 1:1000, Rockland Immunochemicals Inc.). Secondary antibodies from goat or donkey coupled with Cy3- (ICC 1:1000) or peroxidase- (1:10000) were obtained from Jackson ImmunoResearch Laboratories.

2.1.2 Animals

The cells and the tissues used in the study were obtained from Wistar rats and bassoon gene trap (BGT) (Frank et al., 2010; Hallermann et al., 2010) mouse strains backcrossed to C57BL/6N. BGT mice were obtained from Omnibank ES cell line OST486029 by Lexicon Pharmaceuticals, Inc. (The Woodlands, TX). All experiments were performed in accordance with the European Committees Council Directive (86/609/EEC) and approved by the local animal care committee (Landesverwaltungsamt Sachsen-Anhalt, AZ: 42502-2-1303 LIN).

2.1.3 Molecular biology reagents

Table1

Item	Company
Endonucleases (Restriction enzymes)	Biozym; Thermo Scientific

Taq DNA polymerase	QIAGEN
Phusion DNA Polymerase	Thermo Scientific
Alkaline Phosphatase from calf intestine (CIAP)	Thermo Scientific
Deoxynucleoside Triphosphate Set (dNTPs)	Thermo Scientific
T4 DNA ligase	Thermo Scientific
T4 Polynucleotide Kinase (PNK)	Thermo Scientific
Klenow Fragment	Thermo Scientific
Oligonucleotides (Primer)	Invitrogen
Nucleospin PCR cleanup gel extraction Kit	Macherey-Nagel
NucleoBond Xtra EF Midi/Maxi	Macherey-Nagel

2.1.4 Cell culture media and reagents for mammalian cells

Table2

Media and Reagents	Ingredients / Companies
HBSS+ (with Mg ²⁺ and Ca ²⁺)	Gibco
HBSS-	Gibco
DMEM	Gibco
DMEM (10% FCS)	10% FCS (Gibco); 1% Peniciline/Streptomycine 100x (Gibco); 2mM L-Glutamine (Gibco) in DMEM (Gibco)
Opti-MEM medium	Gibco
Neurobasal medium	Gibco
NB medium	2% B27 (Gibco); 2mM L-Glutamine (Gibco); 1% Peniciline/Streptomycine (Gibco) in Neurobasal
Ara C 1.5mM	Calbiochem
10x Trypsin	Gibco
1X Trypsin	10% 10x Trypsin (Gibco); DMEM (10% FCS)
Paraffin	Paraplast embedding medium (Fisher)
Poly-D-lysin	100mg/l poly-D-lysin in 100mM boric acid, pH 8.5, sterile filtered.
Poly-L-lysin	100mg/l poly-L-lysin in 100mM boric acid, pH 8.5, sterile filtered.

2.1.5 Culture media for bacterial cells and yeast

Table3

Media	Composition
LB-medium	20g LB Broth Base (Invitrogen) / 1000ml H ₂ O
SOC-medium	20g/l peptone 140 (Gibco); 5g/l yeast extract (Gibco); 10mM NaCl; 2.5mM KCl; 10mM MgSO ₄ ; 20 mM

Results

LB-Agar	15g Select Agar (Invitrogen) / 1000ml LB-medium
YPDA-medium yeast	50 Broth (Gibco) / 1000ml H ₂ O

2.1.6 Pharmacological reagents

Table4

Compound (working concentration)	Biological activity	Company
D-(-)-2-Amino-5-phosphonopentanoic acid (APV, 50 μ M)	competitive NMDA antagonist	Tocris
6-Cyano-7-nitroquinoxaline-2,3-dione disodium (CNQX, 10 μ M)	AMPA/kainate antagonist	Tocris
Bafilomycin A1 (1 μ M)	Specific inhibitors of vacuolar-type H ⁺ -ATPase	Calbiochem
MG132 (10-20 μ M)	Reversible proteasome inhibitor	Calbiochem
Lactacystin (10 μ M)	Selective and irreversible proteasome inhibitor	Enzo Life Sciences
Epoxomicin (10 μ M)	Selective and irreversible proteasome inhibitor	Enzo Life Sciences
N-ethylmaleimide (NEM, 2 mM)	Covalent modification of cysteine residues in proteins, prevents deubiquitination	Sigma-Aldrich
PhosStop (1x)	Phosphatase inhibitor cocktail	Roche
Complete (1x)	Protease inhibitor cocktail	Roche

2.1.7 Commonly used buffers and reagents for biochemical /imaging experiments

Table5

HEK293T cells lysis buffer (immunoprecipitation)	50mM Tris HCl, pH 8.0; 1% Triton X-100; 150mM NaCl containing Complete protease inhibitors
HEK293T cells lysis buffer (native gel electrophoresis)	25mM Tris HCl; pH 7.5, 5mM MgCl ₂ ; 1mM DTT; 2mM ATP; 0.025% digitonin
HEK293T cells lysis buffer (proteasome activity assay)	50mM Tris-HCl, pH 7.5; 250mM sucrose; 5mM MgCl ₂ , 1mM DTT; 2mM ATP; 0.5mM EDTA; 0.025% digitonin
PBS	2.7mM KCl; 1.5mM KH ₂ PO ₄ ; 8mM Na ₂ HPO ₄ , pH 7.4
PBS-T	2.7mM KCl; 1.5mM KH ₂ PO ₄ ; 8mM Na ₂ HPO ₄ , pH 7.4; 0.1% Tween20
Sucrose buffer A	5mM Tris-HCl pH 7.4; 5mM MgCl ₂ ; 0.32M sucrose; 1mM DTT; 2mM ATP

Results

Sucrose buffer B	5mM Tris-HCl, pH 8.1; 5mM MgCl ₂ ; 0.32M sucrose; 1mM DTT; 2mM ATP
In-gel activity assay buffer	100μM Suc-LLVY-MCA; 20mM Tris-HCl, pH 7.5; 5mM MgCl ₂ ; 2mM ATP
Proteasome activity assay buffer	100μM Suc-LLVY-MCA; 50mM Tris-HCl, pH 7.5; 5mM MgCl ₂ ; 40mM KCl; 1mM DTT; 2mM ATP
Tyrodes buffer	119mM NaCl, 2.5mM KCl, 25mM HEPES pH 7.4, 30mM glucose, 2mM MgCl ₂ and 2mM CaCl ₂
Solutions used for Native Gels	
5x loading buffer	200mM Tris-HCl, pH 8.6; 50% glycerol; 0.005% bromophenol blue
Electrophoresis buffer	192mM glycine; 25mM Tris-base
Blotting buffer	25mM Bicine; 25mM Bis-Tris; 1mM EDTA
LDS sample buffer	Life Technologies
Solutions used for Tris-glycine SDS-PAGE	
5xSDS loading buffer	250mM Tris-HCl pH 6.8; 30% Glycerol; 7.5% SDS; 0.25% Bromophenol blue
Electrophoresis buffer	192mM glycine, 1 % (w/v) SDS, 25mM Tris-base, pH 8.3
4x separating buffer	1.5M Tris/HCl, pH 8.8
4x stacking buffer	0.5M Tris/HCl, pH 6.8
Separation gel (20 %)	8.25 ml separation buffer; 7.5ml 87 % Glycerol; 16.5 ml 40 % Acrylamide; 330μl EDTA (0.2M); 330μl SDS; 22μl TEMED; 120μl 0.5% Bromophenol blue and 85μl 10 % APS
Separation gel (5 %)	8.25 ml separation buffer; 17.94 ml dH ₂ O; 1.89 ml 87% Glycerol; 4.12ml 40% Acrylamide; 330μl EDTA (0.2M); 330μl SDS; 22μl TEMED and 128μl APS.
Stacking gel (5 %)	6ml stacking buffer; 7.84ml dH ₂ O; 5.52 ml 87% Glycerol, 3.90 ml 30% Acrylamide; 240 μl EDTA (0.2 M); 240μl 10% SDS, 17.2μl TEMED; 140
Blotting buffer	192 mM glycine, 0.2 % (w/v) SDS, 25mM Tris-base,

2.2. Methods

2.2.1 Genotyping of mutant mice

DNA for genotyping was extracted from the tail cuts of P0 mice. The tail cuts were incubated in the lysis buffer (10 mM Tris-HCl pH 8.0, 100 mM NaCl supplemented with 0.4 mg/ml Proteinase K) at 55°C in a thermoshaker (Eppendorf) at 1000 rpm for 30-40 min. Subsequently, the enzyme was heat inactivated (10 min, 95°C) and PCR master mix was

prepared. The mix comprised 4 µl of DNA extract, 1 pM of both forward and reverse primer, 2.5 mM MgCl₂, 0.1units/µl Taq-polymerase, 0.2 mM dNTPs and 1x PCR buffer (Qiagen). The table describes temperature profile used for the PCR reaction:

Table6

Process	Time and temperature	Cycles
Initial denaturation	5 min at 95°C	1
Denaturation	45 sec at 95°C	35
Annealing	45 sec at 65°C	
Extension	60 sec at 72°C	
Final extension	30 sec at 72°C	1

After PCR, reaction mixtures were run on 1 % agarose gel (Biozym LE agarose, dissolved in TAE buffer) for 1 h (Biorad) and then visualised by illuminating the pre-stained gel (GelRed, red fluorescent nucleic acid dye) with UV light (Science Imaging, Intas).

2.2.2. Cloning of DNA constructs

Bsn fragments Bsn4 (aa 2715–3013) and Bsn1 (aa1692-3263) (Dresbach et al., 2003) as well as Bsn2 (aa1653-2082) (tom Dieck et al., 2005) were described previously. pEGFP-Bsn2 and pEGFP-Bsn4 were subcloned into RFP-C2 vector as well as FUGW lentiviral transfer vector. Bsn5 (aa 2715-2820 of NP_062019.2) was created from pEGFP-Bsn4 as a template using PCR with extended primers, thereby introducing EcoRI and BamHI restriction sites at 5' and 3' ends, respectively. Added restriction sites were used for in-frame cloning of the fragment into the pBS SK(+) vector and subsequent subcloning into pEGFP-C2. Bsn3 and Bsn6 were generated using PCR on rat cDNA of Bsn as template with extended primers to add EcoRI and XhoI restriction sites at the 5' and 3' ends of the fragments, respectively. Bsn constructs: Bsn7 (aa 1653-1878), Bsn8 (aa 1963-2086) and Bsn9 (aa 1653-1963) were generated using PCR on Bsn2 as a template, with extended primers to add EcoRI and XhoI, whereas Bsn10 (aa 2013-2087) was produced using PCR on Bsn8 as a template, with extended primers, therefore adding EcoRV and XhoI restriction sites at the 5 and 3 ends of the fragments, respectively. The introduced restriction sites were used for in-frame cloning of fragments into pGADT7, pCMV-3B and pBS SK(+) vectors. All the fragments were subcloned into pEGFP-C2 vector. Bsn3 was created from GFP-Bsn95-3938 as a template. Added restriction sites (EcoRI and BamHI) were used for in-frame cloning into the pBS SK(+) vector and pEGFP-C2. All constructs were verified by sequencing.

Results

PSMB4 covering nucleotides (nt) nt 161-820 and amino acids (aa) aa 45-263 and Δ C-PSMB4: nt 1615-7668, aa 45-246 of rat Psm4 (NM_031629.2, NP_113817.2) were produced by PCR using the pACT2 rat brain Matchmaker cDNA library (Clontech Laboratories, Inc.) as a template with extended primers, adding EcoRI and XhoI restriction sites at the 5' and 3' ends of the fragments, respectively. Inserted restriction sites were used for in-frame cloning of the fragment into the pBS SK(+), pCMV-Tag2B and pCMV-Tag3B vectors. PCR reaction included 10 pmol/ μ l of forward and reverse primers, distinct for each cDNA construct, 0.2 mM dNTPs, 2U Phusion DNA Polymerase in GC buffer (Finnzymes). The following temperature profile was employed for the PCR reaction:

Table7

Process	Time and temperature	Cycles
Initial denaturation	98°C; 5min	1
Denaturation	95°C; 15sec	35
Annealing	59°C; 30sec	
Extension	72°C, 40sec	
Final extension	72°C, 5min	1

After PCR reaction the amplified DNA fragments were separated according to their size by the means of agarose gel electrophoresis and purified using PCR clean-up gel extraction kit (Macherey-Nagel). Thereafter, ligation reaction consisting of 1 μ l T4 DNA ligase, 2 μ l of 1x ligase buffer (Life Technologies), DNA fragment/vector in a molar ratio 15:1 was prepared and incubated overnight at 16°C. 1 μ l of the ligation mixture was subsequently transformed into *E.coli* XL10 Gold competent cells. The ligation reaction was incubated with the bacteria for 10 min on ice. Next, the bacteria were subjected to heat shock at 42°C for 45 sec, returned immediately to ice to allow for the recovery and incubated in SOC medium (20 g/l peptone 140 (Gibco), 5 g/l yeast extract (Gibco), 10 mM NaCl, 2.5 mM KCl, 10 mM MgSO₄, 20 mM Glucose) at 37°C under constant shaking. After 1 h, 100 μ l of bacterial suspension was plated on LB (20 g LB Broth Base (Invitrogen) / 1000 ml H₂O) agar plates with suitable antibiotics and incubated overnight at 37°C. The plasmids were purified from LB bacterial culture using the alkaline lysis method (endotoxin-free DNA purification kit from Macherey-Nagel). In detail, bacterial cells were pelleted, and re-suspended in a buffer containing 50 mM Tris/HCl pH 8.0, 10 mM EDTA, 100 μ g/ml RNase A, followed

by lysis in 200 mM NaOH with 1% (w/v) SDS. Chromosomal DNA and bacterial proteins were precipitated using neutralization buffer (3 M potassium acetate, pH 5.5). The suspension was loaded onto the column, washed three times and eluted with elution buffer. Isopropanol was added to the eluate containing plasmid of interest and DNA was precipitated by centrifugation at 15000 g for 30 min. After washing with 70 % (v/v) ethanol, DNA was dissolved in either TE buffer or H₂O and stored at -20°C. All constructs were verified by sequencing.

RFP-CtermPSMB4 (nt 767-820, aa 247-263) construct was created by annealing of complementary oligonucleotides (C-terminus of PSMB4 is a very short sequence spanning only 19 aa) and subsequent insertion of this short DNA fragment into pEGFP-C2 and RFP-C2 vectors. Briefly, equimolar amounts of two complementary oligos were mixed and placed in the PCR machine. The samples were heated to 95°C for 2 min and slowly cooled down at the rate of approximately 0.5°C/sec. Next, ligation reaction was set at 3:1 fragment/vector molar ratio at RT for 1 h.

2.2.3. Mapping of interaction domain by yeast two hybrid screening (Y2H)

For cDNA library screening, the Matchmaker TwoHybrid System 2 (Clontech Laboratories, Inc.) was employed with a rat Matchmaker cDNA library 2 (Clontech Laboratories, Inc.) as a prey and Bsn1 fragment as a bait. Yeast cells were transformed using standard transformation protocols. Co-transformed cells were selected by growth on Leu- and Trp-lacking medium and reporter gene expression was evaluated as growth on medium deficient in Leu, Trp, adenine and His in the presence of 1 mM 3-amino-1, 2, 4-triazole. Growth was assessed and scored after 7 to 10 days. Possible self-activation of constructs was monitored in parallel by co-transformation with empty prey or bait vectors.

2.2.4. Lentiviral particles production

Lentiviral particles were generated in HEK293T cell line (ATTC, Manassas, VA) using three vectors: FUGW-based transfer, psPAX2 packaging and pVSVG pseudotyping vectors (Lois et al., 2002). HEK293T cells were grown in media containing 10% fetal calf sera (FCS) to 60% confluence in the 75 cm² flasks. Cells were transfected using standard calcium phosphate method. For transfection of a single flask, 500 µl of solution A (0.5 M CaCl₂) was mixed with a total of 20 µg of DNA (FUGW: psPAX2: pVSVG 5,5:9:5,5 µg). In the next

step, 500 μ l of solution B (140 mM NaCl, 50 mM HEPES, 1.5 mM Na₂HPO₄, pH 7.05) was added and, after 1 min, the mixture was applied to the cells in culture. Cells were incubated for 4 to 6 h and after this period of time, medium was changed to 10 ml Neurobasal production medium supplemented with 1% penicillin/streptomycin, 1 mM sodium pyruvate (Life Technologies), B27 and 2% Glutamax (Life Technologies). After 48 h virus-containing media was separated from large, cellular debris by centrifugation for 20 min at 2,000 g. Virus-containing supernatant was aliquoted and stored at -80°C until further use.

2.2.5. Primary neuronal cultures and viral infections

Primary cultures of cortical neurons were prepared as described previously (Lazarevic et al., 2011). In brief, 18-19 days rat embryos (E18–E19) were sacrificed by decapitation. The brains were removed and deprived of meninges. After treatment with 0.25% trypsin for 15 min and mechanical trituration cell suspension was plated in DMEM containing 10% FCS, 1 mM glutamine and antibiotics (100 U/ml penicillin, 100 μ g/ml streptomycin) onto poly-D-lysine coated glass coverslips (Sigma, 18 mm diameter). 24 h after plating, the medium was exchanged for Neurobasal medium supplemented with B27, antibiotics, and 0.8 mM glutamine. The cells were maintained in a humidified incubator with 5 % CO₂. For biochemical experiments cells were plated either in 75 cm² flask at a density of 5 million/75 cm² or in 6-well plates at a density of 300000 cells/well.

Primary rat hippocampal cultures were prepared according to a modified original protocol from (Banker, 1980) as described in (Frischknecht et al., 2008). Primary hippocampal cultures from mice were prepared as specified elsewhere (Kaech and Banker, 2006; Davydova et al., 2014) with minor modifications. Briefly, newborn animals of the desired genotype and their respective WT siblings were killed by decapitation. The brains were removed, hippocampi extracted and deprived of meninges. After 0.25 % trypsin treatment and mechanical trituration cell suspension was plated in DMEM containing 10% FCS, 1 mM glutamine and antibiotics onto poly-L-lysine coated glass coverslips. One hour later, coverslips were placed into dishes with 70–80% confluent feeding layer of astrocytes and Neurobasal A medium containing B27, 1 mM sodium pyruvate, antibiotics and 4 mM GlutaMax. On 1 DIV AraC was added to prevent glia proliferation, on 3 DIV additional dose of AraC was applied to reach the final concentration of 1.2 μ M. For live-cell imaging experiments, neurons were plated either at a density of 35000 cells/18 mm (mouse hippocampal neurons) or 25000 cells/18 mm coverslip (rat hippocampal neurons) in a 60 mm Petri dish.

Until otherwise stated, rat and mouse hippocampal as well as cortical cultures were infected with lentivirus at 4 DIV with almost 100% efficiency. For the infection of rat and mouse hippocampal neurons; 80 μ l of virus-containing supernatant was applied onto coverslips. Coverslips were returned to the original dishes with conditioned media after 7-8 h. For the infection of rat cortical cultures in 6-well plates or 75 cm² flasks between 2 and 3 ml of virus particles were used. After 8 h viral particles were removed and replaced with conditioned media. Neuronal cells were subjected to imaging after about two weeks at 16-18 DIV and to biochemical assays at 17 DIV.

2.2.6. Co-recruitment assays in COS7 cells

COS-7 cells grown on the glass coverslips were transfected using Polyfect reagent (QIAGEN) according to the manufacturer's instructions. After 24 h the cells were fixed with 4% paraformaldehyde, 4% sucrose in PBS (*Phosphate-buffered saline*) for 3 min at RT. Then, the samples were blocked and permeabilized with 10 % FCS, 0.1 % glycine, and 0.3 % Triton X-100 in PBS for 40 min. The coverslips were incubated with primary antibodies overnight at 4°C, and secondary antibodies for 1 h at RT. The primary and the secondary antibodies were diluted in PBS containing 3 % FCS. The coverslips were mounted on slides with Mowiol or FluorSave Reagent (Calbiochem). Images were acquired with Zeiss Axio Imager A2 microscope with Cool Snap EZ camera (Visitron Systems) and MetaMorph Imaging software (MDS Analytical Technologies).

2.2.7. Immunoprecipitation from HEK293T cells and Western blotting

HEK293T cells were transfected using standard calcium phosphate method. Briefly, solution A (250 μ l for 25 cm² flask and 500 μ l for 75 cm² flask) was mixed with DNA. In the next step solution B was added (the same amount as for the solution A), the mixture was incubated for 1 min and applied to the cells. 6 to 8 h later, medium were exchanged for an equal amount of fresh medium. One day after the transfection cells were lysed for 5 to 10 min on ice in the buffer containing 50 mM Tris-HCl, pH 8.0, 1% Triton X-100, 150 mM NaCl supplemented with complete protease inhibitors and PhosStop and cleared by centrifugation. The co-immunoprecipitation (Co-IP) was performed using MicroMACS anti-GFP Microbeads and Micro Columns (Miltenyi Biotec) according to the provided protocol from the manufacturer, except for the washing steps where the lysis buffer was utilized.

Bound proteins were eluted in SDS-loading buffer, heated for 5 min at 95°C and analysed by immunoblotting. Briefly, the samples were separated on 5%-20% Tris-glycine gradient polyacrylamide gels and blotted onto PVDF membrane (Millipore) by wet electroblotting system (Amersham, Biosciences). The membranes were incubated with primary antibody (diluted in PBS containing either 1% or 5% BSA and supplemented with 0.1% Tween 20) overnight at 4°C with gentle agitation, followed by 3 washes with PBS-T and incubation with HRP-conjugated secondary antibody (diluted in 5% non-fat dry milk/PBS-T) for 1 h at RT. Immunodetection was performed using Pierce ECL WB Substrate (Thermo Scientific) and ChemoCam Imager (Intas).

2.2.8. Mouse brain subfractionation

6-7 weeks mice were sacrificed by cervical fracture. Cortex and hippocampi were dissected and homogenized in sucrose buffer containing 0.32 M sucrose, 5 mM Tris-HCl, pH 7.4, 5 mM MgCl₂ supplemented with 1 mM DTT and 2 mM ATP, with glass-Teflon homogenizer using 12 strokes at 900 rpm. This and all the following procedures were carried out at 4°C. The homogenate (H) was centrifuged at 1,000 g for 10 min to sediment nuclear fraction and cell debris (P1). For native gel electrophoresis and WB, the supernatant (S1) was collected and centrifuged at 10,000 g for 15 min, yielding pellet (P2, membrane-enriched fraction) and supernatant (S2, cytosol). P2 fraction was resuspended and subjected to the hypotonic lysis and 7 strokes of glass-Teflon homogenizer at 1,5000 rpm. The resulting lysate was immediately transferred to a tube containing 1 M HEPES-NaOH pH 7.4, kept on ice for 30 min and subsequently spun for 20 min at 25,000 g. This produced pellet LP1 (plasma membrane enriched fraction) as well as supernatant LS1 (crude synaptic vesicle fraction). For proteasome activity assay, P1 fraction was resuspended in 2.5 mL of sucrose buffer and centrifuged for 10 min at 1000 g, yielding supernatant (S1') and pellet (P1'). The supernatant S1 and S1' were pooled and centrifuged for 15min at 12000g. The resulting P2 fraction was resuspended in 1.750 ml of buffer containing 0.32 M sucrose, 5 mM Tris-HCl pH 8.0 and 10 mM ATP, laid atop a discontinuous sucrose gradient: 0.8 M/1.0 M/1.2 M sucrose gradient (3 ml per step) and centrifuged for 2 h at 85000 g. The separation rendered pure synaptosomal fraction that was collected from the interface between 1.0 M/1.2 M sucrose.

2.2.9. Native gel electrophoresis and Zymography

To resolve proteasome complexes either HEK293T cell lysate (lysis buffer: 25 mM Tris-HCl, pH 7.5, 5 mM MgCl₂, 1 mM DTT, 2 mM ATP, 0.025% digitonin) or brain fractions (prepared as described in 2.2.8) were subjected to the native gel electrophoresis. The lysis buffer was supplemented with ATP as a regenerating system to enhance isolation of the intact 26S proteasomes and with DTT to prevent oxidation of the proteasomes. Samples were mixed with loading buffer (200 mM Tris-HCl, pH 8.6, 50 % glycerol, 0.005 % bromophenol blue) and 50 µg of the brain fractions lysate or 20 µg of HEK293T cell lysate was separated on 3 %-8 % NuPAGE Tris-Acetate Mini Gels (Life Technologies). The samples did not include any reducing/denaturing agents nor were they boiled, which allows preserving the integrity of the complexes. The gels were run at 4°C, first at 150 V for 1.30 h, thereafter, the voltage was increased to 200 V for the next 2.30 h. In-gel activity of the 26S proteasome was revealed by the incubation of the gel in buffer (20 mM Tris-HCl, pH 7.5, 5 mM MgCl₂, and 2 mM ATP) containing 100 µM Suc-LLVY-AMC for 20 min at 37°C. Proteasome activity was detected upon illumination with UV light (excitation 366 nm, emission 440/40 nm) using ChemoCam Imager (Intas). Fluorescence intensity was quantitated using ImageJ software.

2.2.10. Proteasome activity assay from HEK293T cells, cortical cultures and brain fractions

One day after transfection or 14 days after infection, HEK293T cells or rat cortical neurons, respectively, were lysed in buffer containing 50 mM Tris-HCl, pH 7.5, 250 mM sucrose, 5 mM MgCl₂, 1 mM DTT, 2 mM ATP, 0.5mM EDTA, and 0.025 % digitonin for 10 min at 4°C. The lysate was cleared by centrifugation for 15 min at 20.000g. Protein concentration was measured by Coomassie Plus Bradford Assay according to manufacturer instructions (Thermo Scientific). Protein concentration after subcellular brain fractionation was determined using BCA kit (Pierce BSA). For the assessment of proteasome activity from HEK239T cells and cortical cultures, equal amounts of total protein (5 µg/100 µl well) were incubated with assay buffer (50 mM Tris-HCl, pH 7.5, 5 mM MgCl₂, 40 mM KCl, 1 mM DTT, 2 mM ATP) containing 100 µM Suc-LLVY-AMC (N-Succinyl-Leu-Leu-Val-Tyr-7-amino-4-methylcoumarin, Enzo Life Science) (Kisselev and Goldberg, 2005). For the determination of proteasome activity from different brain fractions, equal amounts of protein extracts (5 µg/100 µl well) were incubated with assay buffer (0.5 mM EDTA, 50 mM Tris-

HCl, pH 8) containing 40 μ M Suc-LLVY-AMC (Snider et al., 2002). Proteasome activity was recorded as a fluorescent signal generated by the release of fluorogenic AMC (380 nm/440 nm excitation/emission spectra). Fluorescence was detected as an end-point measurement after 10 min using the Fluostar Omega microplate reader with appropriate fluorescence filters (BMG Labtech). The samples were read in triplicates or quadruplicates. After background subtraction (taken as the mean of three blank readings) from each data point, the values were normalized to the control (EGFP) and expressed in %. MG-132 (50 μ M) was used to verify the validity of the assay.

2.2.11. Measurement of the UPS activity in HEK 293T cells with the fluorescent proteasome reporter

HEK293T cells were co-transfected with equimolar amounts of bsn constructs and Ub^{G76V}-GFP reporter (Dantuma et al., 2000). At 90% confluence, cells were split at the ratio of 1:8 and the equivalent of 200 μ l was distributed into 96 microwell plates. Cells were allowed to recover for another 24 h and the GFP fluorescence was measured by the Fluostar Omega microplate reader (excitation at 485 nm; emission 530/10 nm). After background subtraction (taken as the mean of blank readings) from each data point, the values were normalized to the control (EGFP) and expressed in %.

2.2.12. Glycerol density gradient ultracentrifugation

One day after transfection, HEK293T cells were lysed in 25 mM Tris-HCl, pH 7.5, 5 mM MgCl₂, 1 mM DTT, 2 mM ATP, 0.025% digitonin. Protein concentration was measured by Coomassie Plus Bradford Assay. Equal amount of samples (450 μ g protein/300 μ l) were overlaid on the top of 5 %-25 % glycerol gradient prepared by Gradient master (BIOCOMP). Samples were centrifuged at 35,000 rpm for 6.30 h at 4^oC using MLS-50 rotor (Optima Max Ultracentrifuge, Beckman Coulter) and 14 fractions of 300 μ l were collected manually. Proteins were precipitated by the addition of 1.5 ml of ice-cold acetone, incubated for 1 h at -80^oC and centrifuged at 20.000 g for 15 min. Supernatant was removed and pellet was allowed to dry. Pellet was resuspended in LDS sample buffer (supplemented with 100 mM DTT, Life Technologies). Samples were analysed by SDS-PAGE, followed by western blotting.

2.2.13. CypHer5E and synapto-pHluorin imaging

In order to monitor synaptic vesicle recycling in rat hippocampal neurons, cypher5E -labelled anti-synaptotagmin1 antibody (aSyt1-cypHer5) uptake was employed. CypHer5E is a pH-sensitive dye, fluorescent in the acidic environment of the synaptic vesicles. Fluorescence of CypHer5E is quenched upon fusion of SVs with plasma membrane and exposure to slightly basic conditions. Therefore, this dye is suitable for the visualisation of the synaptic vesicle cycle and monitoring of any changes in RRP and RP. Imaging experiments were performed in the presence of bafilomycin A, an inhibitor of the vesicular proton pump that prevents reacidification of SVs upon their compensatory endocytosis.

Rat hippocampal cultures, infected either at 4 DIV or 14 DIV were incubated in Tyrodes buffer (119 mM NaCl, 2.5 mM KCl, 25 mM HEPES pH 7.4, 30 mM glucose, 2 mM MgCl₂ and 2 mM CaCl₂) with aSyt1-cypHer5 antibody (1:200, Synaptic Systems) for 2-3 h. Thereafter, coverslips were washed with Tyrodes buffer to minimize unspecific signal, installed in the imaging chamber (Warner Instruments, RC-49MFS) and imaged at RT on inverted microscope (Observer. D1; Zeiss) equipped with 63x objective and GFP ET filter set (exciter 470/40, emitter 525/50, dichroic 495 LP) and Cy5 ET filter set (exciter HC628/40 emitter HC692/40, dichroic BS660) and EMCCD camera (Evolve 512; Delta Photometrics) controlled by MetaMorph Imaging (MDS Analytical Technologies). Transduced axons were recognised by green fluorescence signal. Neurons were imaged in Tyrodes buffer containing bafilomycin A (1 μ M) as well as APV (50 μ M) and CNQX (10 μ M) to block recurrent network activity. Electrical field stimulation was applied to release RRP (40 AP at 20 Hz) and RP (200 AP at 20 Hz) using S48 stimulator (GRASS Technologies). Images were recorded every 100 ms at 10 Hz. 5 sec of the baseline was recorded before the stimulation, followed by imaging of the recovery phase for another 60 sec. Stacks for RP and RRP were acquired separately. After subtraction of the background values from the images, mean fluorescence intensities were measured in the round regions of interest (ROIs with a width of 8x8) placed over each responding synapse using Time Series Analyzer V2.0 plugin in ImageJ and corrected for bleaching. Briefly, the average fluorescence time course of unresponsive boutons was modelled into the exponential curve fitter and the returned b value together with row fluorescent values of responding ROIs were fitted in the exponential equation. RRP and RP are calculated as averaged mean of 100 values per cell (representative of the frames 130-230 for RRP and 440-540 for RP and corresponding to time points 13-23 sec and 44-54 sec,

respectively on the XY graph). The data are expressed as the mean fluorescence at each time point normalised to averaged intensity values before the stimulation.

For synapto-pHluorin imaging, the original mRFP-synaptophysin-pHluorin (sypHy) construct was obtained from the lab of Thomas Oertner (Rose et al., 2013) and subcloned into FUGW backbone vector. SypHy is a genetically encoded probe tailored to measure vesicle release and cycling (Burrone et al., 2006; Royle et al., 2008). SypHy fluorescence is quenched at low, acidic pH of SVs, but rises upon SV fusion and exposure of their lumen to the neutral pH of the extracellular media. Prior to the experiments, cells were incubated for 2 h with different proteasome inhibitors: MG-132 (50 μ M), lactacystin (10 μ M), epoxomicin (10 μ M) or DMSO as a control. Since MG-132 is a reversible inhibitor, it was included in the buffer solution throughout recording. Microscope specifications were as for cypHer5 imaging with the exception of the filters used: GFP/mCherry single band excitors ET filter set (exciter 470/40, exciter 572/35, emitter 59022m, dichroic 59022BS). Individual transduced boutons were detected by red fluorescence signal. RRP was revealed by electrical field stimulation with 40 AP at 20 Hz. This was followed by 2 min break, after which RP was released by 900 AP at 20 Hz. Subsequently, NH₄Cl was applied to reacidify the vesicular lumen and visualize all sypHy-expressing vesicles (Burrone et al., 2006). The stimulation was delivered by Master-8 stimulator (Master-8, A.M.P., Jerusalem, Israel). Images were recorded every 80 ms at 10 Hz. Other recording parameters were as stated for cypHer5 experiments. Synaptic boutons responsive to stimulation were selected by subtracting the first 10 frames of the baseline (before stimulation) from the 10 frames directly after the stimulus. Only neurons showing $\leq 20\%$ increase in fluorescence after NH₄Cl application were considered viable and metabolically active and processed for the analysis. Further analysis was performed as described for cypHer5 imaging. The relative sizes of the RRP and the RP are expressed as fractions of the total sypHy-expressing pool detected after addition of 60 mM NH₄Cl and plotted as time courses of normalised fluorescence intensity. RRP and RP were quantified by averaging the mean of 100 values per each cell (representative of the frames 197-297 for RRP and 560-660 for RP and corresponding to time points 15.84-23.84 sec and 44.88-52.88 sec, respectively on the XY graph).

2.2.14. Statistical analysis

All the results of quantitative analyses are expressed as means \pm standard errors of the mean (SEM). Statistical analyses were executed with Prism 5 software (GraphPad Software, Inc.).

Results

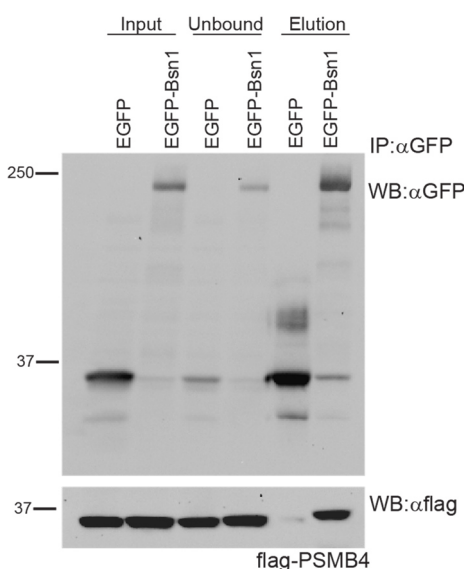
The normal distribution of the data was assessed by D'Agostino-Pearson omnibus test. One-way ANOVA with Bonferroni correction or Student's t-test was used for comparison of the groups. In all graphs numbers within bars depict the numbers of analysed cells or independent loadings obtained from at least two different experiments. Statistical significance is marked as * ≤ 0.005 , ** ≤ 0.001 , *** ≤ 0.0001 in all the graphs.

3. Results

3.1 Bsn interacts with the proteasomal subunit β 7 (aka PSMB4)

Multidomain structure of bsn engages it in the numerous interactions with many proteins inhabiting the presynaptic compartment. To shed light on the complexity of these interactions and to pinpoint plausible components, we performed yeast two hybrid (Y2H) experiments. Amongst multiple proteins, PSMB4 emerged as an interesting candidate. This protein, also known as β 7 subunit of 20S CP, plays a critical role in the proteasome assembly, namely, it drives dimerization of two half-proteasomes and thereby formation of the functional 20S proteasome. At this point, it seemed exciting to study this interaction, as by binding to the proteasomal subunit, bsn could potentially participate in the regulation of the activity and/ or assembly of the proteasome and thereby contribute to the control of presynaptic ubiquitin-proteasome system and consequently influence presynaptic proteostasis.

In order to confirm the results obtained in the Y2H, we designed co-immunoprecipitation (Co-IP) experiments in the heterologous expression system of mammalian HEK293T cell line. These cells are perfectly suited for biochemical experiments owing to their easy maintenance and reproduction, simplicity and high efficiency of transfection and faithfulness of post-translational processing. We first verified the interaction between bsn fragment Bsn1(1692-3263), used as a prey in Y2H assay and PSMB4. Initially, we took advantage of a plasmid vector, readily available in our laboratory that expresses N-terminally truncated flag-tagged



PSMB4 (aa 32-263). The N-terminus of PSMB4 contains propeptide sequence that is normally cut off after formation of the mature 20S proteasome. Studies conducted by *Hirano et al.* in HEK293T cell line indicate that this domain is dispensable for their proper growth and survival as well as effective proteasome biogenesis (Hirano et al., 2008) and as such the exact role of this propeptide has not yet been fully elucidated. In the first set of experiments, we co-transfected HEK293T cells with plasmids encoding flag-tagged PSMB4 and EGFP-tagged bsn fragment- Bsn1 (EGFP-Bsn1) or EGFP construct alone as a control. GFP-coupled beads were used to

Figure 6. Bsn fragment EGFP-Bsn1 interacts with 20S CP subunit PSMB4. Flag-PSMB4 is successfully precipitated by EGFP-Bsn1, but no EGFP alone from HEK293T cell lysates with GFP antibodies. Size markers are indicated in kDa.

immunoprecipitate bsn fragments. As shown in the Figure 6, PSMB4 can be detected in the elution fraction together with EGFP-Bsn1 fragment, however it is absent in the control elution fraction, that contains only EGFP protein. These results validate previous Y2H experiments and reveal that bsn could be, indeed, involved in the interaction with 20S proteasome via binding to $\beta 7$ subunit. Since EGFP-Bsn1 represents a large, central portion of bsn, we sought to narrow down the PSMB4-binding domain on bsn. For this purpose, we carried out Co-IP experiments using flag-PSMB4 and different EGFP-tagged bsn constructs. Two smaller bsn fragments EGFP-Bsn2 (aa 1653-2087) and EGFP-Bsn4 (aa 2715-3013), but not EGFP-Bsn3 (aa 2088-2563) successfully precipitated proteasome subunit PSMB4 (Figure 7), establishing two PSMB4-interaction motifs on bsn.

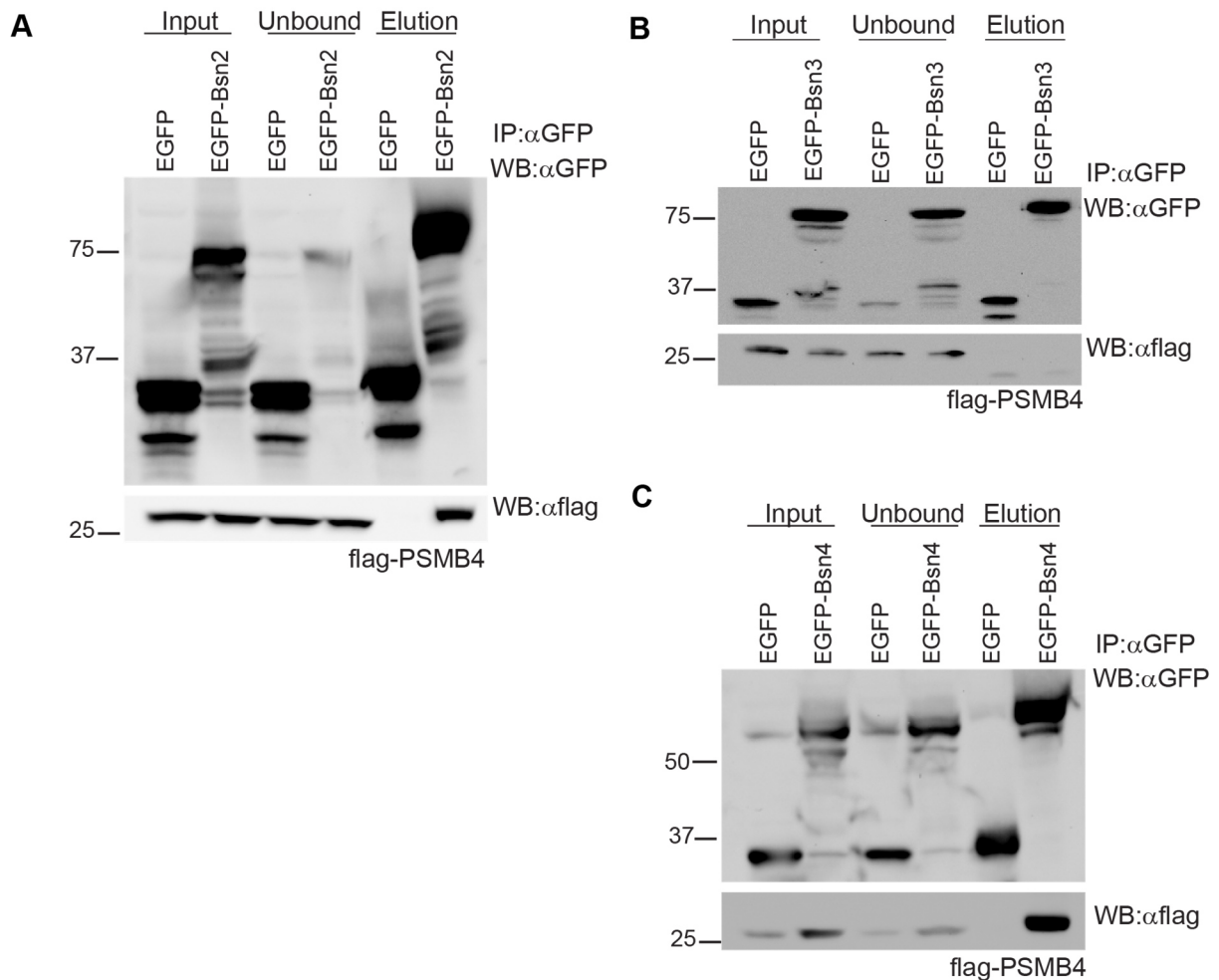


Figure 7. Bsn fragments EGFP-Bsn2 and EGFP-Bsn4 interact with PSMB4. Immunoprecipitation experiments from HEK293T cells demonstrate that while (B) bsn fragment EGFP-Bsn3 does not mediate interaction with PSMB4, two shorter pieces of bsn (A) EGFP-Bsn2 and (C) EGFP-Bsn4 effectively bind this proteasome subunit. Size markers are indicated in kDa.

EGFP-Bsn4 construct contains the third coiled-coil (CC3) domain of bsn. As coiled-coil domains are generally known to mediate protein-protein interactions, we examined whether this domain is important for binding of bsn with PSMB4. To this end, we dissected EGFP-Bsn4 construct into two parts: EGFP-Bsn5 (aa 2715-2820) and EGFP-Bsn6 (aa 2821-3013). EGFP-Bsn5 failed to associate with PSMB4, similarly, EGFP-Bsn6 was not co-immunoprecipitated with the proteasomal subunit, although it contains intact CC3 domain (Figure 8). These results prompted us to reason that not only coiled-coil domain but also additional regions of EGFP-Bsn4 fragment regulate interaction, with PSMB4. Alternatively, the binding domain could be buried on the interface of these two fragments (when the possibility of the incorrect folding of the smaller fragments is excluded).

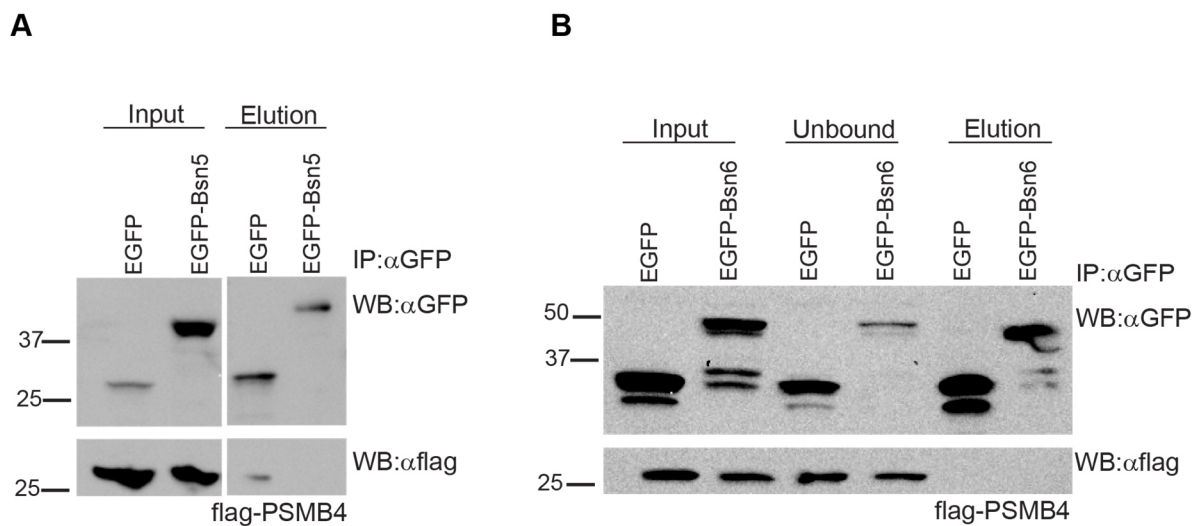


Figure 8. Intact EGFP-Bsn4 fragment is essential for interaction with PSMB4. Co-IP experiments reveal that neither EGFP-Bsn5 (A) nor EGFP-Bsn6 (B) interact with PSMB4 subunit of 20S proteasome. Size markers are indicated in kDa.

In order to unequivocally demonstrate that N-terminal propeptide region is not required for the binding between bsn and the proteasome subunit, we designed a deletion mutant construct completely deprived of the propeptide sequence and co-expressed it with interacting bsn fragments EGFP-Bsn4 and EGFP-Bsn2 in HEK293T cells. Co-IP studies demonstrated that both bsn fragments precipitated Δ NPSMB4, indicating that propeptide does not affect interaction between bsn and PSMB4 (Figure 9).

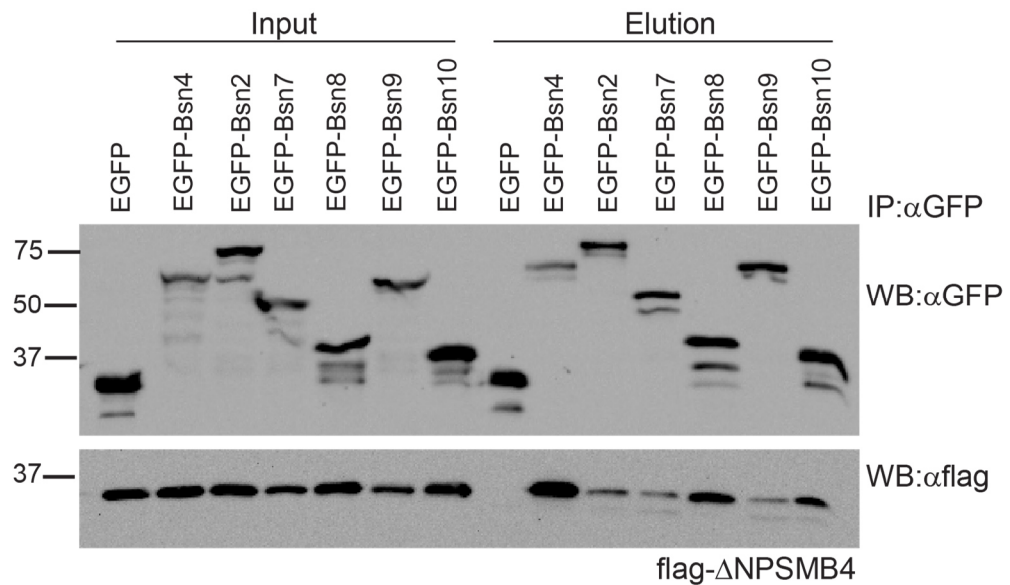


Figure 9. Multiple independent motifs of bsn interact with flag- Δ NPSMB4. Fragments derived from EGFP-Bsn2 were screened for the interaction with the proteasome subunit deprived of the N-terminus. Co-IP experiments from HEK293T cells revealed two major interaction interfaces on EGFP-Bsn2, namely EGFP-Bsn7 and EGFP-Bsn10. Size markers are indicated in kDa.

We, then, attempted to further examine bsn-proteasome interaction, focusing on the second bsn binding fragment, EGFP-Bsn2. Available constructs, produced by Dr. Marija Rankovic and subcloned into pEGFP-C2 vector, were used for the screening. We tested four shorter pieces of EGFP-Bsn2 fragment, namely: EGFP-Bsn7 (aa 1653-1878), EGFP-Bsn8 (aa 1964-2087) EGFP-Bsn9 (aa 1653-1963) and EGFP-Bsn10 (aa 2013-2087) for interaction with Δ NPSMB4 in the Co-IP assays. Figure 9 illustrates the outcome of the experiments, where all examined fragments were detected in a complex with β 7 subunit of the 20S proteasome. Altogether, these experiments revealed two shorter binding motifs within EGFP-Bsn2 fragment: EGFP-Bsn7 and EGFP-Bsn10 and further added up to the complexity of bsn-proteasome interaction, indicating that numerous structural elements of bsn including aa sequences: 1653-1878, 2013-2087 and 2715-3013 contribute to proteasome binding (Figure 10)

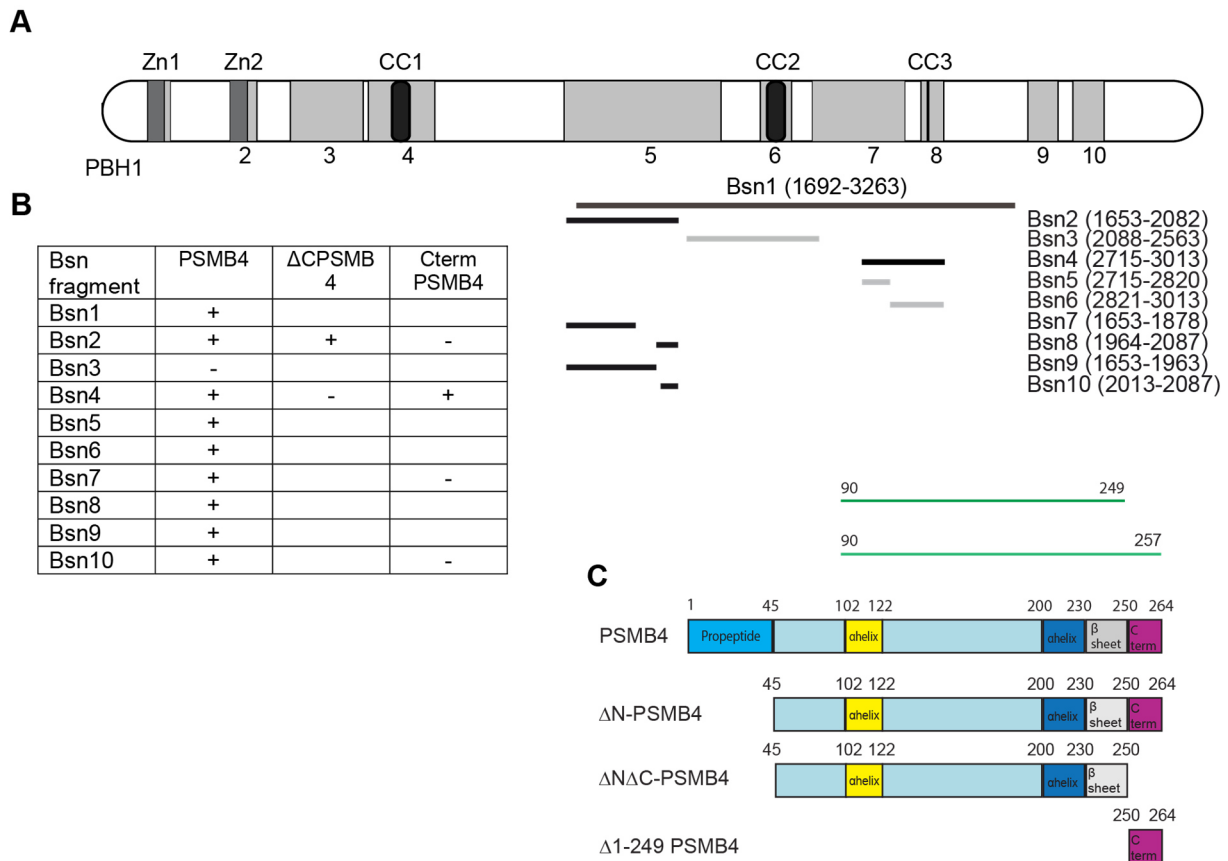


Figure 610. Summary of bsn fragments interacting with PSMB4 protein. (A) Structure of bsn is depicted. The position of the PSMB4-interaction interface in bsn and all bsn fragments used in the interaction studies are illustrated. Black bars denote constructs that bind to, whereas grey bars constructs that do not associate with PSMB4. Abbreviations: Zn1/2, zinc fingers; CC1-3, coiled-coil regions; PBH1-10, piccolo-bassoon homology regions. Numbers in brackets correspond to amino acid (aa) residues of rat bsn. **(B)** A table summarizing the ability of different bsn fragments to associate with distinct regions of PSMB4. **(C)** Schematic diagram depicting the structure of the intact PSMB4 as well as fragments used in Co-IP experiments. The diagram was drawn on the basis of PSMB4 structure as published in (Loscher et al., 2005). Green lines depict two PSMB4 constructs used as preys in Y2H screen.

In contrast to the N-terminal propeptide, the C-terminal tail of PSMB4 protein has a well-recognized function and is of great importance for the correct proteasome maturation, as it is involved in the last steps of the 20S CP assembly. To test whether bsn associates with the C-tail of PSMB4, we generated mRFP-tagged COOH-terminal PSMB4 construct and examined its potential binding to bsn fragments. mRFP-CtermPSMB4 was precipitated exclusively with EGFP-Bsn4, but not with EGFP-Bsn2 or its shorter interacting fragments EGFP-Bsn7 and EGFP-Bsn10. These experiments highlight that C-terminus of the proteasomal subunit is a major region mediating specific interaction with EGFP-Bsn4 fragment, favoring the hypothesis that bsn could interfere or conceivably act as a negative regulator of the proteasome assembly (Figure 11).

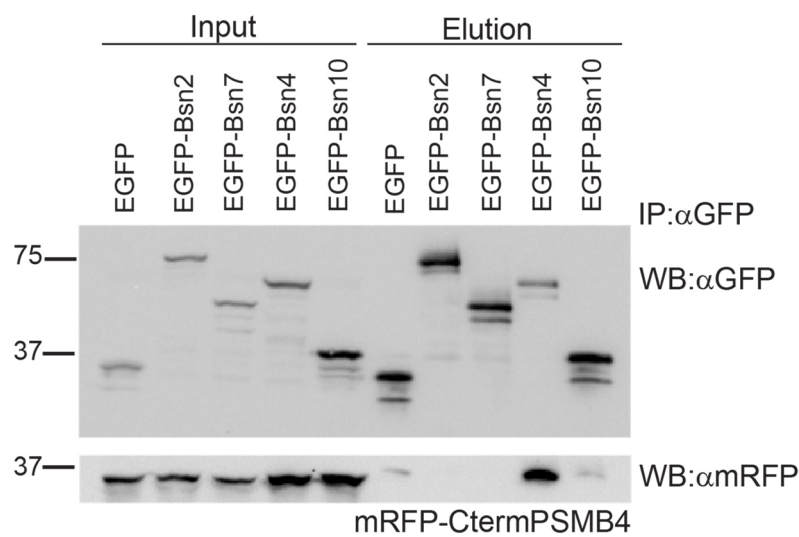


Figure 11. Only EGFP-Bsn4 effectively binds C-terminus of PSMB4 proteasome subunit. Co-IP studies conducted in HEK293T cells disclose that solely one of the bsn fragments-EGFP-Bsn4 precipitates C-terminal extension of PSMB4 (mRFP-CtermPSMB4) that drives dimerization of two half-proteasomes. Size markers in Western blot images are indicated in kDa.

In the last set of Co-IP studies we scrutinized the interaction between bsn and a deletion mutant of PSMB4 lacking N-terminal prosequence as well as C-terminal tail. Only EGFP-Bsn2 showed successful binding to flag- $\Delta\Delta$ CPSMB4 (Figure 12), providing a possibility for multiple roles of bsn in the modulation of the proteasome function, dependently on the interacting domain.

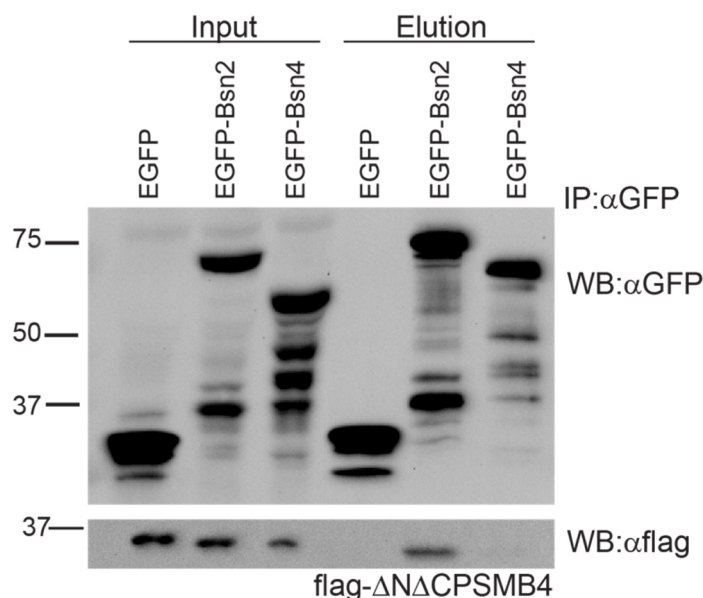


Figure 12. Flag- $\Delta\Delta$ CPSMB4 is found in the complex with EGFP-Bsn2. Immunoprecipitation experiments from HEK293T cells demonstrate that proteasome subunit deprived of N- as well as C-terminus (flag- $\Delta\Delta$ CPSMB4) binds exclusively EGFP-Bsn2 bsn fragment. Size markers in Western blot images are indicated in kDa.

3.2 Bsn recruits endogenous UPS

Co-IP experiments suggested a strong interaction between bsn and the subunit of 20S CP-PSMB4. To further support these data we performed co-clustering studies in COS-7 cells that endogenously do not express bsn. To this end, we primarily expressed GFP-tagged bsn fragment EGFP-Bsn1 together with RFP-tagged PSMB4 and looked at their possible co-localization. In line with already published data (Maas et al., 2012), when expressed in the heterologous cell line, EGFP-Bsn1 formed cytosolic clusters. RFP-PSMB4 was recruited to these intracellular inclusions (Figure 13), implying, thus, that both proteins concentrate in the intimate vicinity. Consistently, deletion of the whole interacting domain (aa 1692-3263) introduced in bsn construct spanning aa sequence 609-3938 (EGFP-Bsn609-3938 Δ Bsn1) effectively abolished binding of bsn and PSMB4 in the cellular co-recruitment assay (Figure 13).

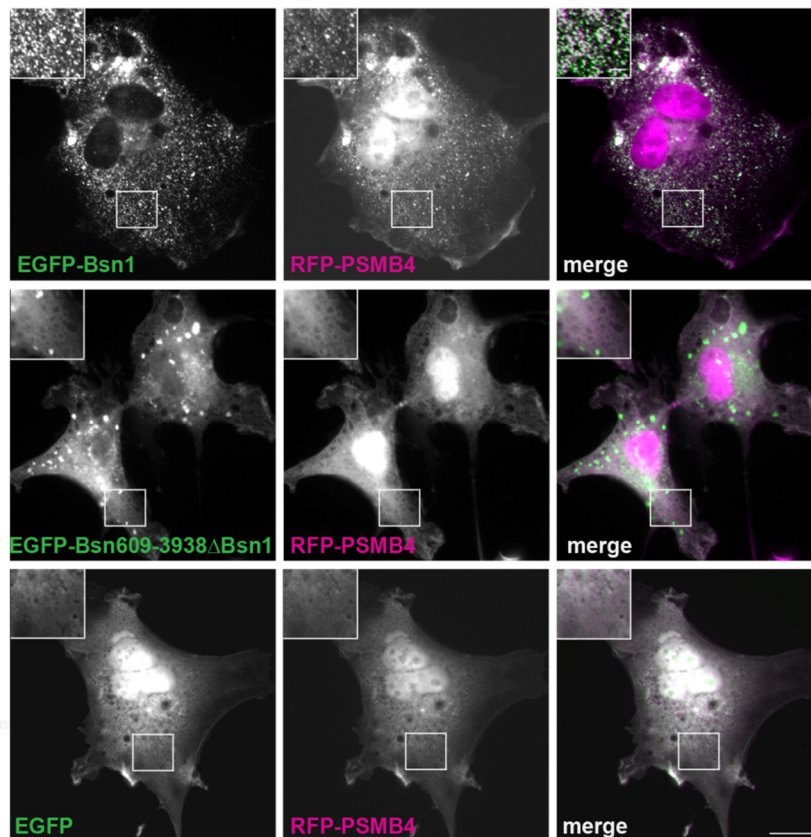


Figure 13. PSMB4 is mobilized to EGFP-Bsn1-enriched clusters. Expression of both proteins: EGFP-Bsn1 and RFP-PSMB4 in COS-7 cells reveals their interaction. Deletion of the entire binding interface-aa 1692-3263, hampers recruitment of RFP-PSMB4. Scale bar represents 10 μ m in overview and 2 μ m in inset. Data provided by Prof. Dr. Anna Fejtova.

We further screened shorter bsn fragments EGFP-Bsn2 and EGFP-Bsn4 for interaction with the proteasome subunit in the co-clustering experiments. EGFP-Bsn2 retained ability to form punctate clusters in the cytoplasm and successfully recruited flag-PSMB4 (Figure 14).

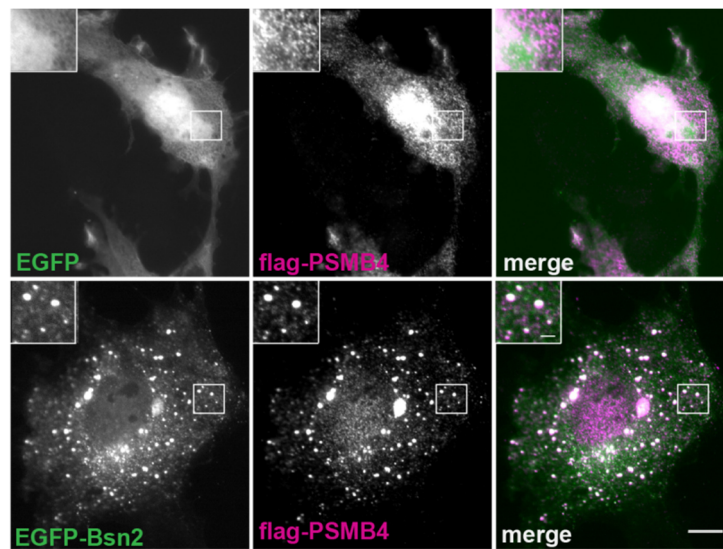


Figure 14. PSMB4 is recruited to EGFP-Bsn2 containing clusters. When both proteins: EGFP-Bsn2 and flag-PSMB4 are co-expressed in COS-7 cells they show marked colocalisation. Scale bar represents 10 μm in overview and 2 μm in inset.

Conversely, EGFP-Bsn4 construct displayed diffused localization in COS-7 cells, reminiscent of EGFP (Figure 14, first panel), precluding us from withdrawing any vital conclusions regarding colocalisation of this fragment with the proteasome (Figure 15).

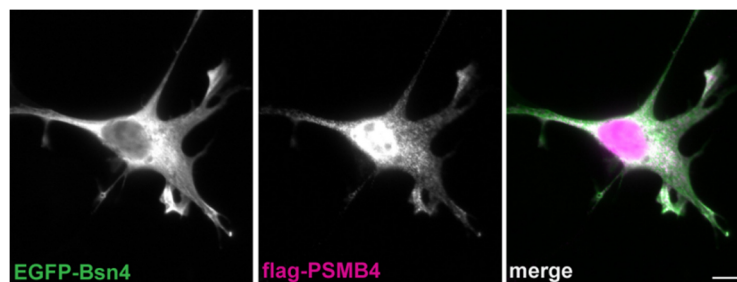


Figure 15. EGFP-Bsn4 fragment exhibits diffuse localization. EGFP-Bsn4 similarly to the EGFP alone shows diffuse expression pattern, therefore its colocalisation with the proteasome subunit PSMB4 is difficult to infer. Scale bar represents 10 μm .

To reinforce our co-recruitment experiments, we inspected the colocalisation of EGFP-Bsn2 with endogenous ubiquitin-proteasome machinery. Proteasome was stained with $\alpha 4$ antibody, whereas ubiquitin was visualized with FK2 antibody. Similarly to the earlier experiments relying on the overexpression of the proteasomal subunit, endogenous proteasome as well as ubiquitin revealed co-localization with EGFP-Bsn2 (Figure 16). Thus, we propose that, in the

living cells, bsn is found in the close proximity to the proteasome and that it potentially interacts with the functional 20S, as envisaged by $\alpha 4$ staining.

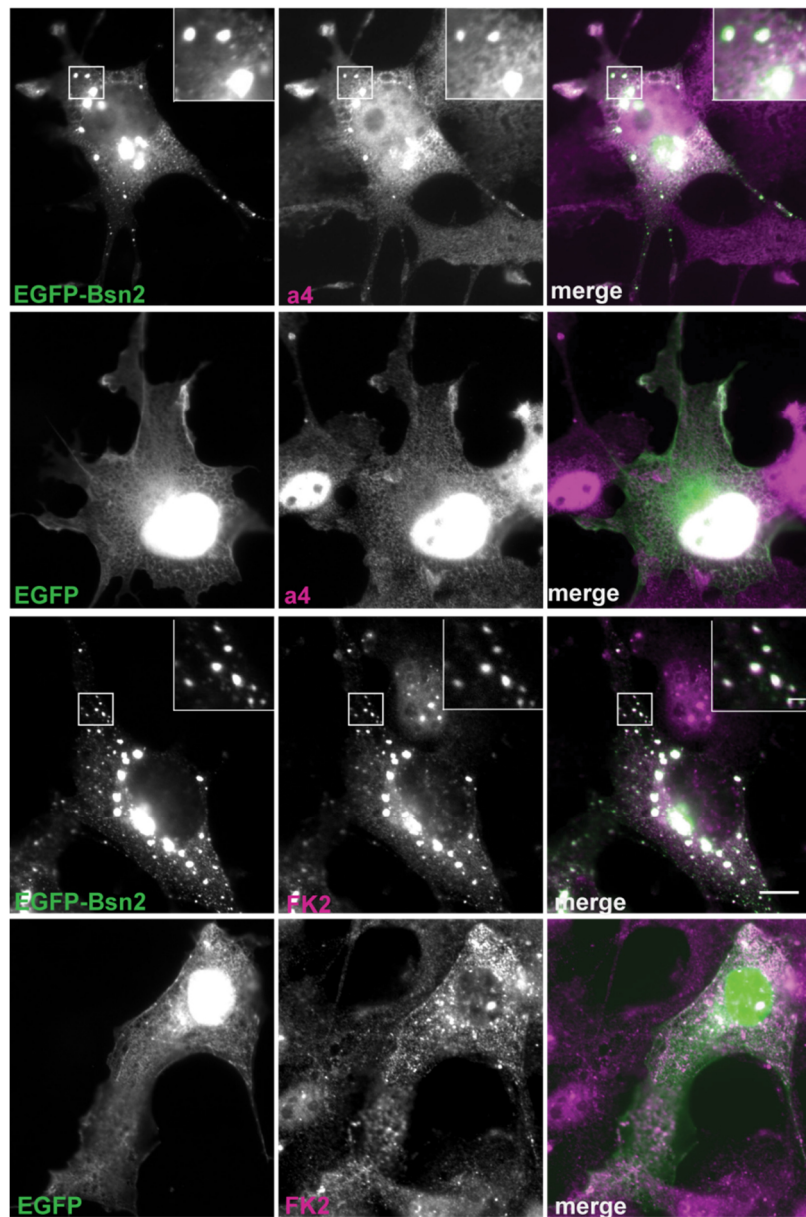


Figure 16. EGFP-Bsn2 recruits endogenous components of the UPS machinery. When overexpressed in COS-7 cells, EGFP-Bsn2 is localised in the cytoplasmatic inclusions. Endogenous proteasome, revealed by staining against $\alpha 4$ subunit and ubiquitin, stained with FK2 antibody, are mobilized to these clusters. Regions in squares are shown magnified in the inset in the upper left corner. Scale bar represents 10 μm overview and 2 μm in inset.

3.3 Bsn is ubiquitinated but not constitutively degraded

Polyubiquitination is a posttranslational modification that marks proteins for proteasomal degradation (Glickman & Ciechanover, 2002). To determine whether PSMB4-interacting fragments are subjected to polyubiquitination, we overexpressed bsn fragments together with HA-ubiquitin (HA-Ub), commonly used to increase ubiquitination in HEK293T. We detected a marked association of HA-Ub with EGFP-Bsn2 and thereof derived fragments: EGFP-Bsn7 and EGFP-Bsn10, while the degree of HA-Ub association with EGFP-Bsn4 and EGFP control was comparable. The interaction of bsn with the proteasome might indicate that bsn is degraded by this proteolytic machinery. In order to address this issue, we treated HEK293T cells transfected with bsn constructs or EGFP, for either 3h or 6h, with the proteasome inhibitor MG132 and monitored the amount of bsn by Western blots. These experiments revealed no major increase in the protein levels of Bsn2 and Bsn4 fragments in comparison with the endogenous actin or overexpressed EGFP upon inhibition of the proteasome (Figure 17A,B; 3 h: EGFP: 103 ± 4 %, EGFP-Bsn2: 99 ± 9 %, EGFP-Bsn4: 96 ± 4 %; 6 h: EGFP: 95 ± 4 %, EGFP-Bsn2: 101 ± 11 %, EGFP-Bsn4: 103 ± 6 %), implying that these fragment are not targeted for the proteasomal degradation.

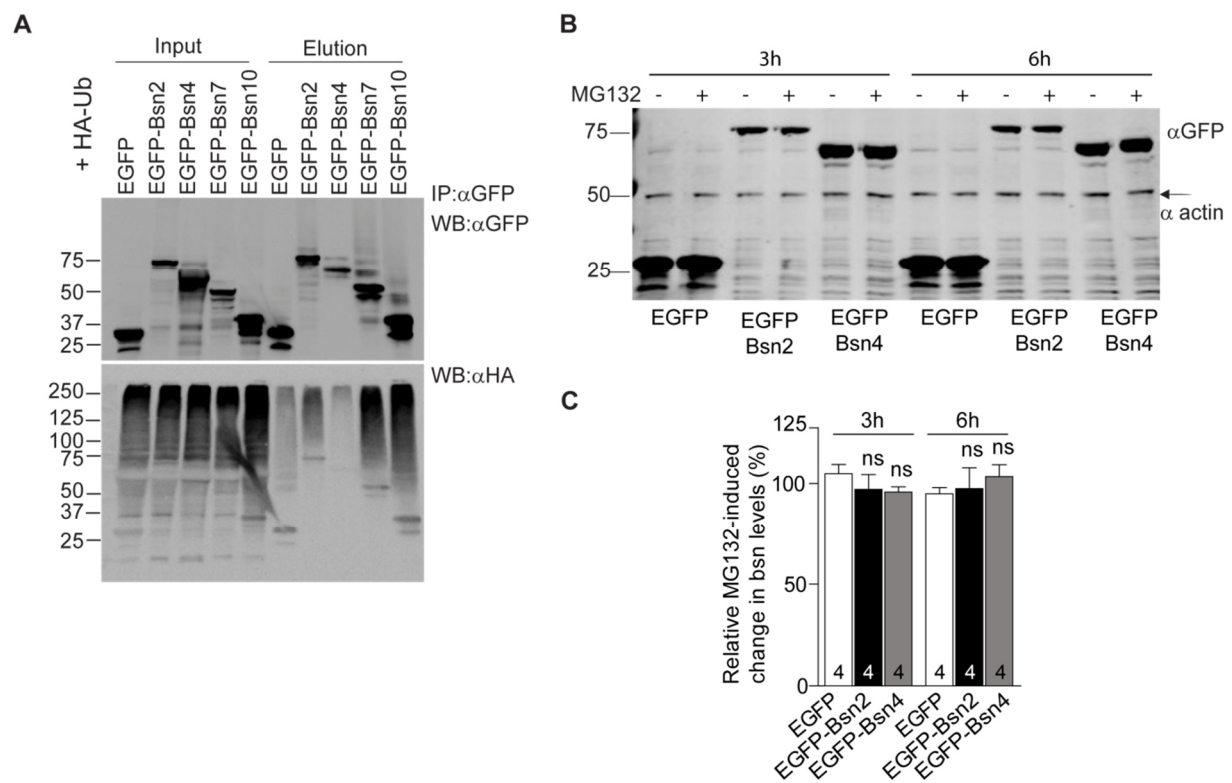


Figure 17. Bsn fragments are differently ubiquitinated but not degraded by the proteasome. (A) HEK 293T cells were transfected with EGFP, EGFP-Bsn2 or EGFP-Bsn4 as well as HA-Ub. Bsn

fragments were immunoprecipitated with specific GFP antibodies. Linkage of ubiquitin moieties was detected by immunoblotting with anti-HA antibody. (B) Western blot of HEK293T cell extracts treated with either 10 μ M MG132 or DMSO as a control solution for 3 h or 6 h. Equal amount of protein was loaded, actn served as a loading control. The levels of EGFP-Bsn2 and EGFP-Bsn4 do not change upon proteasome inhibition. Size markers are indicated in kDa. (C) Quantitative assessment of the abundance of bsn levels.

3.4 Bsn overexpression impairs proteasome activity

A growing body of evidence suggests a role of specialized proteasome interacting proteins (PIPs) in the control and support of the proteolytic activity (Schmidt et al., 2005), however, little is known about brain-specific factors that would help to maintain proteasome homeostasis. We wondered, therefore, whether bsn could have a role in the regulation of the proteasome activity.

In order to approach this question, we set a battery of experiments. First, we carried out 20S proteasome activity assay, which is based on a fluorogenic peptide substrate N-Succinyl-Leu-Leu-Val-Tyr-7-amino-4-methylcoumarin (Suc-Leu-Leu-Val-Tyr-AMC). The substrate consists of a chain of aminoacids (Suc-LLVY), specific for chymotrypsin activity of the proteasome and a small fluorophore molecule (AMC) quenched in the absence of the proteolytic activity. Upon the onset of the proteasome activity the fluorophore is cleaved and fluorescence is emitted (Figure 18). The intensity of the fluorescence signal is proportional to the activity of the proteasome and can be monitored fluorimetrically at 440/40 nm with excitation at 366 nm. Since proteasome activity is highly sensitive to the different types as well as concentrations of detergents, we initially decided to screen an array of detergents for their effect on proteasome activity. As previously reported (Kisselev and Goldberg, 2005), common detergents, including Triton X-100, Tween20 and NP-40, each one frequently used at a concentration of 0.2%, considerably impeded proteasome activity in comparison with milder non-ionic detergents such as DDM and digitonin, usually employed at lower 0.02% concentrations (Figure 18). Taking these results into consideration, we performed all subsequent proteasome activity assays in the presence of low percentage-0.02%- digitonin.

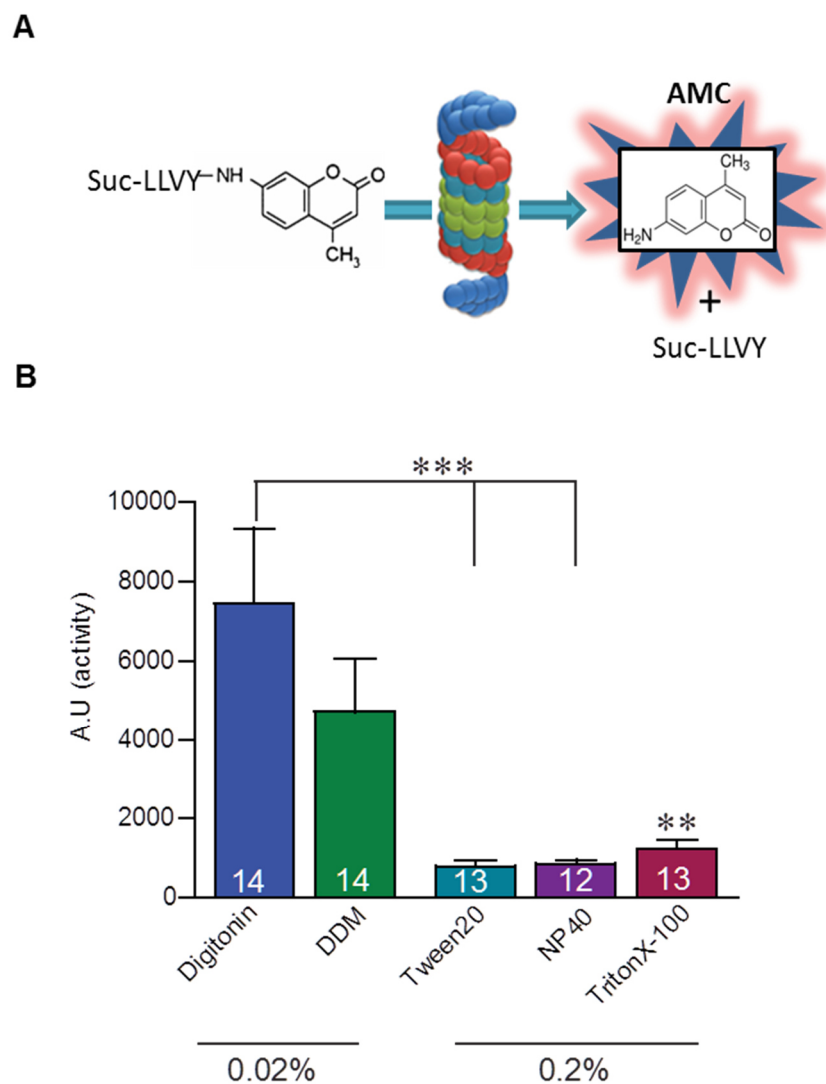


Figure 18. Impact of various detergents upon proteasome activity. (A) Simplified cartoon of the proteasome activity assay. Substrate for the chymotrypsin-like proteasome activity is coupled to the fluorophore which is cleaved by the proteasome activity, subsequently; the emitted fluorescent signal is quantified. (B) Effect of different detergents on the hydrolysing activity of the proteasomes. Abbreviation: a.u., arbitrary units. Values in bars indicate *n* number which corresponds to the number of readings from three distinct experiments, performed on three independent HEK293T cell cultures. The graphs display mean \pm SEM. Statistical significance was assessed by one-way ANOVA with Bonferroni post-test, ** $p < 0.01$, *** $p < 0.001$

Next, we measured the activity of the proteasome from the extracts of HEK293T cells overexpressing interacting bsn fragments EGFP-Bsn2 and EGFP-Bsn4. After cell lysis and centrifugation, the supernatant was collected and the protein concentration was quantified. In the next step equal amounts of cell extracts were mixed with the proteasome buffer containing aforementioned fluorogenic substrate for the determination of chymotrypsin-like activity. We measured a significant downregulation of the proteasomal activity in the lysates of cells

expressing either bsn interacting fragments (Figure 19). Expression of EGFP-Bsn2 and EGFP-Bsn4 decreased proteasome activity by roughly 20% (EGFP-Bsn2: 72 ± 14 % of ctrl; EGFP-Bsn4: 71 ± 5 %),

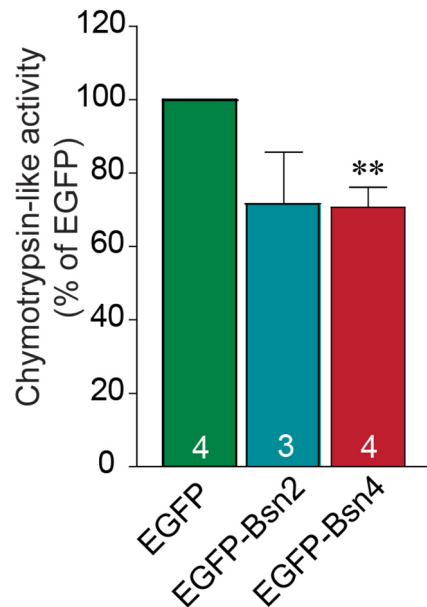


Figure 19. Proteasome activity is significantly decreased upon bassoon expression in heterologous system of HEK293T cells. Proteasome activity assay using fluorogenic proteasome substrates revealed a marked downregulation of the activity of proteasome in the presence of both EGFP-Bsn2 and EGFP-Bsn4. Values in bars indicate *n* number which corresponds to the number of flasks from three independent experiments performed on independent HEK293T cell cultures. Data indicate mean \pm SEM. Unpaired Student's *t*-test was used for statistics, ***p*<0.01

These results suggest that both bsn fragments impede proteasome activity to similar extent, by interfering with 20S-dependent degradation. To further scrutinize the inhibitory effect of bsn on the proteasomal degradation, we took advantage of native gel electrophoresis (native-PAGE). This method allows to separate intact proteasome complexes in the native environment without use of denaturing or reducing agents. It is therefore well suited to visualize activities of the main active proteasome subspecies including 20S and 26S. After native-PAGE, we bathed the gels in the solution containing proteasome substrate against chymotrypsin activity to reveal proteolytic action. Although, as evaluated by Western blotting, the levels of 20S proteasomal α and β subunits were unaltered in control and bsn-expressing HEK293T cells, proteasomal activity was substantially decreased in the cells transfected with bsn fragments (Figure 20). Interestingly, the in-gel activity assay enables visualization of the intact double- and single-capped proteasomes as well as 20S CP activity. The activity of 20S CP is disclosed after addition of low percentage SDS that is said to mildly denature the 20S

barrel and therefore promote gate opening and peptide access to normally latent CP. In our experimental set-up SDS treatment, indeed, increased 20S CP activity, however the results were not consistent throughout the experiments, for this reason, they were excluded from the further analysis. The activity of the 26S organelle, however, could be reliably quantified and amounted to $74 \pm 5\%$ upon EGFP-Bsn2 expression and $76 \pm 5\%$ upon EGFP-Bsn4 expression (Figure 20).

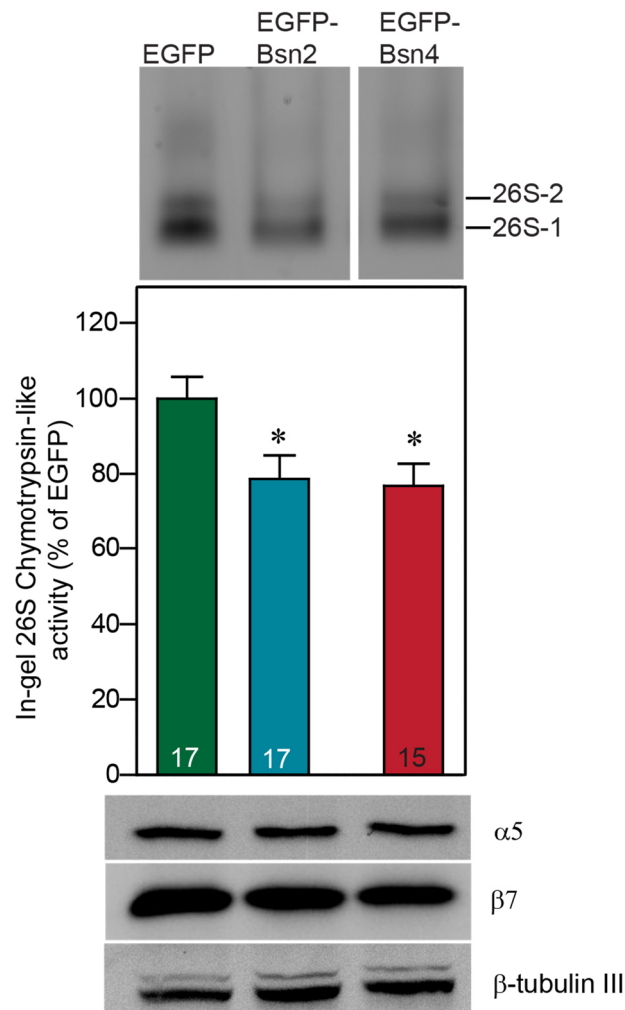


Figure 20. Proteasomal activity is downregulated by bsn overexpression. Cell extracts from EGFP-Bsn2, EGFP-Bsn4 or EGFP-expressing HEK293T cells were subjected to native-PAGE and examined for proteasome activity by the in-gel overlay activity assay using Suc-LLVY-AMC. Quantification of 26S band intensity revealed a substantial decrease in the activity of the proteasome in cells expressing bsn fragments, without concomitant alternations in the protein levels of 20S proteasomal α and β subunits as represented by staining against $\alpha 5$ and $\beta 7$. β -tubulin III served as a loading control. Proteasome configurations are assigned. 26S-2 represents doubly capped proteasome, 26S-1-singly capped proteasome. Values in bars indicate *n* number which corresponds to the number of loadings from three different experiments, performed on three independent HEK293T cell cultures. Data indicate mean \pm SEM. One-way ANOVA with Bonferroni post-test was used for statistics. * $p < 0.05$

Thus far, our data establish that bsn exerts negative control over proteasome, curbing effectively its activity. This is an exciting discovery, as bsn could potentially play a role in the regulation of presynaptic proteostasis.

Although, proteasome activity assay with fluorogenic peptides represents a widely used method to monitor proteasome activity, it does not consider the importance of ubiquitination reaction for the efficient protein degradation. In order to characterize the effect of bsn on the entire ubiquitin-proteasome machinery, we took advantage of the fluorescent ubiquitin-proteasome reporter. This reporter consists of a destabilized GFP molecule coupled to an Ub moiety with a mutation introduced in the last glycine residue, Gly76, in order to prevent the action of deubiquitinating enzymes (Dantuma et al., 2000). Under normal conditions this reporter is constantly sent for proteasomal degradation and emits fluorescence only at a low level. Upon proteasome inhibition/impairment the fluorescence increases substantially due to the accumulation of the fluorescent reporter protein (Figure 21A). Thus, this probe reflects changes in the UPS that depend on the concerted action of both ubiquitination and proteasome degradation. To evaluate the impact of bsn on UPS function, we expressed the reporter in HEK293T cells together with mRFP-tagged bsn fragments: mRFP-Bsn2 and mRFP-Bsn4. Next, we measured the fluorescent signal of UbG76V-GFP reporter from cells expressing either of bsn pieces or RFP as a control. We observed a significant increase in the fluorescence signal, which is inversely proportional to the activity of 26S, indicating that UPS activity is considerably impeded in presence of both interacting bsn fragments (Figure 21B; mRFP-Bsn2: $134 \pm 12\%$ of ctrl, mRFP-Bsn4: $394 \pm 48\%$ of ctrl). A huge increase in the fluorescence upon mRFP-Bsn4 expression was somehow unexpected and does not go in line with our previous experiments, where we demonstrated essentially smaller activity changes in the presence of this fragment, however this rise was consistently observed in each experiment (Figure 21C). As ubiquitin-proteasome pathway is not only restricted to hydrolytic activity of the proteasomes but also includes E1-E3 enzymatic cascade and a plethora of deubiquitinating enzymes, the extreme increase in the fluorescence signal in mRFP-Bsn4-expressing cells could be a complex result of deregulation of the proteasome activity and plausible impact of bsn on the distinct members of the ubiquitination pathway.

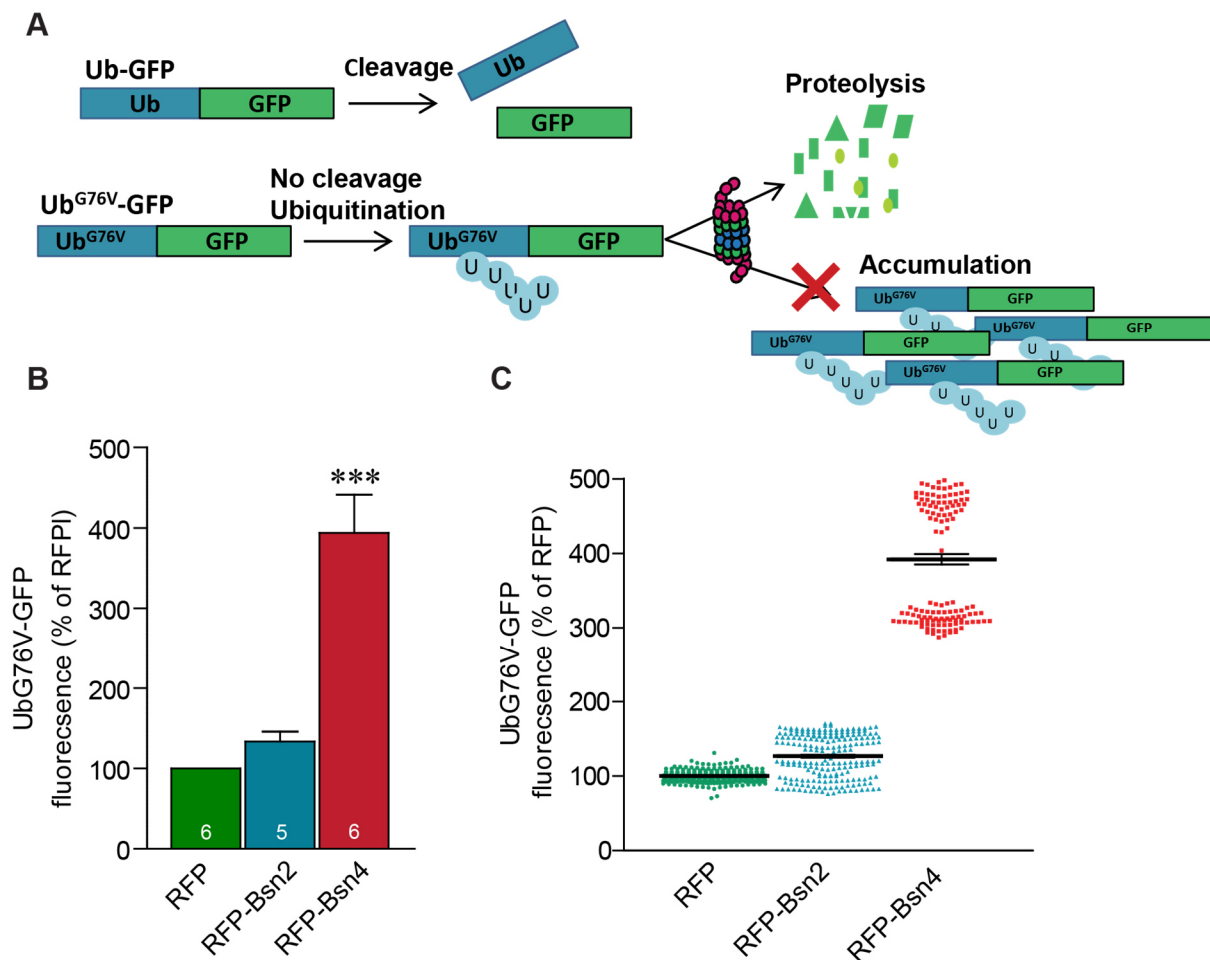


Figure 21. Bsn overexpression induces accumulation of ubiquitin-proteasome reporter. (A) Schematic cartoon of Ub-GFP and Ub^{G76V}-GFP. The Ub-GFP is cleaved, leading to release of a stable GFP molecule. Contrary, the Ub^{G76V}-GFP reporter, that contains a mutation in the terminal residue of ubiquitin, cannot undergo cleavage and as a result is polyubiquitinated and send for degradation by the proteasome. Block of proteasome activity triggers accumulation of the reporter and increase in the fluorescence signal. (B) Co-expression of Ub^{G76V}-GFP and RFP-Bsn2, RFP-Bsn4 or RFP as a control reveals a marked accumulation of the reporter upon bsn expression, with a bigger effect of RFP-Bsn4 fragment. (C) Scatter plot of all normalized values from four to seven independent experiments, shows reproducibility of the assay. Values in bars indicate *n* number which corresponds to the averaged values from five to six different experiments, performed on independent HEK293T cell cultures Data indicate mean ± SEM. Unpaired Student's *t*-test was used for statistics, ****p*<0.001

Since, bsn is a neuron-specific protein, engaged in the coordination of neurotransmitter release, we wondered whether it could impact proteasome activity in the neuron-specific context. To this end, we infected rat cortical neuron cultures with bsn constructs EGFP-Bsn2 and EGFP-Bsn4 or EGFP as a control, using lentiviral vectors. This system is perfectly tailored for gene delivery into neurons as lentiviral vectors transduce post-mitotic, non-dividing cells, a prominent feature of neurons. In addition, this technique is characterised by relatively

low toxicity, large packaging capacity and efficient, long-term expression of the transgene. Two weeks after infection, at 18 DIV, cortical neuronal cultures were subjected to lysis and the activity of the proteasome was assayed by the means of the fluorogenic peptide substrate. The assessment of the proteasome activity revealed a substantial downregulation upon expression of the two bsn fragments (Figure 22; EFP-Bsn2: $80 \pm 5\%$ of ctrl, EFP-Bsn4: $83 \pm 3\%$ of ctrl). These experiments are crucial as they demonstrate that bsn can, indeed, function as the neuron-specific inhibitor of the proteasome activity.

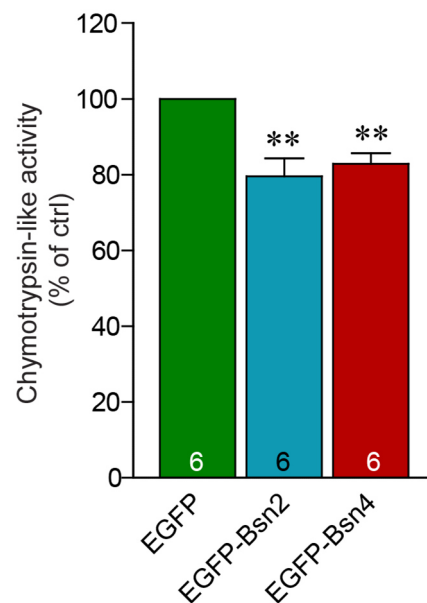


Figure 22. Proteasome activity is significantly decreased upon bsn expression in cortical neuronal cultures. Neurons were infected at 4 DIV with EGFP-Bsn2 and EGFP-Bsn4 or EGFP alone as a control. Activity of the proteasome was measured at 17 DIV. Values in bars denote *n* number which corresponds to the number of flasks from three independent experiments performed on three distinct HEK293T cell cultures. Data are displayed as mean \pm SEM. Statistical significance of differences in parameters was evaluated by unpaired Student's *t*-test, ** $p < 0.01$

3.5 Bsn deficiency modulates proteasome activity

The battery of experiments conducted in HEK293T cells as well as cultured cortical rat neurons, showed that bsn overexpression has functional consequences on the proteasome activity- inhibiting the action of 20S and 26S proteasomes *in vitro* as well as in the intact cells. These results hint at the possibility of bsn being negative regulator of the proteasome action.

To further explore this hypothesis, in the first array of experiments, we set to particularly investigate brain proteasomes. Initially, we isolated cortices and hippocampi from wild type C57BL/6 mice and subjected them to differential and density gradient centrifugation. In the following steps, we measured and compared the activity of the proteasome in distinct brain fractions using fluorogenic peptide substrate against chymotrypsin activity. All brain fractions contained active proteasomes with similar activity profiles (Figure 23A; homogenate: 83403 ± 528 a.u, S2: 68084 ± 344 a.u, P2: 53159 ± 998 a.u, synaptosomes: 56240 ± 1366 a.u). It is important to highlight that substantial activity was detected in P2 fraction, representing crude synaptosome pellet as well as in the purified synaptosomal fraction (although the fractions cannot be compared between each other due to the different amount of protein extract in the synaptosomal and other fractions). Importantly, this indicates that functional proteasomes are also present at synapses, where they can influence and modify synaptic strength and plasticity. Moreover, to demonstrate the efficacy of the assay, we investigated the activity of the proteasome upon MG132 treatment. MG132 acts as a specific proteasome inhibitor and in our experimental design, it effectively blocked proteasome activity in each fraction by roughly 70-80% (Figure 23B; homogenate: $18 \pm 1\%$ of ctrl, S2: $14 \pm 1\%$ of ctrl, P2: $22 \pm 4\%$ of ctrl, synaptosomes: $16 \pm 2\%$ of ctrl).

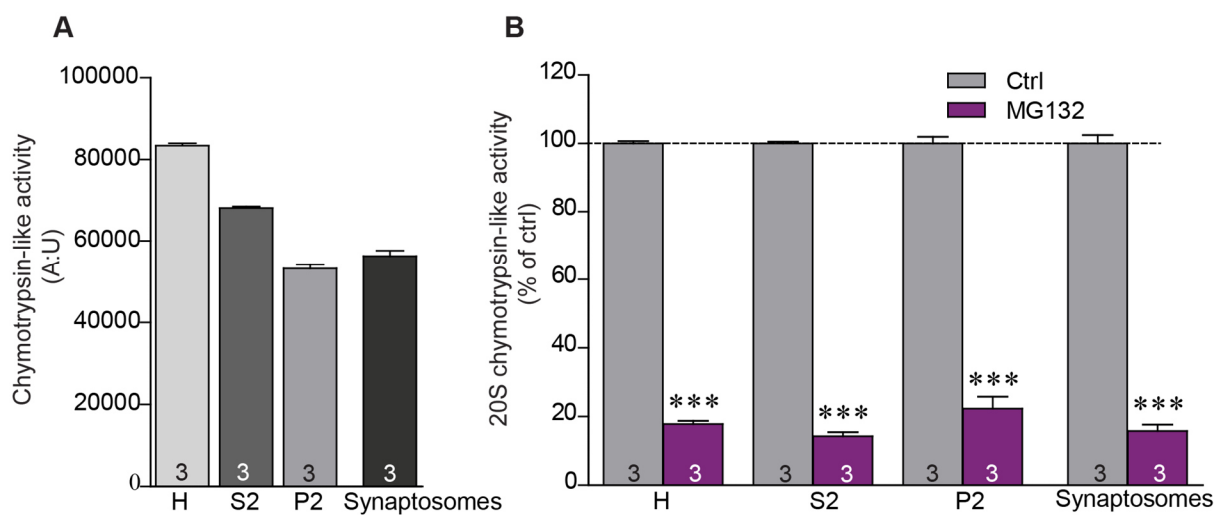


Figure 23. Different brain fractions contain active proteasomes, sensitive to pharmacological inhibition. (A) Equal amount of protein extract from different brain fractions was subjected to proteasome activity measurements. The activity was detected in the cytosolic as well as synaptic extracts and expressed as arbitrary fluorescence units (A.U). (B) Proteasome activity from different brain fractions is essentially impeded by the treatment with widely-used proteasome inhibitor MG132. Individual brain fractions are indicated: H, homogenate; S2, crude cytosolic; P2 crude synaptosomal fraction. Values in bars represent *n* number which corresponds to the number of animals. Data are representative of two independent experiments and indicate mean \pm SEM. Student's *t*-test was used for statistics.

Results

These experiments were performed by Eneko Pina and constitute a part of the Master thesis: “The role of UPS-dependent protein degradation in amyloid beta induced presynaptic plasticity”.

To gain insight into the role of bsn in the regulation of the proteasome activity, we performed similar experiments as described in the previous section. Cortices and hippocampi from bsn knockout animals (BGT) as well as their wild type littermates were isolated and submitted to subcellular brain fractionation. Compellingly, we observed a significant increase in proteasome activity in BGT animals in each investigated fraction (Figure 24; homogenate: $195 \pm 6\%$ of wt, S2: $163 \pm 6\%$ of wt, P2: $1601 \pm 3\%$ of wt, synaptosomes: $148 \pm 19\%$ of wt). These results are highly encouraging, as they suggest that constitutive deprivation of bsn induces alternations in the proteasome activity.

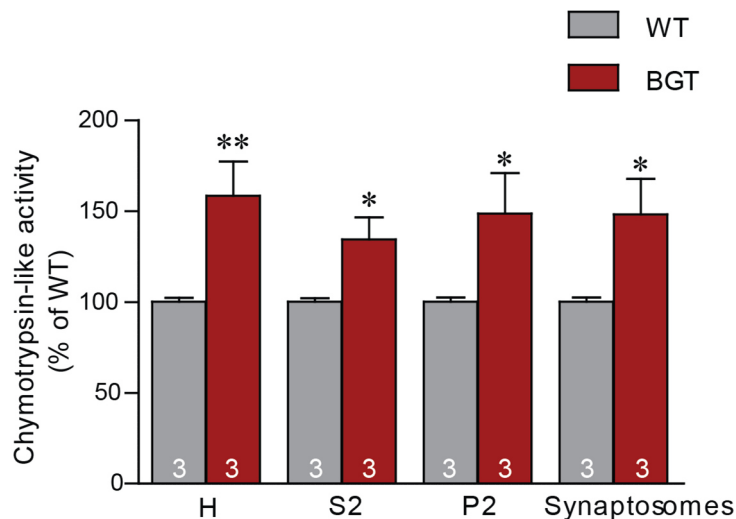


Figure 24. Proteasome activity is increased in fractions of brain lysate of BGT mice. Equal amount of protein extract from different brain fractions of BGT mice and their wild type littermates was assayed for proteasome activity using Suc-LLVY-AMC. These experiments revealed a significant upregulation in chymotrypsin-like proteasome activity in all brain fractions from BGT mice under investigation. Individual brain fractions are indicated: H homogenate, S2 crude cytoplasmic fraction, P2 crude synaptosomal extract. Values in bars denote *n* number which corresponds to the number of animals. Data are representative of two independent experiments, performed in duplicates or triplicates from three mice per genotype and indicate mean \pm SEM. Statistical analysis was done using Student's *t*-test. **p* < 0.05, ***p* < 0.01. These experiments were performed by Eneko Pina and constitute a part of the Master thesis: “The role of UPS-dependent protein degradation in amyloid beta induced presynaptic plasticity”.

To further corroborate these data, we performed native-PAGE, followed by in-gel overlay assay. Slightly modified protocol for subcellular brain fractionation, relying on differential centrifugation and including hypotonic lysis of the crude synaptosome fraction, was

implemented. However, we were only able to visualize proteasome subspecies originating from homogenate and S2 fractions, probably because the activity of the proteasome from synaptic preparation was too low to be detected, as the presence of the proteasome at synaptic sites was substantiated by Western blotting against proteasomal core subunits (Figure 25C). Albeit the overall level of 20S proteasomes, assessed by immunoblotting against $\alpha 5$ core subunit, was unchanged in BGT mice and their WT littermates, a considerable increase of proteasomal activity in BGT animals was observed. Noteworthy, this increase was not only restricted to 26S but included also 20S CP (Figure 25B; 26S homogenate $175 \pm 12\%$ of wt, S2 $183 \pm 15\%$ of wt; 20S homogenate $187 \pm 18\%$ of wt, S2 $186 \pm 12\%$ of wt).

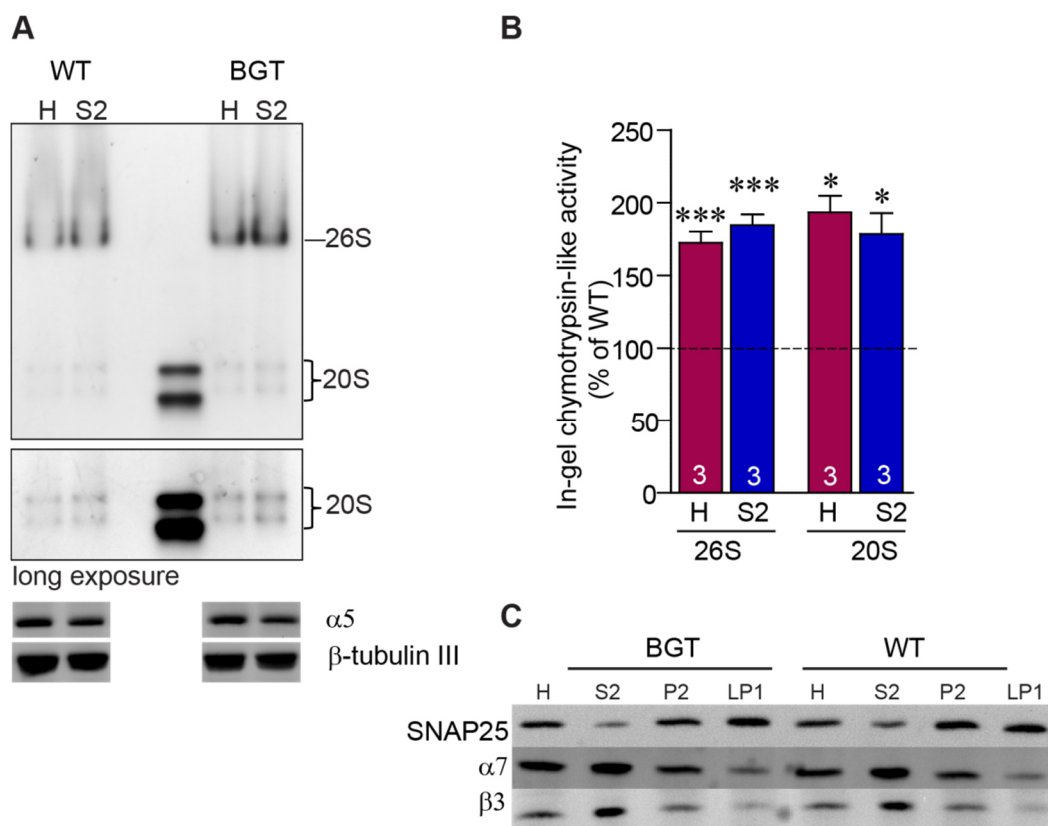


Figure 25. Mice deficient in bsn upregulate the activity of both 26S and 20S proteasome. Subcellular fractionation of brain tissue was followed by native-PAGE electrophoresis that preserves complex integrity. Activity of the proteasomes from distinct brain fractions was analysed by (A) in-gel activity assay. Protein levels of 20S component- $\alpha 5$ subunit, are not changed in the absence of bsn as verified by Western blot. β -tubulin III served as a loading control. (B) Quantification of 26S as well as 20S proteasome activity revealed an upregulation of the activity of both proteasome subspecies in homogenate (H) and crude cytoplasmic (S2) fraction from BGT mice. Values in bars denote *n* number which corresponds to the number of animals. Data are representative of two to three independent experiments, performed in duplicates or triplicates from three mice per genotype and indicate mean \pm SEM. Statistical analysis was done using Student's *t*-test, * $p < 0.05$, *** $p < 0.001$. (C) Subcellular brain fractionation from BGT and their WT littermates demonstrates that proteasome can be found

at synapses and in association with plasmatic membranes. Respective brain fractions are designated: H homogenate, S2 crude cytoplasmic fraction, P2 crude synaptosomal extract, LP1 synaptosomal plasmatic membrane fraction. SNAP25 served as a marker for plasma membrane fraction.

Altogether, our data imply that proteasome activity is greatly enhanced in the absence of bsn, which may bear major consequences for the correct neuronal function and ultimately influence synaptic health.

3.6 Bsn interferes with proteasome assembly

Thereafter, we wondered what could be the underlying mechanism behind bsn-mediated reduction of the proteasome activity. Proteasome is an extremely intricate organelle and its assembly into 20S as well as 26S complex is a stepwise process that requires a set of dedicated chaperon proteins. Since our interaction studies implied that bsn binds PSMB4, a 20S proteasome subunit indispensable for the successful dimerization of two half-proteasomes, we tested whether bsn hampers this step. The assembly of 20S CP proceeds through a few intermediate species and is accompanied by two pairs of heterodimer chaperons PAC1-PAC2 and PAC3-PAC4 as well as Ump1.

To differentiate between distinct proteasome species and assembly intermediates we employed density glycerol gradient ultracentrifugation. This method relies upon rate zonal centrifugation in a linear glycerol gradient, where molecules migrate according to their mass and shape and can be subsequently collected into separate fractions.

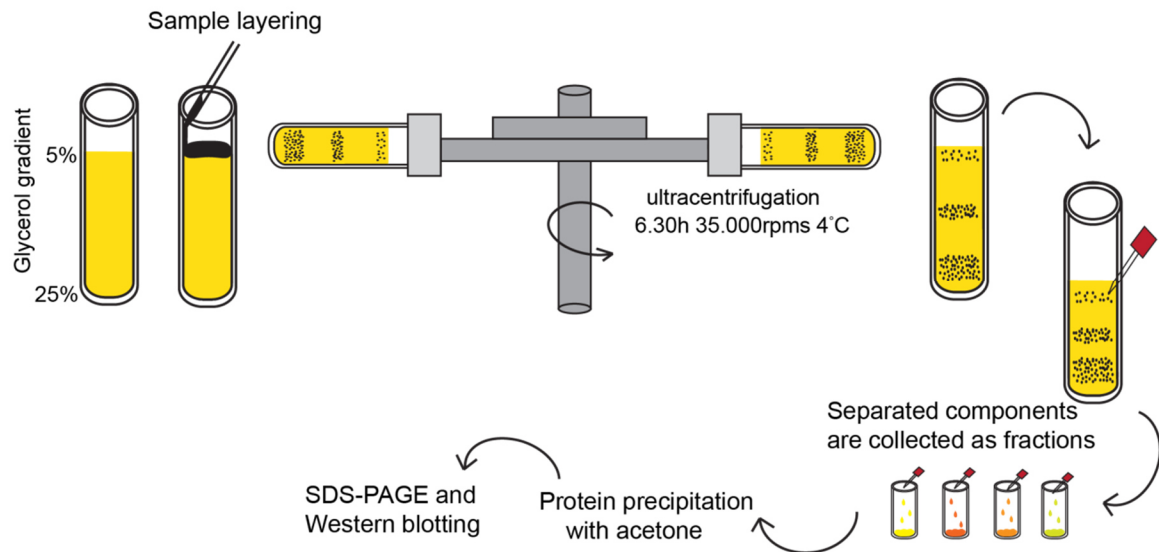


Figure 26. Separation of proteasome species by density glycerol gradient ultracentrifugation. Schematic representation of glycerol gradient ultracentrifugation. Light (5%) and heavy (25%) glycerol fractions are layered and the continuous gradient is generated automatically. Subsequently, the sample (HEK293T lysate) is laid atop the gradient and centrifuged at 4°C for 6.30 h at 35.000 rpm. Separated components are collected, from the top, into distinct fractions, precipitated by acetone and analyzed by SDS-PAGE and Western blotting.

To test the experimental set-up we first applied purified human 20S as well as 26S proteasomes on top of a preformed 5-25% glycerol gradient and centrifuged for 6.30 h in a swinging bucket type rotor (MLS-50) at 35.000 rpm. After the run, samples were collected into 14 fractions and subjected to acetone precipitation to concentrate proteins. Subsequently, fractions were resolved by SDS-PAGE electrophoresis and analysed by Western blotting (Figure 26A). Membranes were probed with antibodies against proteasome integral subunits and chaperons. Our results demonstrate that fractions 6 and 7 contain mostly 20S particles as these fractions consist of a large amounts of $\alpha 6$, $\alpha 7$, $\beta 2$ and $\beta 7$ subunits but lack immunoreactivity for PAC1 chaperon, $\beta 2$ propeptide and Rpt3 and Rpt6 19S/26S components. Fractions 9-11 are enriched in Rpt3 and Rpt6 as well as α and β subunits and thus represent 26S proteasomes (Figure 27A-D). Fractions 2-4 were assigned as assembly intermediates characterised by the presence of PAC1 chaperone and unprocessed $\beta 2$ propeptides. Quantitative analysis of these experiments revealed a significant enrichment of PAC1 in the fractions 2-4, containing assembly intermediates, in cells expressing bsn fragments compared to EGFP expressing control (Figure 27E). Moreover, the quantification revealed a shift in the distribution of $\beta 2$ and $\beta 7$ subunit towards lighter fractions upon

overexpression of EGFP-Bsn4, further supporting that this fragment might interfere with the normal proteasome assembly (Figure 27F,G).

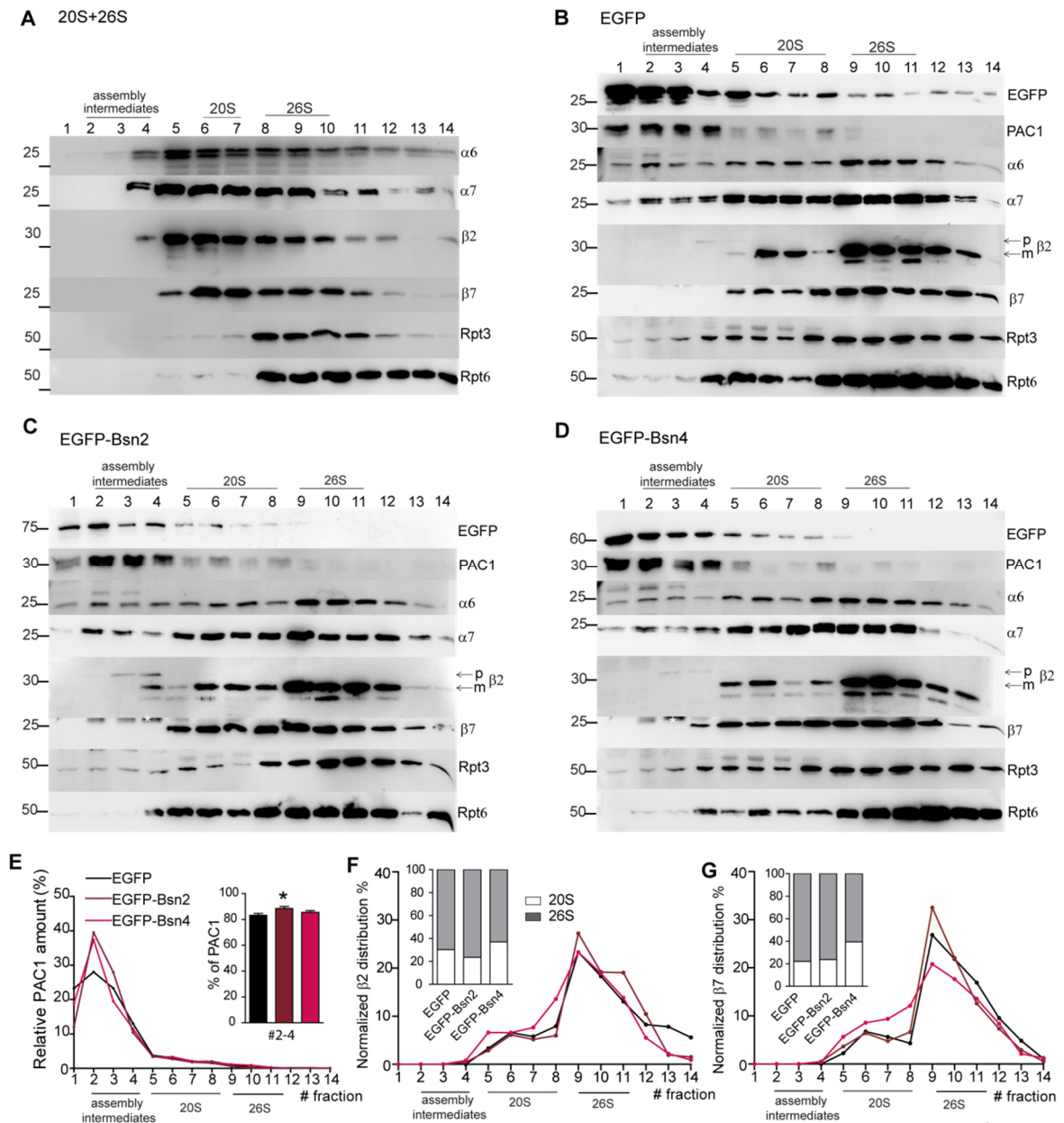


Figure 27. Bsn overexpression impairs proteasome assembly. (A) Glycerol density gradient centrifugation (5%-25%) of purified human 26S and 20S proteasomes. The resultant fractions were immunoblotted with the indicated antibodies.(B, C, D) Glycerol density gradient centrifugation of extracts of HEK293T cells transfected with EGFP, EGFP-Bsn2 or EGFP-Bsn4. Fractions were immunoblotted for indicated proteins. Asterisks denote nonspecific bands. p, precursor; m, mature. (E) Relative protein distribution for PAC1 plotted from glycerol density gradient fractionation experiments normalized to the total protein and expressed in %. The inset depicts accumulation of PAC1 in the assembly intermediate fractions (2-4) from HEK293T cells expressing either EGFP, EGFP-Bsn2 or EGFP-Bsn4. (F, G) Normalized protein distribution for $\beta 2$ and $\beta 7$ subunits plotted from glycerol density gradient fractionation experiments and expressed in %. The inset contains stacked bar graph illustrating accumulation of $\beta 2$ and $\beta 7$ subunits in 20S and 26S fractions from HEK293T cells expressing EGFP, EGFP-Bsn2 or EGFP-Bsn4. The graph depicts the data quantified from seven

different experiments performed on seven independent HEK 293T cell cultures. *p*-values versus control (EGFP) by unpaired two-tailed Student's *t*-test, **p*<0.05

3.7 Bsn overexpression does not induce changes in the SV pool sizes

Recent evidence suggests that proteasome supports neurotransmitter release and modulates synaptic vesicle pool sizes (Willeumier et al., 2006; Yao et al., 2007). Importantly, active zone proteins can also coordinate the function of the UPS. Essentially, bsn and pclo are involved in the regulation of presynaptic ubiquitination and proteostasis by directly binding E3 ligase SIAH1 (Waites et al., 2013).

To directly examine whether the interaction between bsn and proteasome could have an impact on the release efficacy by modifying SV pool sizes, we measured the SV pool turnover at individual synapses by the means of pH-sensitive cyanine dye, CypHer5E (CypHer). This dye is coupled to the antibody against luminal domain of synaptotagmin1 (Syt1-CypHer), an integral synaptic vesicle protein, and exhibits maximal fluorescence in the acidic (pH≈5.5) milieu of the synaptic vesicle. Upon exocytosis and exposure to more neutral pH its fluorescence is quenched (Figure 28B). Following compensatory endocytosis and reacidification, however, the fluorescence of the dye increases again. This assay is, thus, perfectly tailored to sense and indicate differences in the pH between SV lumen and extracellular environment to reliably report presynaptic activity. In order to accurately estimate the size of the synaptic vesicle pools, we applied bafilomycin, a vesicular proton pump (V-type ATPase) inhibitor that prevents reacidification and traps vesicles in the alkaline state, so that they cannot contribute to the further increases in fluorescence upon another fusion cycle (Burrone et al., 2006).

Using lentiviral vectors, we transduced cultured hippocampal neurons with either control, EGFP-Bsn2 or EGFP-Bsn4-expressing constructs. Mature neurons (16-17 DIV) were labelled with anti-Syt1-CypHer antibody during 2-3 h incubation and imaged. To trigger firing of action potentials, we used electric field stimulation. First, we delivered 40 pulses to release all the vesicles that are in the close vicinity to the presynaptic membrane and are therefore competent for the immediate exocytosis (so called readily releasable pool, RRP), next, after brief (2 min) period of recovery, we applied 200 AP to deplete entire recycling population of vesicles. Only synapses showing simultaneously expression of bsn fragments and Syt1-CypHer staining were considered for the analysis. Initially, we assessed the efficiency of dye labelling during spontaneous anti-Syt1-CypHer antibody uptake. Quantification of

Results

fluorescence intensity at rest, before the onset of stimulation, revealed no major changes between control and bsn-infected neurons (Figure 28D; EGFP: 516 ± 53 a.u.; EGFP-Bsn2: 548 ± 101 a.u.; EGFP-Bsn4: 523 ± 103 a.u.) Calculation of synaptic vesicular pool sizes reported no alternations in the RRP fraction upon bsn expression (Figure 28E, F; **RRP**, EGFP: -0.14 ± 0.006 ; EGFP-Bsn2: -0.14 ± 0.006 ; EGFP-Bsn4: -0.13 ± 0.008), nor in the RP fraction (Figure 26E, F; **RP**, EGFP: -0.33 ± 0.02 ; EGFP-Bsn2: -0.32 ± 0.02 ; EGFP-Bsn4: -0.30 ± 0.02). A possible explanation for this set of data is that modulation of SVs pools by the short bsn fragments is not fully manifested in the presence of endogenous bsn, moreover the short fragments contain only partial information about bsn structure and function and are not precisely localized to the presynaptic active zone but rather diffusely expressed in the presynapse, as suggested by previous studies (Dresbach et al., 2003; Maas et al., 2012).

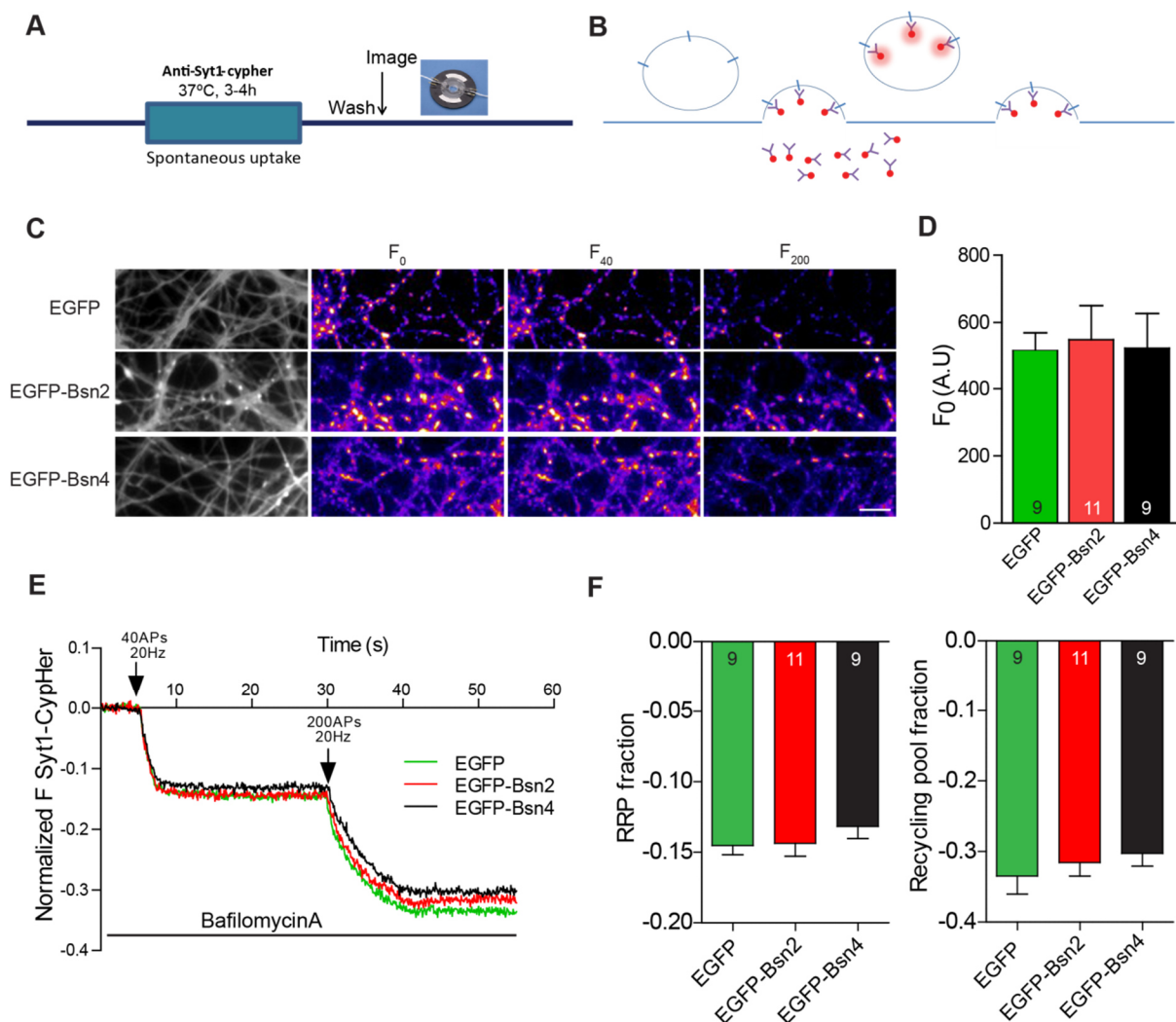


Figure 28. Long term expression of short bsn fragments does not modulate synaptic vesicle pool sizes. (A,B) Schematic representation of the imaging protocol: three to four hours prior to imaging

neurons were incubated with anti-Syt1-cypHer antibody that labels recycling vesicles. Just before the experiment, cells were washed with Tyrode's buffer, placed in the imaging chamber and imaged. (C) Representative images of mature hippocampal neurons expressing EGFP, EGFP-Bsn2 or EGFP-Bsn4 and incubated with anti-Syt1-cypHer antibody. The images before the stimulus (F_0), after 40APs (F_{40}) and after 200APs (F_{200}) are shown. Neurons were infected at 4 DIV and imaged at day 16-17. Scale bar is 5 μm . (D) Quantification of the intensity of the dye uploading after spontaneous labelling for 2-3 h. (E) Averaged time traces from neurons expressing EGFP, EGFP-Bsn2 or EGFP-Bsn4. Statistical analysis of (F) RRP fraction as well as RP pool. Numbers within columns denote the number of analysed cells. Data are representative of three to four independent experiments and indicate mean \pm SEM. One-way ANOVA with Bonferroni post-test was used for statistics.

We also surmised that such a long overexpression of bsn fragments (about two weeks) might mask possible changes in the pool sizes due to the contribution of the compensatory mechanisms that would become activated to maintain SV homeostasis. Therefore, we infected mature hippocampal neurons (14 DIV) with lentiviral bsn vectors and performed live cell imaging two days after. Acute overexpression of bsn fragment EGFP-Bsn4, at a later stage of maturation, substantially compromised neuronal health, hence only control neurons and EGFP-Bsn2-expressing cells were analysed. Here again, we noticed no alternations in the size of the RRP (Figure 29A, B; **RRP**, EGFP: -0.17 ± 0.01 ; EGFP-Bsn2: -0.17 ± 0.01), nor in the content of RP in neurons expressing EGFP-Bsn2 bsn fragment (Figure 29A, C; **RP**, EGFP: -0.42 ± 0.02 ; EGFP-Bsn2: -0.39 ± 0.03).

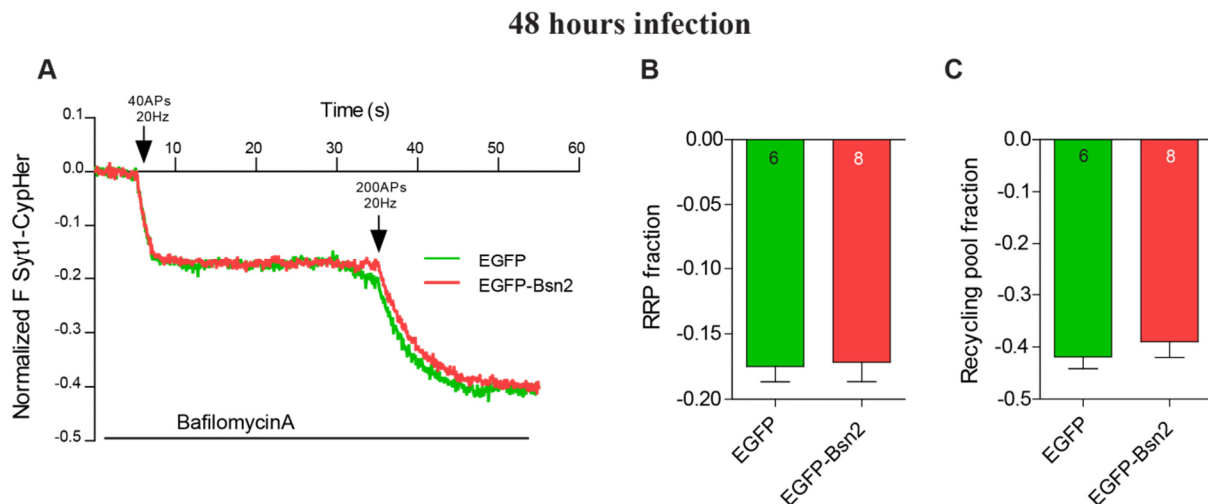


Figure 29. Short term expression of short bsn fragments does not influence synaptic vesicle pool sizes. (A) Representative time traces of neurons expressing EGFP or EGFP-Bsn2. Cells were infected at 14 DIV and imaged at 16 DIV. Quantification of (B) RRP and (C) recycling pool fraction. Numbers within columns represent the number of analysed cells. Data are from three independent experiments and indicate mean \pm SEM. Statistical analysis was done using Student's *t*-test.

3.8 Bsn and proteasome intersect to trigger alternations in the SV pool sizes

These results prompted us to scrutinize the effect of bsn-proteasome interaction on the bsn knockout background. To this end, we monitored the size of SVs pools in the mouse hippocampal knockout neurons using a genetically encoded GFP-derived probe, called pHluorin, introduced to the cultures by the means of lentiviral expression plasmid. This probe consists of another synaptic vesicle protein: synaptophysin fused to a pH-sensitive variant of GFP molecule (sypHy), whose fluorescence is quenched in the acidic environment of SV lumen, however becomes visible following exocytosis and exposure to extracellular pH- the change in fluorescence is therefore opposite to that reported by CypHer (Figure 30A) (Burrone et al., 2006). Vesicles refractory to the simulation, so called resting pool (RtP), are visualized by NH₄Cl application, which alkalizes SV lumen and thereby unquenches entire sypHy-expressing vesicle population.

To investigate the contribution of the proteasome to vesicle pool regulation on the bsn knockout background, we treated neurons with different proteasome inhibitors 2 h prior to imaging experiments. 2 h treatment is a well-established time window that has been shown to induce a substantial increase in the recycling pool of SVs (Willeumier et al., 2006). We applied different proteasome inhibitors as these drugs display distinct pharmacodynamics. We employed two naturally occurring microbial proteasome inhibitors: lactacystin and epoxomicin as well as a synthetic blocker of the proteasomal activity MG132. Although all the compounds target chymotrypsin-like activity of the 20S proteasome, they vary in selectivity, potency and reversibility of inhibition. Consequently, MG132 is the most widely used, reversible inhibitor, which at the same time is the least selective of the three drugs as it also blocks calpains and disparate lysosomal cathepsins. Therefore, in order to confirm the involvement of proteasome it is necessary to implement more specific inhibitors. However, because lactacystin has been shown to inhibit lysosomal cathepsin A, epoxomicin constitutes the most selective and irreversible inhibitor of the proteasome activity (Kisselev and Goldberg, 2001). After incubation with the proteasome inhibitors, neurons were subjected to imaging. We delivered 40 AP at 20 Hz to release RRP and 900 AP at 20 Hz to mobilize RP, followed by NH₄Cl pulse to visualize RtP.

Results

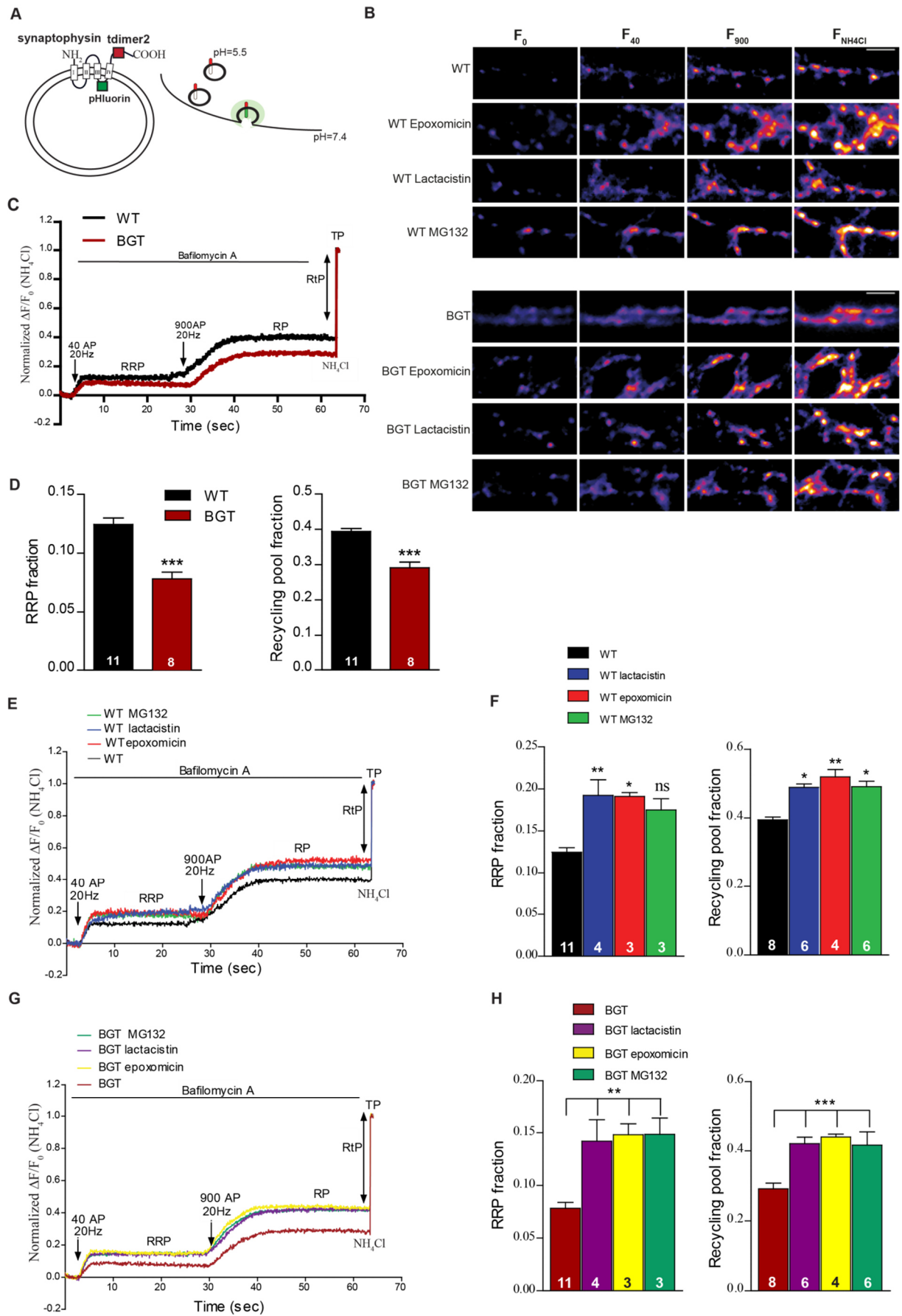


Figure 30. Bsn and proteasome collectively participate in the regulation of synaptic vesicle pools. (A) Schematic cartoon of synaptophysin (sypHy) and the principle behind it. Superecliptic pHluorin is introduced between third and fourth transmembrane domains of synaptophysin and faces the vesicular lumen, whereas dimeric RFP (t-dimer2) is localised to the C-terminus. At rest, the fluorescence of sypHy is quenched. Upon fusion of the vesicles with the plasma membrane and exposure to more neutral extracellular environment fluorescence increases. (B) Representative images of mature hippocampal neurons expressing sypHy before the stimulation (F_0), after 40APs (F_{40}), 900APs (F_{900}) and NH_4Cl application ($F_{\text{NH}_4\text{Cl}}$) (C) Representative average traces from WT and BGT cells. (D) Quantification of the responses in (C) reveals a substantial decrease in RRP and RP in BGT neurons. (E) Representative average traces from WT cells treated with three independent proteasome blockers. Inhibition of the proteasome activity triggers a significant increase in (F) RRP as well as recycling pool of synaptic vesicles. (G) Representative average traces from BGT neurons incubated with three independent proteasome inhibitors. (H) Quantification of mean values of RRP and RP reveals a considerable upregulation of both pools in BGT neurons. Number of analysed cells is indicated within columns. Data are pooled from at least three independent experiments, analysed format least two independent cultures and indicate mean \pm SEM. One-way ANOVA with Bonferroni post-test was used for statistical comparison, * $p < 0.05$, ** $p < 0.01$, *** $p < 0.001$. These experiments were performed by Dr. Carolina Montenegro.

Quantification of the responses revealed a considerable decrease in the size of RRP as well as RP in the BGT neurons as compared to neurons from their wt littermates (Figure 30C, D; **RRP**: wt 0.124 ± 0.00545 ; BGT 0.0787 ± 0.0056 ; **RP**: wt 0.39 ± 0.008 ; bgt 0.29 ± 0.016). In line with already published literature, inhibiting proteasomal activity, with three different, structurally unrelated blockers, triggered a significant upregulation of both RRP and RP in wt cells (Figure 30E, F; **RRP**: wt 0.12 ± 0.005 ; wt/lactacystin 0.19 ± 0.02 ; wt/epoxomicin 0.19 ± 0.005 ; wt/MG132 0.18 ± 0.13 ; **RP**: wt 0.39 ± 0.008 ; wt/lactacystin 0.49 ± 0.01 ; wt/epoxomicin 0.5 ± 0.02 ; wt/MG132 0.05 ± 0.02). Under proteasomal inhibition, BGT cells were still able to substantially increase RRP (Figure 30G, H; **RRP**: BGT 0.08 ± 0.006 ; wt 0.12 ± 0.005 ; BGT/lactacystin 0.14 ± 0.02 ; BGT/epoxomicin 0.15 ± 0.01 ; BGT/MG132 0.15 ± 0.015). Interestingly, pharmacological block of the proteasome activity in BGT cells also restored RP fraction (Figure 30G, H; **RP**: BGT 0.29 ± 0.016 ; wt 0.39 ± 0.008 ; BGT/lactacystin 0.42 ± 0.02 ; BGT/epoxomicin 0.44 ± 0.008 ; BGT/MG132 0.42 ± 0.04). These data imply that impeding overactive proteasome in bsn-deprived neurons may rescue defects in the pool of the recycling vesicles.

To better illustrate the impact of the proteasome on synaptic vesicle pool sizes on bsn knockout background, we quantified fold changes in the increase of vesicular pools upon treatment with diverse proteasome inhibitors relative to the size of the respective pool before the proteasome block in each genotype. If proteasome plays a role in the SV pool turnover via interaction with bsn, a bigger effect of inhibition on the SVs pools fraction in BGT animals

should be observed. Indeed, our results reveal that proteasome assists in the recruitment of synaptic vesicles to releasable pool, partially, in bsn-dependent fashion. We noticed a significantly higher increase in the RP, but not in RRP fraction, in proteasome blocker-treated BGT animals (Figure 31A,B; **RPP**: wt/lactacystin $155 \pm 15\%$; wt/epoxomicin $153 \pm 4\%$; wt/MG132 $141 \pm 11\%$; bgt/lactacystin 182 ± 26 ; bgt/epoxomicin $189 \pm 13\%$; BGT/MG132 $190 \pm 20\%$; Figure 31A,C; **RP**: wt/lactacystin $125 \pm 3\%$; wt/epoxomicin $132 \pm 5\%$; wt/MG132 $124 \pm 4\%$; BGT/lactacystin $144 \pm 7\%$; BGT/epoxomicin $151 \pm 3\%$; BGT/MG132 $133 \pm 17\%$). Collectively, our data demonstrate that bsn is an essential organiser of the SV pool sizes and that SVs homeostasis becomes easily upset in the absence of this protein. Essentially, we also show that proteasome acts as a major contributor to SV pool turnover and that curbing its activity in the BGT animals might have beneficial effects.

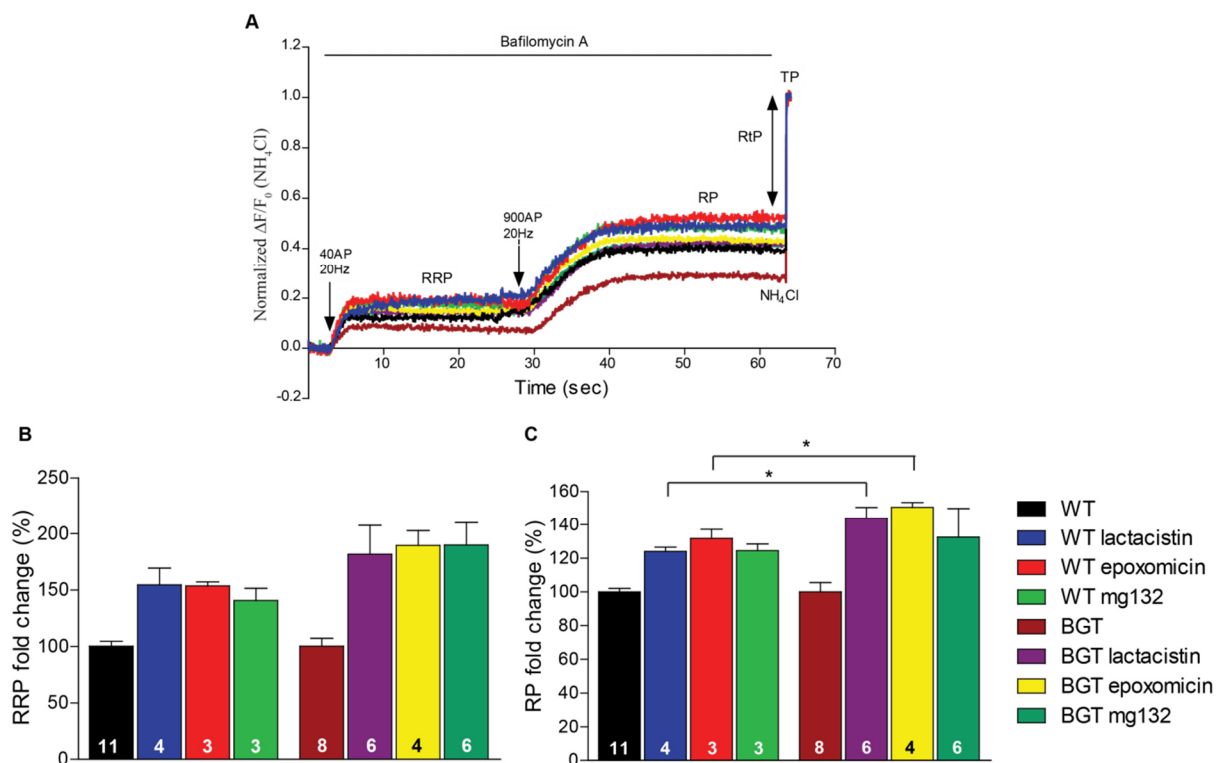


Figure 31. Proteasome inhibition partially rescues decreased pool of synaptic vesicles in BGT animals. (A) Overlaid average times traces for WT as well as BGT neurons. (B) RRP fraction calculated and expressed as a percentage change. Values were normalized to the control of the respective genotype. (C) the same for RP. Number of analysed cells is illustrated within columns. Data are representative of at least three independent experiments, analysed from two independent cultures. Graphs show mean \pm SEM. Student's *t*-test was used for statistical comparison, $*p < 0.05$. Data were provided by Dr. Carolina Montenegro.

4. Discussion

The role of degradation pathways in the support and sustenance of synaptic function is gaining increasing attention. In this work, we identify bsn as an important interacting partner and activity regulator of the presynaptic proteasome. This interplay has crucial implications for synaptic vesicle cycling and maintenance of SV pool homeostasis. Our data set a platform for further studies on presynaptic proteasome and its intersecting pathways with active zone proteins.

4.1 Functional interaction of the active zone protein bsn with a crucial subunit of the 20S proteasome

Presynaptic terminals are structures devised for rapid and reliable release of synaptic vesicle-containing neurotransmitter, which occurs at the specialized regions of presynaptic membrane-AZs. AZs are enriched in a number of proteins important for spatio-temporal organization of synaptic vesicle cycling. In the present study, we focused on one of the biggest constituents of AZs- bsn. We identified a novel interaction partner of bsn, namely a proteasome subunit PSMB4 (called also $\beta 7$). Currently, proteasome is a subject of intense research and together with autophagy-lysosome degradative pathway, it seems to essentially contribute to the clearance of misfolded or no longer needed SV-associated proteins and thus maintenance of SV protein homeostasis and neurotransmitter release (Waites et al., 2013; Okerlund et al., 2017).

Primary, Y2H studies determined Bsn1 (aa 1692-3263), which contains a large central portion of bsn, as a binding partner for PSMB4. Subsequent co-immunoprecipitation experiments, performed from bsn- and PSMB4-expressing HEK293T cell lysates, corroborated binding between these two proteins and, what is more, identified two shorter bsn fragments namely Bsn2 and Bsn4, as major independent interacting regions for the proteasome subunit. Interestingly, further molecular mapping experiments revealed another two individual regions in Bsn2- Bsn7 (aa 1653-1878) and Bsn10 (aa 2013-2087) that associate with PSMB4, suggesting that elaborate intramolecular interactions in bsn might determine its binding with proteasome.

4.1.1 Multiple binding interfaces in Bsn2 are involved in the interaction with PSMB4

We have established Bsn2 (aa 1653-2082) as one of the PSMB4-interacting segments. This interaction was additionally confirmed by the means of co-clustering studies in the living mammalian cells, where overexpressed Bsn2 formed cytoplasmatic inclusions and recruited not only exogenously expressed PSMB4 but also endogenous proteasome as well as ubiquitin apparatus. These experiments unequivocally corroborated that bsn can be found in the complex with or in the vicinity of the functional ubiquitin-proteasome system. Our data, however, do not exclude the possibility that cytoplasmatic bsn clusters induce unfolded protein response and recruit UPS components to direct bsn for degradation, although inhibition of the proteasome did not provoke any accumulation of Bsn2 or Bsn4 fragments as inspected by Western blotting, largely eliminating the assumption that bsn could act as a UPS substrate.

Moreover, we report the presence of two independent PSMB4-interacting regions within Bsn2. A cluster of two closely spaced PSMB4-binding motives implies that multivalent interaction interfaces in bsn are probably involved to correctly establish PSMB4–bsn association.

Curiously, Bsn2 fragment not only binds the proteasome subunit but it also has another binding partner, namely CtBP1, a transcriptional co-repressor protein. Via interaction with CtBP1, bsn regulates its subcellular localization and is therefore indirectly involved in the transcriptional control of neuronal activity-dependent genes (Ivanova et al., 2015). How could one bsn fragment be potentially engaged in the interaction with two distinct proteins? It has been reported that elevating NADH levels substantially increases binding between bsn and CtBP1. Because NADH is largely produced during glycolysis stimulated by high neuronal activity, cellular metabolic state seems to greatly influence the affinity of CtBP1 for bsn. It could be speculated that, whereas, heightened neuronal activity promotes association and retention of CtBP1 at the presynapse, reduced synaptic activity and/or alternations in the cell redox status would encourage interaction between bsn and proteasome. Such an interaction, that prompts proteasome inhibition, could constitute a homeostatic system to spare presynaptic proteome during the times of low synaptic activity and/or direct bsn for degradation. Interestingly, activity-dependent remodeling of pre- as well as postsynaptic proteome has already been investigated (Ehlers, 2003; Lazarevic et al., 2012) and shown to be influenced by the proteasome. Strikingly, it has been suggested that bsn is processed by the

proteasome when neuronal network activity is substantially dampened. Of note is also a recent report which postulates that proteasome, particularly its regulatory 19S complex, can sense changes in the NADH levels, with increased NADH/NAD⁺ ratio culminating in increased 26S level and activity (Tsvetkov et al., 2014). Therefore, metabolic status of the cell seems to affect proteasome activity and conceivably also interaction between proteasome and other proteins.

4.1.2 Bsn4 associates specifically with C-terminus of PSMB4 and acts as a hub for many protein interactions

Further co-immunoprecipitation analysis identified another PSMB4-binding site on bsn -Bsn4 (aa 2715-3013). Bsn4 has already been described to participate in the phosphorylation-dependent interaction with adaptor protein 14-3-3 (Schroder et al., 2013). Therefore, it could be envisaged that while phosphorylation of this bsn fragment by the family of RSK protein kinases enhances binding between bsn and 14-3-3 and favors disassociation of bsn from CAZ constituents, dephosphorylation of Bsn4 or its phosphorylation by another protein kinase encourages bsn-proteasome interaction and presumably recruits proteasome in the vicinity of the AZ. This recruitment would be of utmost importance for molecular remodeling of CAZ network and induction of synaptic plasticity. This idea is quite conceivable as proteasome has been shown to be redistributed from dendritic shafts to dendritic spines in response to increased neuronal activity. Moreover, recruitment of postsynaptic proteasomes is highly dependent on phosphorylation, with kinase CAMKII α acting as a major effector of this process (Bingol and Schuman, 2006; Bingol et al., 2010). Additionally, association of bsn with 14-3-3 could promote its interaction with proteasome. Indeed, studies by *Tai et al* demonstrate that 14-3-3 specifically co-purifies with the synaptic 26S proteasomes. Although a direct interplay between proteasome and 14-3-3 has not yet been established, 14-3-3 proteins have been shown to either prevent or enhance proteasomal degradation of its binding partners. In rat hippocampal neurons, overexpression of 14-3-3 triggers phosphorylation of tau at Ser²⁶², destabilizes microtubules and stimulates proteasomal clearance of synaptophysin (Qureshi et al., 2013), whereas in mammalian HeLa cells, 14-3-3 binds to Cdt2, a component of CRL4^{Cdt2} E3 ligase and rescues it from SCF^{FbxO11}-mediated degradation, promoting, thus, cell cycle progression and proliferation (Dar et al., 2014). However, regardless of a strong link between 14-3-3 proteins and proteasomal degradation, the role of 14-3-3 adaptors in

bridging the interaction between its binding partners and proteasome, to promote non-proteolytic functions, has not been elucidated and awaits further scrutiny.

Furthermore, Bsn4 is involved in the interaction with other two vital AZ constituents, namely RBP and CAST (Wang et al., 2009; Davydova et al., 2014). Via interaction with RBP, bsn specifically recruits P/Q calcium channels to AZs and thus largely contributes to determination of presynaptic efficiency at individual release sites (Davydova et al., 2014). Intriguingly, it has been reported that regulatory subunits of proteasome contain KEKE motifs that bind Ca^{2+} ions, which impedes hydrolysis of peptides (Realini and Rechsteiner, 1995). Intracellular calcium could, thereby, directly regulate proteasomal degradation and bsn, via association with PSMB4 and RBP, would act to position proteasome in the vicinity of calcium channels. Such positioning of proteasomes would allow for the precise remodeling of presynaptic proteome upon action potential-driven calcium influx, simultaneously affecting synaptic strength and plasticity. Bsn4 fragment of bsn, therefore, provides high potential for a crosstalk between molecules found at the presynaptic AZs. Currently, mechanisms implicated in the regulation of these interactions remain elusive. Posttranslational modifications, including not only phosphorylation, but also sumoylation or ubiquitination, could act as a molecular switch to direct interactions between bsn and its multiple binding partners. Such regulation has already been reported for one of the AZ constituents-RIM1 α . When sumoylated, RIM1 α shows increased binding to Cav2.1 calcium channels and thus facilitates vesicle exocytosis and synchronous neurotransmitter release, instead its desumoylation leads to decreased binding and supports maintenance of the AZ structure (Girach et al., 2013). It should be also emphasized that Bsn4 contains coiled-coil domain, which normally promotes formation of homo- or heterooligomeric protein complexes. Liprin- α constitutes a prominent example of a molecule that via its coiled-coil region participates in numerous protein-protein interactions. Its N-terminally located coiled-coil domain contains binding sites for CAZ members: RIMs and ELKS: this domain is also engaged in the establishment of liprin- α homodimers (Schoch et al., 2009).

However, our co-immunoprecipitation experiments revealed that intact Bsn4 fragment is critical in moderating the interaction with PSMB4, and two smaller pieces, Bsn5 as well as Bsn6, which comprises entire third coiled-coil domain, do not exhibit any binding to the proteasome subunit. This indicates that shorter segments of Bsn4 do not possess enough binding interfaces with PSMB4 and that along with coiled-coil regions other structural elements of bsn are essential for its association with the proteasome subunit.

Intriguingly, we also show that association between Bsn4 and PSMB4 was not affected by N-terminal propeptide of PSMB4, but was specifically mediated by C-terminal extension of PSMB4, critical for half-proteasome dimerization. This indicates that bsn could participate in the biogenesis of the proteasome and act as the neuron specific factor responsible for the regulation of the assembly of presynaptic proteasomes. At present, only few proteins are known to interact specifically with PSMB4 subunit of 20S proteasome. Binding between U-box E3 ligase SNEV and mature form of PSMB4 has been proposed to escort ubiquitinated client proteins to the proteasome for their subsequent degradation (Loscher et al., 2005). Furthermore, Nef and Tax, two HIV-derived proteins associate with PSMB4 and presumably modulate proteasome function (Rousset et al., 1996; Rossi et al., 1997), while Smad1, a family member of Smad proteins that act as a major signal transducers of TGF- β family type I receptors and play a prominent role in neuronal development and differentiation, forms a complex with PSMB4 as well as another protein- Az (antienzyme) (Lin et al., 2002) This interaction that occurs at the step of proteasome precursor assembly facilitates targeting and docking of Smad1 to the proteasome for its consecutive degradation (Gruendler et al., 2001; Lin et al., 2002). Yet another protein that functions in an exclusively neuronal context and is involved in autosomal-recessive non-syndromic mental retardation, namely-cereblon (CRBN) has been described to interact with PSMB4 (Lee et al., 2012).

Our studies are of utmost significance as they help to understand structural relationship between bsn and PSMB4 as well as make presumptions about possible functional outcome of this interaction. However, we do not provide evidence that bsn directly interacts with PSMB4. We did not consider mutational analysis due to the fact that these bsn motifs bind other proteins and deleting them would probably have a pleiotropic effect. Therefore, we recognize that other proteins, cofactors or posttranslational modifications could mediate the association between bsn and proteasome.

4.2 Bsn acts as a major regulator of the presynaptic proteasome activity

In order to maintain constant excitability levels in check and ensure physiologically relevant synaptic function, synaptic activity is subjected to extensive control by various cellular mechanisms. Protein degradation by the proteasome constitutes one of the pathways that play active role in the remodeling of synaptic connections. In turn, proteasome itself can be locally modulated in response to changes in neuronal activity (Ehlers, 2003; Djakovic et al., 2009; Djakovic et al., 2012). Nevertheless, most of the studies focus on the postsynaptic

compartment, abundant in neurotransmitter receptors, scaffolding molecules and signaling proteins, but overlooks the contribution of the presynaptic sites. Many proteins that interact with proteasome are simultaneously processed for degradation (Sanchez-Lanzas and Castano, 2014), thus we first inspected whether bsn is a substrate of proteasome. Consequently, no evident accumulation of bsn, was observed upon treatment of bsn-transfected HEK293T cells with proteasome inhibitors, implying that bsn is not targeted for degradation.

Next, to verify whether bsn could modulate presynaptic proteasome activity, we conducted a series of experiments to address this question. Evaluation of the proteasome activity in the heterologous system of HEK293T cells by the means of degradation of a fluorogenic peptide substrate, specific for the chymotrypsin-like proteasomal activity, revealed a considerable decrease in the activity of the proteasome upon expression of bsn fragments independently interacting with PSMB4. Furthermore, zymography-based visualization of the proteasomal activity from cell lysates transfected with Bsn2 and Bsn4 showed that both fragments have inhibitory effect on proteasome. Since employing fluorogenic peptide substrates constitutes readout for the activity of 20S proteasome but does not rely upon preceding ubiquitination of the proteasome client proteins, we took advantage of a GFP-based fluorescent reporter (Dantuma et al., 2000) that measures ubiquitin-proteasome-dependent proteolysis in the living cells. Overexpression of both bsn segments- Bsn2 and Bsn4 resulted in the accumulation of the Ub^{G76V}-GFP reporter, which indicates a downregulation of degradation rates of ubiquitinated proteins. Interestingly, Bsn4 consistently triggered much higher increase in the reporter signal. This might indicate that this specific fragment of bsn, does not only inhibit enzymatic activity of the proteasome, but could also interfere with proteasome assembly and/or other aspects of the ubiquitination machinery. In line with this idea is the recent study by Hipp et al., which showed that aggregation-prone mutant form of protein huntingtin, involved in the pathogenesis of Huntington's disease, triggers accumulation of the fluorescent UPS reporter without clogging the proteasome (Hipp et al., 2012). The increase in the fluorescence signal of this reporter was attributed to the impaired protein folding homeostasis and competition of ubiquitinated substrates, including UPS reporter molecules, for the restricted 26S capacity. Moreover, available data indicate that in the absence of deubiquitinating enzyme Ubp6 (yeast homolog of human Usp14), UPS reporter proteins are turned over faster, suggesting that Ubp6 acts to delay proteolysis. Ubp6 not only trims ubiquitin chains, but also directly inhibits proteasome, promoting dissociation of the substrate from the proteasome and rescuing it from degradation (Hanna et al., 2006). It is therefore plausible that by interfering with different components of Ub conjugation cascade, Bsn4

triggers massive accumulation of Ub^{G76V}-GFP reporter. Additionally, the increase in the fluorescence of Ub^{G76V}-GFP protein could also reflect elevated levels of reporter mRNA (Bowman et al., 2005), however it is rather difficult to conceive how Bsn4, whether directly or obliquely, could transcriptionally regulate Ub^{G76V}-GFP levels in our experimental set-up.

In order to unambiguously illustrate that short PSMB4-interacting fragments of bsn are responsible for modulation of the proteasome activity on neuronal background, we assessed enzymatic capability of the proteasome in cultured cortical primary neurons. Degradation of the model fluorogenic substrate was decreased in the cortical neurons overexpressing Bsn2 and Bsn4 fragments, confirming that bsn can act as the neuron-specific inhibitor of the proteasome activity.

Moreover, almost two-fold increase in the proteasome activity in the BGT animals further supports the role of bsn as the negative regulator of the proteasome activity *in vivo*. To our knowledge this is the first demonstration of the presynapse-specific mode of the proteasome control. However, because proteasomes are diffusely distributed in neurons and can be found not only in the cytosol and neuritic process but also in the cell body (Ding and Keller, 2001), bsn, abundantly present in the cell soma at trans-Golgi compartment (Dresbach et al., 2006), could potentially regulate proteasome activity at distinct subcellular localizations.

Curiously enough, proteasome species are subjected to the active anterograde transport which is dependent on the molecular motor kinesin-1 and interaction with intracellular membranes (Otero et al., 2014). It has been postulated, therefore, that proteasomes bind synaptic vesicles or 'hitch-hike' on membranous cargos along axons which might favour degradation of particular proteins either in the course of their transfer or upon arrival at the place of destination (Otero et al., 2014). Intriguingly, bsn and pclo, along with other proteins, associate with Golgi-derived dense core vesicles- called Piccolo-Bassoon transport vesicles (PTV) and are delivered to the nascent synapses in a microtubule-based, kinesin motor-driven axonal transport (Zhai et al., 2001; Shapira et al., 2003; Cai et al., 2007). Although highly speculative, an exciting possibility exists that proteasome could bind PTVs for the transport and subsequent deposition at the sites of presynaptic assembly. In accordance with this idea, recently published data suggests that proteasome locally modulates formation of presynaptic terminals (Pinto et al., 2016). Additionally, a novel type of proteasome termed neuronal membrane proteasome (NMP) has been described that directly regulates neuronal function by processing intracellular proteins into extracellular peptides that in turn affect neuronal signaling (Shapira et al., 2003; Ramachandran and Margolis, 2017). Although, at present, specific localization of these particular proteasomal species to pre- or postsynaptic

membranes is unknown, interestingly, their expression begins at 8 DIV which coincides with emergence of PTVs (Shapira et al., 2003; Ramachandran and Margolis, 2017).

In line with already published data (Colledge et al., 2003; Ehlers, 2003; Tai et al., 2010), we detected proteasome activity in the different subcellular brain compartments. Furthermore, we show that proteolytically active proteasomes are present not only in the cytosolic extracts but also in the synaptosomes, i.e. the fraction enriched in synaptic junctions, where they participate in the modulation of synaptic strength and plasticity. We also demonstrate that the activity of the proteasome is higher in the cytosolic than in the synaptosomal preparation as already reported by *Tai et al.* (Tai et al., 2010) as well as *Wang et al.* (Wang et al., 2008). Nevertheless, by the means of native gel electrophoresis followed by the in-gel overlay analysis that essentially utilizes the same fluorogenic substrate as the previous assay, but allows for more qualitative assessment of the proteasome composition, we were only able to identify proteasome species in the total brain as well as cytoplasmatic fractions, likely because the activity of the proteasomes in other fractions was either lost during sample preparation/electrophoresis or was too low to be detected by the assay. This assumption was further confirmed by Western blotting which revealed the presence of proteasomal subunits in synaptosomes, ultimately corroborating that proteasomes are also localized at the synaptic sites.

Our data provides a strong hint that in the presynaptic compartment bsn might curtail proteasome activity. Several studies report that proteasome activity can be monitored by interactions with proteasomal subunits. Of note is cereblon protein, that binds to PSMB4 and reduces proteasome activity (Lee et al., 2012). Although the authors do not elucidate mechanism behind cereblon-mediated downregulation of proteasome hydrolysis, they postulate that CRBN could impede proteasome assembly. CRBN is widely expressed in the brain and, most likely, it can be found in both pre- and postsynaptic compartments, where it binds different partners (Lee et al., 2012; Lee et al., 2014). Currently, it is not known if CRBN specifically regulates pre- and/or postsynaptic proteasome, however it is compelling to speculate that activity of the synaptic proteasome is governed by a class of distinct negative regulators. Notably, an array of monomeric as well as aggregated proteins, mostly implicated in the neurodegenerative diseases, has been discovered to interact with the members of either 19S or 20S. (Snyder et al., 2003; Um et al., 2010). For example, parkin, a protein involved in the familial form of Parkinson's disease, interacts with 19S regulatory subunits- Rpn1, Rpn10, Rpt5 as well as Rpt6 and boosts formation of not only 19S particles but also 26S proteasomes, what results in the increase of 26S proteasome activity and implies that mutations in parkin

could contribute to the proteasomal dysfunction observed in PD (Um et al., 2010). α -synuclein, another protein implicated in PD, when aggregated, suppresses proteasomal function by binding to Rpt5 subunit of 19S regulatory complex (Snyder et al., 2003), whereas tau, strongly associated with Alzheimer's disease, associates with several proteasome subunits, including Rpt5 and Rpt6 as well as 20S core α subunits and impedes proteasomal degradation (Myeku et al., 2017). Additionally, misfolded β -sheet-rich prion protein (PrP), a prion disease-related molecule, has been reported to interfere with 20S gate opening, considerably inhibiting proteasome activity and precluding consecutive substrate entry (Andre and Tabrizi, 2011; Deriziotis et al., 2011). Altogether, our studies as well as available literature demonstrate that proteasome is subjected to avid regulation by proteins commonly located at the synapses.

Although, up to date special architectural features of proteasome binding proteins remain uncharted, it is commonly held that HbYX motif, present in 19S RP and PA200, has highly activating potential and that it can stimulate proteasome activity (Li et al., 2014). An intriguing question for future studies is whether proteasome inhibitors are also equipped with a distinct structural motif that confers its inhibitory potential.

4.3 Potential role of bsn in the assembly of 20S proteasomes

Alternations in the activity of the proteasome might severely compromise cell health and have salient consequences for cellular viability (Glickman and Ciechanover, 2002; Ciechanover and Brundin, 2003). Studies show that proteasomes represent highly dynamic and extremely heterogeneous molecules and double-capped, single-capped, uncapped as well as distinct assembly intermediate species all coincide in the single cell (Asano et al., 2015). To better understand the origins of the altered proteasomal activity in BGT animals and to pinpoint possible mechanisms underlying the modulation of the proteasome activity by bsn, we set to investigate the integrity of the proteasome. Our immunoprecipitation studies revealed that bsn interacts with PSMB4 subunit of the proteasome, incorporation of which is a rate limiting step in dimerization of two half-proteasomes. Dimerization of two proteasome half-mers occurs when C-terminal extension of PSMB4 intercalates into the groove between β 1 and β 2 subunits on the opposing β -ring, creating, therefore, a strong dimer comprised of two half-proteasomes and coinciding with emergence of the functional 20S proteasomes. HEK293T cells deprived of the C-terminal tail of PSMB4 hardly produce 20S proteasomes and show markedly

increased amount of precursor complexes as well as impaired enzymatic activity (Hirano et al., 2008). To study proteasome biogenesis and distinguish various proteasome assembly intermediate species, we employed glycerol density gradient ultracentrifugation. In our experiments, higher levels of PAC1, an auxiliary protein, normally degraded upon completion of the proteasome assembly and formation of competent 20S proteasomes, were observed upon bsn overexpression in the fractions containing proteasome assembly intermediates, moreover propeptides of $\beta 2$ subunit were clearly increased in bsn-expressing cells whereas $\beta 2$ and $\beta 7$ subunits themselves were enriched in the lighter fractions upon bsn expression. Collectively, these results suggest that bsn could act as negative regulator of the 20S biogenesis, efficiently controlling proteasomal content at the presynaptic terminals. However, the exact mechanism by which bsn is involved in the 20S assembly remains quite elusive. Here, we speculate that by binding to C-terminal extension of PSMB4 bsn might hinder its intercalation into the pocket between $\beta 1$ and $\beta 2$ subunits on the opposing β -ring and therefore prevent or substantially impede dimerization of two half-proteasomes. Our findings reveal that formation of 20S proteasomes, in neuron-specific environment, might not be exclusively mediated by dedicated chaperons but might also involve other proteins that have broader roles in neuronal homeostasis.

Intriguingly, work by *Waites et al.* has already demonstrated that bsn is implicated in the control of another component of the UPS, namely E3 ligase action (Waites et al., 2013). In their study, knock down of bsn as well as another highly homologous AZ protein pclo led to enhanced ubiquitination and degradation of multiple presynaptic proteins, including synaptophysin and VAMP2, upregulation of endo-lysosomal organelles and gradual degeneration of synapses (Waites et al., 2013). This phenotype is mediated by E3 ligase-Siah1, which in the absence of bsn and pclo exerts detrimental effect on the synaptic health and structure. These large, multidomain proteins, thus, promote synaptic integrity by binding to Siah1 and negatively regulating its activity. What is more, *Okerlund et al.* reported that via interaction with E3-like ligase, namely, Atg5, bsn governs presynaptic autophagy (Okerlund et al., 2017). Knockdown of bsn and pclo triggered generation of presynaptic autophagosomes as well as autolysosome formation, however selective loss of bsn was enough to induce presynaptic autophagy. Here, polyubiquitination also played essential role in the activation of the autophagy process, yet this was independent of Siah1 (Okerlund et al., 2017). Work by these authors, thus, shows that bsn normally acts to limit autophagy at presynaptic boutons. Our results, in turn, unearth that bsn is specifically involved in the modulation of the proteasome activity via regulation of its assembly. We reveal increased proteasome activity in

BGT animals and defective proteasome biogenesis in the HEK293T cells overexpressing bsn Bsn2 and Bsn4 fragments that interact with 20S proteasome. Although preservation of homeostatic proteasome levels is fundamental for cell fitness, mechanisms regulating the assembly of this degradative machinery remain largely elusive. Many reports demonstrate that proteasome biogenesis can be efficiently controlled at the step of 20S and 19S association. However, even docking of 19S to 20S particle is mainly governed either by posttranslational modifications or assembly chaperon proteins (Cho-Park and Steller, 2013; Day et al., 2013; Im and Chung, 2016). Our data, thus, would be the first to describe a protein that could act as a locally specific modulator of 20S proteasome assembly. We claim that via binding to proteasome and negatively regulating its activity, bsn could participate in the supervision of CAZ as well as synaptic vesicle (SV) pool integrity. Collectively, our results and the published research suggest that bsn acts as the negative regulator of several cellular programs, including polyubiquitination, ubiquitin-proteasome system, endo-lysosomal pathway and autophagy, since in the absence of bsn these major degradation programs become deregulated and considerable loss of SV proteins as well as synaptic degeneration are observed. Future studies are required to decipher how bsn converges upon all the described pathways and whether these systems act in concert or are autonomously regulated.

4.4 Increased proteasome activity contributes to the deregulation of synaptic vesicle pool sizes observed in bassoon knockout animals

The ability of bsn to interact, control the activity and seemingly tether proteasome at the sites of synaptic vesicle recycling, further supports the view that proteasome participates in many facets of presynaptic function. Indeed, it has been shown that, at the presynaptic boutons, proteasome is implicated in the surveillance of synaptic vesicle pool sizes, as inhibition of the proteasome activity leads to an increase in the recycling pool of synaptic vesicles, assayed by fluorescent styryl dye FM4-64 (Willeumier et al., 2006). Increase in the size of RP strongly depended on the synaptic activity, thus, proteasome is postulated to function as a presynaptic homeostatic regulator, fine-tuning neurotransmitter release during times of boosted neuronal activity. Since authors did not observe any changes in the amount or kinetics of dye release, they concluded that inhibition of the proteasome activity triggers mobilization of vesicles from the reserve to the recycling pool (Willeumier et al., 2006). Therefore, we presumed that if bsn overexpression impedes proteasome activity, it could as well prompt changes in the SV pool sizes. In our studies, we used pH-sensitive fluorophore-CypHer5E to measure SV pool

turnover at individual synapses expressing either Bsn2 or Bsn4 bsn fragment. To our surprise, these experiments revealed no major changes in the synaptic vesicle pool dynamics upon overexpression of bsn fragments. Considering that endogenous bsn is still present at the presynaptic sites, it is conceivable that it masks potential modulatory effects of the shorter fragments. In addition, as Bsn4 is diffusely distributed in the cells, its presynaptic targeting function might be severely compromised, which has already been proposed by earlier studies (Dresbach et al., 2003; Maas et al., 2012). Although the exact subcellular targeting of Bsn2 fragment has not been verified, a larger segment spanning aa 1692-2563 and still containing Bsn2 piece, is correctly anchored at the presynaptic specializations (Maas et al., 2012). Because long-term expression of bsn segments (12 days) could induce homeostatic mechanisms to counteract plausible, unbalanced changes in the presynaptic vesicle pool sizes, we examined synaptic vesicle recycling after acute expression of bsn interacting fragments. Since, acute expression of Bsn4 at later developmental stages (14 DIV) caused significant neuronal death, we excluded it from the further experiments. However, our data demonstrate that even short-term Bsn2 overexpression did not induce any considerable changes in the presynaptic vesicle cycling.

Bsn has been shown to be essential for neurotransmitter release at ribbon retinal synapses, endbulbs of Held as well as cochlear inner hair cells (Dick et al., 2003; Khimich et al., 2005; Jing et al., 2013; Mendoza Schulz et al., 2014). At cerebellar mossy fiber to granule cell synapses, lack of bsn enhances short-term depression during high-frequency transmission and reduces vesicle reloading at AZ (Hallermann et al., 2010). Previous work from our laboratory indicated that partial bsn deficiency (Bsn Δ Ex4/5) does not affect neither synapse density nor basic criteria characterizing presynaptic nerve terminals but it does induce inactivation of a considerable fraction of excitatory synapses (Altrock et al., 2003). Complete bsn knockout (BGT), however, leads to more severe phenotype including decreased vesicle recycling and lower release probability (Davydova et al., 2014) in hippocampal neurons. Here, we extend these findings and demonstrate that bsn is an important regulator of the presynaptic vesicle pool sizes, including morphologically docked vesicles of RRP and more diversified RP, at hippocampal terminals, as in the absence of this protein both pools are diminished. Since, together with the decrease in the RRP and RP, BGT neurons displayed increase in the size of resting pool of vesicles, we conclude that these neurons fail to efficiently recruit vesicles from RtP to RP, a defect that is partially rescued by proteasome inhibition. Alternations in RP, in turn, will profoundly affect the size of RRP as lower number of releasable vesicles signifies that essentially fewer vesicles are available for mobilization to immediately releasable pool to

efficiently participate in neurotransmission. Importantly, in line with existing literature, inhibition of proteasome activity, with three unrelated blockers, produced significant increase in the size of RRP as well as RP in wild type hippocampal cultures. Interestingly, increase in SVs pool sizes displayed by BGT neurons upon treatment with proteasome inhibitors was greater than in the WT neurons. This indicates that the defect in SVs pool distribution, observed in the absence of bsn, is partly caused by the overactive proteasome, which can be pharmacologically curbed to prevent detrimental changes that would result in impaired synaptic transmission. What could be the underlying mechanism behind bsn-dependent, proteasome-mediated regulation of synaptic vesicle pool sizes? It has been reported that cAMP/PKA pathway participates in the recruitment of vesicles into RP and that proteasome and cAMP/PKA pathway might converge to conjointly organize vesicle mobilization (Willeumier et al., 2006). Since, experiments conducted in our laboratory demonstrated that PKA activity as well as phosphorylation of PKA substrates, including SNAP25 and synapsin, are decreased in BGT neurons, it is conceivable that this deregulation might also account for defects in vesicle recycling pool. Moreover, it has been shown that phosphorylation by PKA decelerates proteasome-dependent degradation of several key proteins, among others, of dunc-13, a *Drosophila* ortholog of mammalian Munc-13, engaged in vesicular exocytosis (Aravamudan and Broadie, 2003) and that elevation in the levels of cAMP inhibit proteasome, leastwise, in the pineal gland (Schomerus et al., 2000). Therefore, proteasome and PKA might work in concert with bsn and other presynaptic proteins to regulate neurotransmitter release. Potentially, other signaling pathways that work collectively with proteasome to govern vesicular pool turnover might be important at the presynaptic terminals. It has been pointed out that activity-dependent phosphorylation of proteasome subunit Rpt6 by CaMKII is vital for synaptic plasticity and remodeling. Albeit, these effects were investigated only in relation to remodeling of the postsynaptic machinery (Djakovic et al., 2009; Bingol et al., 2010; Djakovic et al., 2012), hypothetically, CaMKII-mediated proteasome phosphorylation could also induce alternations in the presynaptic phenotype, for example, in the availability of vesicles for exocytosis. Interestingly, phosphorylation of synapsin by CaMKII regulates vesicle mobilization and release, especially, at relatively low stimulus frequencies (Chi et al., 2003). Moreover, it is now commonly accepted that the balance between two opposing enzymes: phosphatase calcineurin (CaN) and protein kinase CDK5 governs the presynaptic pool homeostasis. CDK5 activity substantially locks entry to the reserve pool of synaptic vesicles, whereas CaN promotes conversion of resting vesicles into release competent ones (Kim and Ryan, 2010). Compellingly, studies conducted in our laboratory revealed that BGT

animals have significantly higher CDK5 activity, what might contribute to the observed increase in RtP of SV. Altogether, data presented in this work as well as experiments performed in our laboratory imply that in the absence of bsn numerous pathways become deregulated and that this dysregulation translates into severe deficits in SVs pool sizes.

Although primary not addressed in our study, a possibility exists that due to the overactive proteasome, BGT display increased levels of synaptic protein degradation, which would promote defective presynaptic function. Indeed, it has been suggested that knock down of both bsn and pclo leads to synaptic disintegration via overactivation of polyubiquitination, endo-lysosomal pathway and autophagy (Waites et al., 2013; Okerlund et al., 2017). Our findings that bsn absence prompts upregulation of proteasome activity, further expand on these research and indicate that underlying mechanism of faulty synaptic recycling, observed in BGT animals, might be more complex. Importantly, not only proteasome itself but also various components of UPS have been shown to substantially contribute to the regulation of neurotransmitter release. Acute inhibition of both ubiquitination and proteasome activity prompts sizeable increase in the frequency of miniature EPSCs, however it is currently unknown, if this increase arises from upregulation of RRP, enhancement of release probability or other mechanisms. It has been proposed, nevertheless, that this feature seems to be triggered by reduction in dynamic protein ubiquitination (Rinetti and Schweizer, 2010). Intriguingly, also deubiquitinating enzymes are of crucial importance for appropriate synaptic transmission, since mice deficient for Usp14 evince, together with 30% decline in the free ubiquitin pool, impaired short-term plasticity at hippocampal synapses and reduced RRP due to decreased recruitment from RP at NMJ (Wilson et al., 2002; Bhattacharyya et al., 2011). Thus, both undisturbed proteasome function as well as ubiquitin homeostasis seems to be tightly connected with normal neurotransmission and synaptic activity.

In conclusion, our data identify proteasome, and specifically one of its major subunits-PSMB4 as a novel interaction partner of bsn. We also argue that this interaction could have salient consequences on presynaptic proteasome activity and assembly, in addition, we highlight the importance of the proteasome in bsn-dependent regulation of SVs pool sizes. We believe that our results significantly broaden the understanding of the physiological role of multifunctional protein bsn and shed light on the regulatory mechanisms of presynaptic proteasome. How and if bsn-proteasome intercommunication is essential during synaptic development and plasticity remains intriguing question for the future studies.

5. Bibliography

- Altrock WD et al. (2003) Functional inactivation of a fraction of excitatory synapses in mice deficient for the active zone protein bassoon. *Neuron* 37:787-800.
- Andre R, Tabrizi SJ (2011) Misfolded PrP and a novel mechanism of proteasome inhibition. *Prion* 6:32-36.
- Aravamudan B, Broadie K (2003) Synaptic Drosophila UNC-13 is regulated by antagonistic G-protein pathways via a proteasome-dependent degradation mechanism. *J Neurobiol* 54:417-438.
- Asano S, Fukuda Y, Beck F, Aufderheide A, Forster F, Danev R, Baumeister W (2015) Proteasomes. A molecular census of 26S proteasomes in intact neurons. *Science* 347:439-442.
- Banker GA (1980) Trophic interactions between astroglial cells and hippocampal neurons in culture. *Science* 209:809-810.
- Bhattacharyya BJ, Wilson SM, Jung H, Miller RJ (2011) Altered neurotransmitter release machinery in mice deficient for the deubiquitinating enzyme Usp14. *Am J Physiol Cell Physiol* 302:C698-708.
- Bingol B, Schuman EM (2006) Activity-dependent dynamics and sequestration of proteasomes in dendritic spines. *Nature* 441:1144-1148.
- Bingol B, Wang CF, Arnott D, Cheng D, Peng J, Sheng M (2010) Autophosphorylated CaMKIIalpha acts as a scaffold to recruit proteasomes to dendritic spines. *Cell* 140:567-578.
- Blitz DM, Foster KA, Regehr WG (2004) Short-term synaptic plasticity: a comparison of two synapses. *Nat Rev Neurosci* 5:630-640.
- Bowman AB, Yoo SY, Dantuma NP, Zoghbi HY (2005) Neuronal dysfunction in a polyglutamine disease model occurs in the absence of ubiquitin-proteasome system impairment and inversely correlates with the degree of nuclear inclusion formation. *Hum Mol Genet* 14:679-691.
- Burri L, Hockendorff J, Boehm U, Klamp T, Dohmen RJ, Levy F (2000) Identification and characterization of a mammalian protein interacting with 20S proteasome precursors. *Proc Natl Acad Sci U S A* 97:10348-10353.
- Burrone J, Li Z, Murthy VN (2006) Studying vesicle cycling in presynaptic terminals using the genetically encoded probe synaptopHluorin. *Nat Protoc* 1:2970-2978.
- Cai Q, Pan PY, Sheng ZH (2007) Syntabulin-kinesin-1 family member 5B-mediated axonal transport contributes to activity-dependent presynaptic assembly. *J Neurosci* 27:7284-7296.
- Chain DG, Casadio A, Schacher S, Hegde AN, Valbrun M, Yamamoto N, Goldberg AL, Bartsch D, Kandel ER, Schwartz JH (1999) Mechanisms for generating the autonomous cAMP-dependent protein kinase required for long-term facilitation in Aplysia. *Neuron* 22:147-156.
- Chen P, Hochstrasser M (1996) Autocatalytic subunit processing couples active site formation in the 20S proteasome to completion of assembly. *Cell* 86:961-972.
- Chen ZJ, Sun LJ (2009) Nonproteolytic functions of ubiquitin in cell signaling. *Mol Cell* 33:275-286.
- Chi P, Greengard P, Ryan TA (2003) Synaptic vesicle mobilization is regulated by distinct synapsin I phosphorylation pathways at different frequencies. *Neuron* 38:69-78.
- Cho-Park PF, Steller H (2013) Proteasome regulation by ADP-ribosylation. *Cell* 153:614-627.
- Ciechanover A (2005) Proteolysis: from the lysosome to ubiquitin and the proteasome. *Nat Rev Mol Cell Biol* 6:79-87.
- Ciechanover A, Brundin P (2003) The ubiquitin proteasome system in neurodegenerative diseases: sometimes the chicken, sometimes the egg. *Neuron* 40:427-446.
- Ciechanover A, Heller H, Elias S, Haas AL, Hershko A (1980) ATP-dependent conjugation of reticulocyte proteins with the polypeptide required for protein degradation. *Proc Natl Acad Sci U S A* 77:1365-1368.
- Citri A, Soler-Llavina G, Bhattacharyya S, Malenka RC (2009) N-methyl-D-aspartate receptor- and metabotropic glutamate receptor-dependent long-term depression are differentially regulated by the ubiquitin-proteasome system. *Eur J Neurosci* 30:1443-1450.

- Colledge M, Snyder EM, Crozier RA, Soderling JA, Jin Y, Langeberg LK, Lu H, Bear MF, Scott JD (2003) Ubiquitination regulates PSD-95 degradation and AMPA receptor surface expression. *Neuron* 40:595-607.
- Dantuma NP, Lindsten K, Glas R, Jellne M, Masucci MG (2000) Short-lived green fluorescent proteins for quantifying ubiquitin/proteasome-dependent proteolysis in living cells. *Nat Biotechnol* 18:538-543.
- Dar A, Wu D, Lee N, Shibata E, Dutta A (2014) 14-3-3 proteins play a role in the cell cycle by shielding cdt2 from ubiquitin-mediated degradation. *Mol Cell Biol* 34:4049-4061.
- Davydova D, Marini C, King C, Klueva J, Bischof F, Romorini S, Montenegro-Venegas C, Heine M, Schneider R, Schroder MS, Altmann WD, Henneberger C, Rusakov DA, Gundelfinger ED, Fejtova A (2014) Bassoon specifically controls presynaptic P/Q-type Ca(2+) channels via RIM-binding protein. *Neuron* 82:181-194.
- Day SM, Divald A, Wang P, Davis F, Bartolone S, Jones R, Powell SR (2013) Impaired assembly and post-translational regulation of 26S proteasome in human end-stage heart failure. *Circ Heart Fail* 6:544-549.
- De Duve C, Pressman BC, Gianetto R, Wattiaux R, Appelmans F (1955) Tissue fractionation studies. 6. Intracellular distribution patterns of enzymes in rat-liver tissue. *Biochem J* 60:604-617.
- Deriziotis P, Andre R, Smith DM, Goold R, Kinghorn KJ, Kristiansen M, Nathan JA, Rosenzweig R, Krutauz D, Glickman MH, Collinge J, Goldberg AL, Tabrizi SJ (2011) Misfolded PrP impairs the UPS by interaction with the 20S proteasome and inhibition of substrate entry. *EMBO J* 30:3065-3077.
- Dick O, tom Dieck S, Altmann WD, Ammermuller J, Weiler R, Garner CC, Gundelfinger ED, Brandstatter JH (2003) The presynaptic active zone protein bassoon is essential for photoreceptor ribbon synapse formation in the retina. *Neuron* 37:775-786.
- Ding Q, Keller JN (2001) Proteasomes and proteasome inhibition in the central nervous system. *Free Radic Biol Med* 31:574-584.
- Djakovic SN, Schwarz LA, Barylko B, DeMartino GN, Patrick GN (2009) Regulation of the proteasome by neuronal activity and calcium/calmodulin-dependent protein kinase II. *J Biol Chem* 284:26655-26665.
- Djakovic SN, Marquez-Lona EM, Jakawich SK, Wright R, Chu C, Sutton MA, Patrick GN (2012) Phosphorylation of Rpt6 regulates synaptic strength in hippocampal neurons. *J Neurosci* 32:5126-5131.
- Dobie F, Craig AM (2007) A fight for neurotransmission: SCRAPPER trashes RIM. *Cell* 130:775-777.
- Dong C, Bach SV, Haynes KA, Hegde AN (2014) Proteasome modulates positive and negative translational regulators in long-term synaptic plasticity. *J Neurosci* 34:3171-3182.
- Dong C, Upadhyaya SC, Ding L, Smith TK, Hegde AN (2008) Proteasome inhibition enhances the induction and impairs the maintenance of late-phase long-term potentiation. *Learn Mem* 15:335-347.
- Dresbach T, Hempelmann A, Spilker C, tom Dieck S, Altmann WD, Zuschratter W, Garner CC, Gundelfinger ED (2003) Functional regions of the presynaptic cytomatrix protein bassoon: significance for synaptic targeting and cytomatrix anchoring. *Mol Cell Neurosci* 23:279-291.
- Dresbach T, Torres V, Wittenmayer N, Altmann WD, Zamorano P, Zuschratter W, Nawrotzki R, Ziv NE, Garner CC, Gundelfinger ED (2006) Assembly of active zone precursor vesicles: obligatory trafficking of presynaptic cytomatrix proteins Bassoon and Piccolo via a trans-Golgi compartment. *J Biol Chem* 281:6038-6047.
- Ehlers MD (2003) Activity level controls postsynaptic composition and signaling via the ubiquitin-proteasome system. *Nat Neurosci* 6:231-242.
- Fejtova A, Gundelfinger ED (2006) Molecular organization and assembly of the presynaptic active zone of neurotransmitter release. *Results Probl Cell Differ* 43:49-68.
- Fernandez-Alfonso T, Ryan TA (2008) A heterogeneous "resting" pool of synaptic vesicles that is dynamically interchanged across boutons in mammalian CNS synapses. *Brain Cell Biol* 36:87-100.

- Ferreira JS, Schmidt J, Rio P, Aguas R, Rooyackers A, Li KW, Smit AB, Craig AM, Carvalho AL (2015) GluN2B-Containing NMDA Receptors Regulate AMPA Receptor Traffic through Anchoring of the Synaptic Proteasome. *J Neurosci* 35:8462-8479.
- Frischknecht R, Fejtova A, Viesti M, Stephan A, Sonderegger P (2008) Activity-induced synaptic capture and exocytosis of the neuronal serine protease neurotrypsin. *J Neurosci* 28:1568-1579.
- Gallastegui N, Groll M (2010) The 26S proteasome: assembly and function of a destructive machine. *Trends Biochem Sci* 35:634-642.
- Girach F, Craig TJ, Rocca DL, Henley JM (2013) RIM1alpha SUMOylation is required for fast synaptic vesicle exocytosis. *Cell Rep* 5:1294-1301.
- Glickman MH, Ciechanover A (2002) The ubiquitin-proteasome proteolytic pathway: destruction for the sake of construction. *Physiol Rev* 82:373-428.
- Greenberg SM, Castellucci VF, Bayley H, Schwartz JH (1987) A molecular mechanism for long-term sensitization in *Aplysia*. *Nature* 329:62-65.
- Gruendler C, Lin Y, Farley J, Wang T (2001) Proteasomal degradation of Smad1 induced by bone morphogenetic proteins. *J Biol Chem* 276:46533-46543.
- Gundelfinger ED, Fejtova A (2012) Molecular organization and plasticity of the cytomatrix at the active zone. *Curr Opin Neurobiol* 22:423-430.
- Gundelfinger ED, Reissner C, Garner CC (2015) Role of Bassoon and Piccolo in Assembly and Molecular Organization of the Active Zone. *Front Synaptic Neurosci* 7:19.
- Guo J, Ge JL, Hao M, Sun ZC, Wu XS, Zhu JB, Wang W, Yao PT, Lin W, Xue L (2015) A three-pool model dissecting readily releasable pool replenishment at the calyx of held. *Sci Rep* 5:9517.
- Hallermann S, Fejtova A, Schmidt H, Weyhersmuller A, Silver RA, Gundelfinger ED, Eilers J (2010) Bassoon speeds vesicle reloading at a central excitatory synapse. *Neuron* 68:710-723.
- Hanna J, Hathaway NA, Tone Y, Crosas B, Elsasser S, Kirkpatrick DS, Leggett DS, Gygi SP, King RW, Finley D (2006) Deubiquitinating enzyme Ubp6 functions noncatalytically to delay proteasomal degradation. *Cell* 127:99-111.
- Hegde AN, Goldberg AL, Schwartz JH (1993) Regulatory subunits of cAMP-dependent protein kinases are degraded after conjugation to ubiquitin: a molecular mechanism underlying long-term synaptic plasticity. *Proc Natl Acad Sci U S A* 90:7436-7440.
- Hegde AN, Inokuchi K, Pei W, Casadio A, Ghirardi M, Chain DG, Martin KC, Kandel ER, Schwartz JH (1997) Ubiquitin C-terminal hydrolase is an immediate-early gene essential for long-term facilitation in *Aplysia*. *Cell* 89:115-126.
- Herrmann J, Lerman LO, Lerman A (2007) Ubiquitin and ubiquitin-like proteins in protein regulation. *Circ Res* 100:1276-1291.
- Hipp MS, Patel CN, Bersuker K, Riley BE, Kaiser SE, Shaler TA, Brandeis M, Kopito RR (2012) Indirect inhibition of 26S proteasome activity in a cellular model of Huntington's disease. *J Cell Biol* 196:573-587.
- Hirano Y, Hendil KB, Yashiroda H, Iemura S, Nagane R, Hioki Y, Natsume T, Tanaka K, Murata S (2005) A heterodimeric complex that promotes the assembly of mammalian 20S proteasomes. *Nature* 437:1381-1385.
- Hirano Y, Kaneko T, Okamoto K, Bai M, Yashiroda H, Furuyama K, Kato K, Tanaka K, Murata S (2008) Dissecting beta-ring assembly pathway of the mammalian 20S proteasome. *EMBO J* 27:2204-2213.
- Hirano Y, Hayashi H, Iemura S, Hendil KB, Niwa S, Kishimoto T, Kasahara M, Natsume T, Tanaka K, Murata S (2006) Cooperation of multiple chaperones required for the assembly of mammalian 20S proteasomes. *Mol Cell* 24:977-984.
- Im E, Chung KC (2016) Precise assembly and regulation of 26S proteasome and correlation between proteasome dysfunction and neurodegenerative diseases. *BMB Rep* 49:459-473.
- Ivanova D, Dirks A, Montenegro-Venegas C, Schone C, Altmann WD, Marini C, Frischknecht R, Schanze D, Zenker M, Gundelfinger ED, Fejtova A (2015) Synaptic activity controls localization and function of CtBP1 via binding to Bassoon and Piccolo. *EMBO J* 34:1056-1077.

- Jarome TJ, Werner CT, Kwapis JL, Helmstetter FJ (2011) Activity dependent protein degradation is critical for the formation and stability of fear memory in the amygdala. *PLoS One* 6:e24349.
- Jarome TJ, Kwapis JL, Ruenzel WL, Helmstetter FJ (2013) CaMKII, but not protein kinase A, regulates Rpt6 phosphorylation and proteasome activity during the formation of long-term memories. *Front Behav Neurosci* 7:115.
- Jiang X, Litkowski PE, Taylor AA, Lin Y, Snider BJ, Moulder KL (2010) A role for the ubiquitin-proteasome system in activity-dependent presynaptic silencing. *J Neurosci* 30:1798-1809.
- Jing Z, Rutherford MA, Takago H, Frank T, Fejtova A, Khimich D, Moser T, Strenzke N (2013) Disruption of the presynaptic cytomatrix protein bassoon degrades ribbon anchorage, multiquantal release, and sound encoding at the hair cell afferent synapse. *J Neurosci* 33:4456-4467.
- Jung T, Grune T (2012) Structure of the proteasome. *Prog Mol Biol Transl Sci* 109:1-39.
- Jurd R, Thornton C, Wang J, Luong K, Phamluong K, Kharazia V, Gibb SL, Ron D (2008) Mind bomb-2 is an E3 ligase that ubiquitinates the N-methyl-D-aspartate receptor NR2B subunit in a phosphorylation-dependent manner. *J Biol Chem* 283:301-310.
- Kaech S, Banker G (2006) Culturing hippocampal neurons. *Nat Protoc* 1:2406-2415.
- Kandel ER, Schwartz JH (1982) Molecular biology of learning: modulation of transmitter release. *Science* 218:433-443.
- Kato A, Rouach N, Nicoll RA, Brecht DS (2005) Activity-dependent NMDA receptor degradation mediated by retrotranslocation and ubiquitination. *Proc Natl Acad Sci U S A* 102:5600-5605.
- Khimich D, Nouvian R, Pujol R, Tom Dieck S, Egner A, Gundelfinger ED, Moser T (2005) Hair cell synaptic ribbons are essential for synchronous auditory signalling. *Nature* 434:889-894.
- Kim SH, Ryan TA (2010) CDK5 serves as a major control point in neurotransmitter release. *Neuron* 67:797-809.
- Kisselev AF, Goldberg AL (2001) Proteasome inhibitors: from research tools to drug candidates. *Chem Biol* 8:739-758.
- Kisselev AF, Goldberg AL (2005) Monitoring activity and inhibition of 26S proteasomes with fluorogenic peptide substrates. *Methods Enzymol* 398:364-378.
- Klare N, Seeger M, Janek K, Jungblut PR, Dahlmann B (2007) Intermediate-type 20 S proteasomes in HeLa cells: "asymmetric" subunit composition, diversity and adaptation. *J Mol Biol* 373:1-10.
- Kock M, Nunes MM, Hemann M, Kube S, Dohmen RJ, Herzog F, Ramos PC, Wendler P (2015) Proteasome assembly from 15S precursors involves major conformational changes and recycling of the Pba1-Pba2 chaperone. *Nat Commun* 6:6123.
- Kononenko N, Pechstein A, Haucke V (2013) Synaptic requiem: a duet for Piccolo and Bassoon. *EMBO J* 32:920-922.
- Kusmierczyk AR, Kunjappu MJ, Funakoshi M, Hochstrasser M (2008) A multimeric assembly factor controls the formation of alternative 20S proteasomes. *Nat Struct Mol Biol* 15:237-244.
- Lazarevic V, Pothula S, Andres-Alonso M, Fejtova A (2013) Molecular mechanisms driving homeostatic plasticity of neurotransmitter release. *Front Cell Neurosci* 7:244.
- Lazarevic V, Schone C, Heine M, Gundelfinger ED, Fejtova A (2011) Extensive remodeling of the presynaptic cytomatrix upon homeostatic adaptation to network activity silencing. *J Neurosci* 31:10189-10200.
- Lazarevic V, Schone C, Heine M, Gundelfinger ED, Fejtova A (2012) Extensive remodeling of the presynaptic cytomatrix upon homeostatic adaptation to network activity silencing. *J Neurosci* 31:10189-10200.
- Lee KM, Lee J, Park CS (2012) Cereblon inhibits proteasome activity by binding to the 20S core proteasome subunit beta type 4. *Biochem Biophys Res Commun* 427:618-622.
- Lee KM, Yang SJ, Choi JH, Park CS (2014) Functional effects of a pathogenic mutation in Cereblon (CRBN) on the regulation of protein synthesis via the AMPK-mTOR cascade. *J Biol Chem* 289:23343-23352.
- Li X, Thompson D, Kumar B, DeMartino GN (2014) Molecular and cellular roles of PI31 (PSMF1) protein in regulation of proteasome function. *J Biol Chem* 289:17392-17405.

- Lin A, Hou Q, Jarzylo L, Amato S, Gilbert J, Shang F, Man HY (2011) Nedd4-mediated AMPA receptor ubiquitination regulates receptor turnover and trafficking. *J Neurochem* 119:27-39.
- Lin Y, Martin J, Gruendler C, Farley J, Meng X, Li BY, Lechleider R, Huff C, Kim RH, Grasser WA, Paralkar V, Wang T (2002) A novel link between the proteasome pathway and the signal transduction pathway of the bone morphogenetic proteins (BMPs). *BMC Cell Biol* 3:15.
- Loscher M, Fortschegger K, Ritter G, Wostry M, Voglauer R, Schmid JA, Watters S, Rivett AJ, Ajuh P, Lamond AI, Katinger H, Grillari J (2005) Interaction of U-box E3 ligase SNEV with PSMB4, the beta7 subunit of the 20 S proteasome. *Biochem J* 388:593-603.
- Lussier MP, Herring BE, Nasu-Nishimura Y, Neutzner A, Karbowski M, Youle RJ, Nicoll RA, Roche KW (2012) Ubiquitin ligase RNF167 regulates AMPA receptor-mediated synaptic transmission. *Proc Natl Acad Sci U S A* 109:19426-19431.
- Maas C, Torres VI, Altmann WD, Leal-Ortiz S, Wagh D, Terry-Lorenzo RT, Fejtova A, Gundelfinger ED, Ziv NE, Garner CC (2012) Formation of Golgi-derived active zone precursor vesicles. *J Neurosci* 32:11095-11108.
- Matias AC, Ramos PC, Dohmen RJ (2010) Chaperone-assisted assembly of the proteasome core particle. *Biochem Soc Trans* 38:29-33.
- Maupin-Furlow J (2011) Proteasomes and protein conjugation across domains of life. *Nat Rev Microbiol* 10:100-111.
- Mendoza Schulz A, Jing Z, Sanchez Caro JM, Wetzel F, Dresbach T, Strenzke N, Wichmann C, Moser T (2014) Bassoon-disruption slows vesicle replenishment and induces homeostatic plasticity at a CNS synapse. *EMBO J* 33:512-527.
- Murata S, Yashiroda H, Tanaka K (2009) Molecular mechanisms of proteasome assembly. *Nat Rev Mol Cell Biol* 10:104-115.
- Myeku N, Clelland CL, Emrani S, Kukushkin NV, Yu WH, Goldberg AL, Duff KE (2017) Tau-driven 26S proteasome impairment and cognitive dysfunction can be prevented early in disease by activating cAMP-PKA signaling. *Nat Med* 22:46-53.
- Okerlund ND, Schneider K, Leal-Ortiz S, Montenegro-Venegas C, Kim SA, Garner LC, Gundelfinger ED, Reimer RJ, Garner CC (2017) Bassoon Controls Presynaptic Autophagy through Atg5. *Neuron* 93:897-913 e897.
- Otero MG, Alloatti M, Cromberg LE, Almenar-Queralt A, Encalada SE, Pozo Devoto VM, Bruno L, Goldstein LS, Falzone TL (2014) Fast axonal transport of the proteasome complex depends on membrane interaction and molecular motor function. *J Cell Sci* 127:1537-1549.
- Pinto MJ, Alves PL, Martins L, Pedro JR, Ryu HR, Jeon NL, Taylor AM, Almeida RD (2016) The proteasome controls presynaptic differentiation through modulation of an on-site pool of polyubiquitinated conjugates. *J Cell Biol* 212:789-801.
- Qureshi HY, Han D, MacDonald R, Paudel HK (2013) Overexpression of 14-3-3z promotes tau phosphorylation at Ser262 and accelerates proteasomal degradation of synaptophysin in rat primary hippocampal neurons. *PLoS One* 8:e84615.
- Ramachandran KV, Margolis SS (2017) A mammalian nervous-system-specific plasma membrane proteasome complex that modulates neuronal function. *Nat Struct Mol Biol* 24:419-430.
- Ramos PC, Dohmen RJ (2008) PACemakers of proteasome core particle assembly. *Structure* 16:1296-1304.
- Realini C, Rechsteiner M (1995) A proteasome activator subunit binds calcium. *J Biol Chem* 270:29664-29667.
- Rinetti GV, Schweizer FE (2010) Ubiquitination acutely regulates presynaptic neurotransmitter release in mammalian neurons. *J Neurosci* 30:3157-3166.
- Rizzoli SO, Betz WJ (2005) Synaptic vesicle pools. *Nat Rev Neurosci* 6:57-69.
- Rose T, Schoenenberger P, Jezek K, Oertner TG (2013) Developmental refinement of vesicle cycling at Schaffer collateral synapses. *Neuron* 77:1109-1121.
- Rosenzweig R, Glickman MH (2008) Forging a proteasome alpha-ring with dedicated proteasome chaperones. *Nat Struct Mol Biol* 15:218-220.

- Rossi F, Evstafieva A, Pedrali-Noy G, Gallina A, Milanese G (1997) HsN3 proteasomal subunit as a target for human immunodeficiency virus type 1 Nef protein. *Virology* 237:33-45.
- Rousset R, Desbois C, Bantignies F, Jalinot P (1996) Effects on NF-kappa B1/p105 processing of the interaction between the HTLV-1 transactivator Tax and the proteasome. *Nature* 381:328-331.
- Royle SJ, Granseth B, Odermatt B, Derevier A, Lagnado L (2008) Imaging phluorin-based probes at hippocampal synapses. *Methods Mol Biol* 457:293-303.
- Sa-Moura B, Simoes AM, Fraga J, Fernandes H, Abreu IA, Botelho HM, Gomes CM, Marques AJ, Dohmen RJ, Ramos PC, Macedo-Ribeiro S (2013) Biochemical and biophysical characterization of recombinant yeast proteasome maturation factor ump1. *Comput Struct Biotechnol J* 7:e201304006.
- Sanchez-Lanzas R, Castano JG (2014) Proteins directly interacting with mammalian 20S proteasomal subunits and ubiquitin-independent proteasomal degradation. *Biomolecules* 4:1140-1154.
- Sasaki K, Hamazaki J, Koike M, Hirano Y, Komatsu M, Uchiyama Y, Tanaka K, Murata S (2010) PAC1 gene knockout reveals an essential role of chaperone-mediated 20S proteasome biogenesis and latent 20S proteasomes in cellular homeostasis. *Mol Cell Biol* 30:3864-3874.
- Schmidt M, Hanna J, Elsasser S, Finley D (2005) Proteasome-associated proteins: regulation of a proteolytic machine. *Biol Chem* 386:725-737.
- Schomerus C, Korf HW, Laedtke E, Weller JL, Klein DC (2000) Selective adrenergic/cyclic AMP-dependent switch-off of proteasomal proteolysis alone switches on neural signal transduction: an example from the pineal gland. *J Neurochem* 75:2123-2132.
- Schroder MS, Stellmacher A, Romorini S, Marini C, Montenegro-Venegas C, Altroock WD, Gundelfinger ED, Fejtova A (2013) Regulation of presynaptic anchoring of the scaffold protein Bassoon by phosphorylation-dependent interaction with 14-3-3 adaptor proteins. *PLoS One* 8:e58814.
- Scudder SL, Goo MS, Cartier AE, Molteni A, Schwarz LA, Wright R, Patrick GN (2014) Synaptic strength is bidirectionally controlled by opposing activity-dependent regulation of Nedd4-1 and USP8. *J Neurosci* 34:16637-16649.
- Shabek N, Ciechanover A (2010) Degradation of ubiquitin: the fate of the cellular reaper. *Cell Cycle* 9:523-530.
- Shapira M, Zhai RG, Dresbach T, Bresler T, Torres VI, Gundelfinger ED, Ziv NE, Garner CC (2003) Unitary assembly of presynaptic active zones from Piccolo-Bassoon transport vesicles. *Neuron* 38:237-252.
- Snider BJ, Tee LY, Canzoniero LM, Babcock DJ, Choi DW (2002) NMDA antagonists exacerbate neuronal death caused by proteasome inhibition in cultured cortical and striatal neurons. *Eur J Neurosci* 15:419-428.
- Snyder H, Mensah K, Theisler C, Lee J, Matouschek A, Wolozin B (2003) Aggregated and monomeric alpha-synuclein bind to the S6' proteasomal protein and inhibit proteasomal function. *J Biol Chem* 278:11753-11759.
- Sorokin AV, Kim ER, Ovchinnikov LP (2009) Proteasome system of protein degradation and processing. *Biochemistry (Mosc)* 74:1411-1442.
- Stadtmueller BM, Kish-Trier E, Ferrell K, Petersen CN, Robinson H, Myszka DG, Eckert DM, Formosa T, Hill CP (2012) Structure of a proteasome Pba1-Pba2 complex: implications for proteasome assembly, activation, and biological function. *J Biol Chem* 287:37371-37382.
- Sudhof TC (2004) The synaptic vesicle cycle. *Annu Rev Neurosci* 27:509-547.
- Tada H, Okano HJ, Takagi H, Shibata S, Yao I, Matsumoto M, Saiga T, Nakayama KI, Kashima H, Takahashi T, Setou M, Okano H (2010) Fbxo45, a novel ubiquitin ligase, regulates synaptic activity. *J Biol Chem* 285:3840-3849.
- Tai HC, Schuman EM (2008) Ubiquitin, the proteasome and protein degradation in neuronal function and dysfunction. *Nat Rev Neurosci* 9:826-838.
- Tai HC, Besche H, Goldberg AL, Schuman EM (2010) Characterization of the Brain 26S Proteasome and its Interacting Proteins. *Front Mol Neurosci* 3.
- Tanaka K (2009) The proteasome: overview of structure and functions. *Proc Jpn Acad Ser B Phys Biol Sci* 85:12-36.

- tom Dieck S, Altmann WD, Kessels MM, Qualmann B, Regus H, Brauner D, Fejtova A, Bracko O, Gundelfinger ED, Brandstätter JH (2005) Molecular dissection of the photoreceptor ribbon synapse: physical interaction of Bassoon and RIBEYE is essential for the assembly of the ribbon complex. *J Cell Biol* 168:825-836.
- Tomko RJ, Jr., Hochstrasser M (2013) Molecular architecture and assembly of the eukaryotic proteasome. *Annu Rev Biochem* 82:415-445.
- Tsvetkov P, Myers N, Eliav R, Adamovich Y, Hagai T, Adler J, Navon A, Shaul Y (2014) NADH binds and stabilizes the 26S proteasomes independent of ATP. *J Biol Chem* 289:11272-11281.
- Um JW, Im E, Lee HJ, Min B, Yoo L, Yoo J, Lubbert H, Stichel-Gunkel C, Cho HS, Yoon JB, Chung KC (2010) Parkin directly modulates 26S proteasome activity. *J Neurosci* 30:11805-11814.
- Unno M, Mizushima T, Morimoto Y, Tomisugi Y, Tanaka K, Yasuoka N, Tsukihara T (2002) The structure of the mammalian 20S proteasome at 2.75 Å resolution. *Structure* 10:609-618.
- Vandenberghe W, Nicoll RA, Brecht DS (2005) Stargazin is an AMPA receptor auxiliary subunit. *Proc Natl Acad Sci U S A* 102:485-490.
- Velichutina I, Connerly PL, Arendt CS, Li X, Hochstrasser M (2004) Plasticity in eucaryotic 20S proteasome ring assembly revealed by a subunit deletion in yeast. *EMBO J* 23:500-510.
- Vitureira N, Goda Y (2013) Cell biology in neuroscience: the interplay between Hebbian and homeostatic synaptic plasticity. *J Cell Biol* 203:175-186.
- Waites CL, Leal-Ortiz SA, Okerlund N, Dalke H, Fejtova A, Altmann WD, Gundelfinger ED, Garner CC (2013) Bassoon and Piccolo maintain synapse integrity by regulating protein ubiquitination and degradation. *EMBO J* 32:954-969.
- Wang J, Wang CE, Orr A, Tydlacka S, Li SH, Li XJ (2008) Impaired ubiquitin-proteasome system activity in the synapses of Huntington's disease mice. *J Cell Biol* 180:1177-1189.
- Wang X, Hu B, Zieba A, Neumann NG, Kasper-Sonnenberg M, Honsbein A, Hultqvist G, Conze T, Witt W, Limbach C, Geitmann M, Danielson H, Kolarow R, Niemann G, Lessmann V, Kilimann MW (2009) A protein interaction node at the neurotransmitter release site: domains of Aczonin/Piccolo, Bassoon, CAST, and rim converge on the N-terminal domain of Munc13-1. *J Neurosci* 29:12584-12596.
- Wani PS, Rowland MA, Ondracek A, Deeds EJ, Roelofs J (2015) Maturation of the proteasome core particle induces an affinity switch that controls regulatory particle association. *Nat Commun* 6:6384.
- Welzel O, Henkel AW, Stroebel AM, Jung J, Tischbirek CH, Ebert K, Kornhuber J, Rizzoli SO, Groemer TW (2011) Systematic heterogeneity of fractional vesicle pool sizes and release rates of hippocampal synapses. *Biophys J* 100:593-601.
- Willeumier K, Pulst SM, Schweizer FE (2006) Proteasome inhibition triggers activity-dependent increase in the size of the recycling vesicle pool in cultured hippocampal neurons. *J Neurosci* 26:11333-11341.
- Wilson SM, Bhattacharyya B, Rachel RA, Coppola V, Tessarollo L, Householder DB, Fletcher CF, Miller RJ, Copeland NG, Jenkins NA (2002) Synaptic defects in ataxia mice result from a mutation in *Usp14*, encoding a ubiquitin-specific protease. *Nat Genet* 32:420-425.
- Wojcik C, Benchaib M, Lornage J, Czyba JC, Guerin JF (2000a) Localization of proteasomes in human oocytes and preimplantation embryos. *Mol Hum Reprod* 6:331-336.
- Wojcik C, Benchaib M, Lornage J, Czyba JC, Guerin JF (2000b) Proteasomes in human spermatozoa. *Int J Androl* 23:169-177.
- Yao I, Takagi H, Ageta H, Kahyo T, Sato S, Hatanaka K, Fukuda Y, Chiba T, Morone N, Yuasa S, Inokuchi K, Ohtsuka T, Macgregor GR, Tanaka K, Setou M (2007) SCRAPPER-dependent ubiquitination of active zone protein RIM1 regulates synaptic vesicle release. *Cell* 130:943-957.
- Yi JJ, Ehlers MD (2007) Emerging roles for ubiquitin and protein degradation in neuronal function. *Pharmacol Rev* 59:14-39.
- Zhai RG, Vardinon-Friedman H, Cases-Langhoff C, Becker B, Gundelfinger ED, Ziv NE, Garner CC (2001) Assembling the presynaptic active zone: a characterization of an active one precursor vesicle. *Neuron* 29:131-143.

6. Abbreviations

% (v/v)	percent by volume
% (w/v)	percent by mass
4AP	4-Aminopyridine
aa	amino acid
Arc	activity-regulated cytoskeleton-associated protein
AD	Alzheimer's disease
AMPA	α -amino-3-hydroxy-5-methyl-4-isoxazolepropionic acid
AMPA	α -amino-3-hydroxy-5-methyl-4-isoxazolepropionic acid receptor
Ap-Uch	Aplysia ubiquitin C-terminal hydrolase
APV	(2R)-amino-5-phosphonovaleric acid
ATF4	activating transcription factor 4
ATP	adenosin triphosphate
AZ	active zone
BMP	bone morphogenetic protein
Bsn	Bassoon
BrAAP	branched chain amino acid peptidase
CaMKII	Calcium/calmodulin-dependent protein kinase type II
cAMP	cyclic adenosine monophosphate
CAST	the active zone-associated structural protein
CAZ	cytomatrix of the active zone
cDNA	complementary DNA
CNQX	6-cyano-7-nitroquinoxaline-2,3-dione
co-IP	co-immunoprecipitation
COS-7	African green monkey cell line
CP	core particle
cTEC	cortical thalamic epithelial cells

Abbreviations

CRBN	cereblon
CREB	cAMP response element-binding protein
DHPG	dihydroxyphenylglycine
DIV	days in vitro
DKD	double knock down
DMEM	Dulbecco's Modified Eagle Medium
DNA	deoxyribonucleic acid
DUB	deubiquitinating enzyme
E.coli	Escherichia coli
EDTA	ethylenediaminetetraacetic acid
EGFP	green fluorescent protein
EGFR	epidermal growth factor receptor
Ep-L-LTP	early phase of late long term potentiation
ER	endoplasmic reticulum
FCS	fetal calf serum
HbYX	hydrophobic-tyrosine-X
HBSS	Hank's Balanced salts
HEK	human embryonic kidney
HEPES	4-(2-hydroxyethyl)-1-piperazineethanesulfonic acid
His	histidin
ICC	immunocytochemistry
IEG	immediate early gene
IF	immunofluorescence
IFN- γ	interferon gamma
IgG	immunoglobulin G
KD	knockdown
kDa	kilo Dalton
KO	knockout
LTD	long term-depression

Abbreviations

LTF	long term facilitation
L-LTP	late long term potentiation
LTP	long term potentiation
Leu	leucine
mEPSCs	miniature excitatory postsynaptic currents
mGluR	metabotropic glutamate receptors
MHC	major histocompatibility complex
mIPSCs	miniature inhibitory postsynaptic currents
mRNA	messenger RNA
Nedd4-1	Neural precursor cell expressed developmentally down-regulated protein 4
Nef	Negative Regulatory Factor
Mib2	Mind Bomb-2
NMDA	N-Methyl-D-aspartic acid
NMDAR	N-Methyl-D-aspartic acid receptor
NTN	hyrolases nuceophilic hydrolases
PAC	proteasome assembly chaperon
PAGE	polyacrylamide gel electrophoresis
Paip2	polyadenylate-binding protein interacting protein 2
Pba	proteasome biogenesis associated protein
PBS	phosphate buffered saline
Pclo	Piccolo
PCR	polymerase chain reaction
PD	Parkinson's disease
PFA	paraformaldehyde
PKC	protein kinase C
PrP	prion protein
PSD-95	postsynaptic density protein 95
PTV	Bassoon-Piccolo transport vesicles
RBP	RIM-binding protein

Abbreviations

RIM	Rab3-interacting molecules
RNA	Ribonucleic acid
RNAi	RNA interference
RP	recycling pool
RP	regulatory particle
rpm	revolutions per minute
Rpn	regulatory particle of non-ATPase
Rpt	regulatory particle of triple ATPase
RRP	readily-releasable pool
RtP	resting pool
SCR-KO	Scrapper-knockout
SDS	sodium dodecyl sulfate
SIAH	seven in absentia homolog
SNAP-25	Synaptosomal-associated protein 25
SNAPP	small neutral amino acid peptidase
SNEV	senescence evasion factor
SV	synaptic vesicle
SVP	synaptic vesicle precursor
Syn	synapsin
sypHy	synaptophysin-pHluorin
Syt1-CypHer	synaptotagmin1- CypHer5E
T.acidophilum	Thermoplasma acidophilum
TAFIIF	Transcription factor II F
TEMED	Tetramethylethylenediamine
TGN	trans-Golgi-network
Thr	threonine
Tris	Tris(hydroxymethyl)-aminomethane
Tris/HCl	Tris(hydroxymethyl)-aminomethanhydrochloride
TrkB	tropomyosin receptor kinase B

Abbreviations

TRP	total recycling pool
Trp	tryptophan
TTX	tetrodotoxin
Ub	ubiquitin
UBL-UBA	ubiquitin-like-ubiquitin-associated
Ubp6	Ubiquitin carboxyl-terminal hydrolase 6
UPP	ubiquitin-proteasome pathway
UPS	ubiquitin-proteasome system
Usp14	Ubiquitin-specific protease 14
VSVG	Vesicular stomatitis virus G protein
WB	Western blotting
Y2H	yeast two hybrid

7. Scientific publications

Physiological Concentrations of Amyloid Beta Regulate Recycling of Synaptic Vesicles via Alpha7 Acetylcholine Receptor and CDK5/Calcineurin Signaling

Vesna Lazarevic, **Sandra Fieńko**, Maria Andres-Alonso, Daniela Anni, Daniela Ivanova, Carolina Montenegro-Venegas, Eckart D. Gundelfinger, Michael A. Cousin and Anna Fejtova, *Frontiers in Molecular Neuroscience* (2017). 10:221. doi: 10.3389/fnmol.2017.00221

Curriculum vitae

Name: Sandra
Family name: Fieńko
Date of birth: April 19th 1988
Place of birth: Zielona Góra, Poland
Nationality: Polish
Parents: Grażyna Fieńko
Piotr Fieńko

Education:

2013-2017 Doctoral Thesis. Otto von Guericke Universität, Leibniz Institute for Neurobiology, Magdeburg, Germany
2010-2012 Master of Sciences in Biomolecular Sciences, Vrije Universiteit Brussel, Brussels, Belgium
2007-2010 Bachelor in Medical Biotechnology, Poznan University of Medical Sciences, Poznań, Poland
2004-2007 E. Dembowski Secondary School of General Education with bilingual classes in Zielona Góra, Poland

Research experience:

03.2013-2017 Research group Presynaptic Plasticity, Leibniz Institute for Neurobiology, Magdeburg, Germany
10.2011-06.2012 Laboratory for Pharmaceutical Chemistry, Drug analysis and Drug Information, Department of Pharmaceutical Sciences, Faculty of Medicine and Pharmacy, Vrije Universiteit Brussel, Brussels, Belgium
06.2009-07.2009 Institute of Bioorganic Chemistry, Polish Academy of Science, Poznań, Poland
01.2008-06.2008 Institute of Biochemistry and Molecular Biology, Poznan University of Medical Sciences, Poznań, Poland

Erklärung zur eigenständigen Abfassung der Arbeit

Hiermit erkläre Ich, Sandra Fienko, dass Ich die von mir eingereichte Dissertation zum dem Thema

Role of active zone scaffold bassoon in the regulation of presynaptic proteasome

selbständig verfasst, nicht schon als Dissertation verwendet habe und die benutzen Hilfsmittel und Quellen vollständig angegeben wurden.

Weiterhin erkläre ich, dass ich weder diese noch eine andere Arbeit zur Erlangung des akademischen Grades doctor rerum naturalium (Dr. rer. nat.) an anderen Einrichtungen eingereicht habe.

Magdeburg,

Unterschrift